CORROSION AND ABRASION OF RINGS AND LINERS FROM MARINE DIESEL ENGINES USING RESIDUAL FUEL

A thesis submitted as partial
fulfilment of the
requirement for the degree of

DOCTOR OF PHILOSOPHY
OF
BRUNEL UNIVERSITY

by

P.E. DALE B.Tech.

APRIL 1982

TABLE OF CONTENTS

SYNOPSIS

The aim of this research was to investigate the interaction of abrasion and corrosion on rings and liners from marine diesel engines using high sulphur residual fuels.

Pure corrosion effects were simulated in a sealed vessel containing emulsified lubricant and acid. Graphite was found to stimulate corrosion of ferrite but phosphide eutectic and iron carbide remained unattacked. A reciprocating test was used to combine the mechanisms of abrasion and corrosion which have been identified as producing normal wear in marine engines. The severity of the mechanisms were balanced to produce surfaces similar to those often encountered over the centre of an engine stroke. Two engine tests, specified to compare the type and extent of wear using high and low sulphur fuels, showed that an increase in corrosion resulting from increased fuel sulphur was not directly responsible for a measured increase in top ring wear rate. Corrosion was thought to dissolve the ferritic phases to release hard phases into the system which intensified abrasion of the surfaces. It was also possible that phosphide eutectic was left at a sufficiently high level above the surface by corrosion of the matrix to cause direct abrasion of the ring.

Throughout the experimental work particular emphasis was placed on examination and interpretation of the interaction of corrosion and abrasion in lubricated acidified environments.

1. INTRODUCTION

Cylinder liners from low speed marine diesel engines using residual fuels have a useful life of around seven years before wear causes significant performance deterioration. During the twenty year service life of a ship therefore, two complete engine overhauls are usually necessary to replace or refurbish cylinder liners. Medium speed engine liners using similar fuels can last the life of a ship but piston rings, which wear at ten times the liner rate, require replacement after only one or two years in both types of engine. Improvements of one to five per cent in ring wear performance therefore, would be more beneficial than similar gains for liner wear and represent considerable savings on major engine overhauls in terms of cost and time. Improvements in ring wear will not be achieved in isolation. Consideration must be given to the whole system to obtain increased ring life.

Although evidence of abrasion, corrosion and scuffing may be identified on rings and liners from engines using high sulphur residual fuels, scuffing may be an intermittent process during engine operation. Abrasion and corrosion are usually considered to be responsible for "normal" marine engine wear and it is the interaction of these mechanisms which is the subject of this experimental work.

Corrosion results from oxidation of fuel sulphur during combustion which subsequently condenses as sulphuric acid on liner surfaces below the acid dew point temperature. Abrasion is caused by surface asperity interaction and loose abrasive particles produced by combustion or wear.

Piston ring wear in these environments can be excessive when corrosion and abrasion interact to produce wear rates greater than the sum of their individual contributions. This interaction has received very little attention, despite the considerable savings in maintenance costs which are available for small improvements in ring wear. Before modification to engine conditions, materials or lubricants can be specified, however, it is necessary to understand in greater detail the mechanism of this interaction.

Three different test methods were employed to investigate the combined effect of abrasion and corrosion. As grey cast irons are almost universally used for rings and liners in marine engines, the mechanisms of corrosion on the composite phases of the material were investigated in the acidified lubricant environment of a corrosion test. Differences were detected between corrosion of steels and cast irons which were thought to be due to the detrimental effect of graphite. A reciprocating wear rig was designed and constructed which simulated the mechanism of abrasion and corrosion simultaneously in a lubricated test. This rig closely reproduced the type of damage often encountered over the centre of the stroke on marine engine liners run with residual fuels.

It was necessary to make direct comparisons of the type of surface damage in both the corrosion and reciprocating tests with service engine wear effects to justify the isolation of the wear mechanisms from the engine system. Finally a small bore Petter AV-1 engine, converted to a crosshead design, was used to compare the effect of high

sulphur fuel on the type and extent of wear on the rings and liners. Wear of the top ring was intensified using high sulphur fuel but this could not be attributed directly to corrosion. Differential corrosion was thought to increase abrasive effects by the preferential removal of the ferritic phases which weakened the surface and released "hard phases" into the system.

An attempt has been made to interpret the information gained from these tests in the light of the recent literature to further the understanding of wear in corrosive marine engine environments.

2. LITERATURE REVIEW

2.1 WEAR MECHANISMS

The simplest definition of wear is "the unwanted removal of solid material from a rubbing surface"[1]. This definition covers all aspects of wear which do not appear to fit into the O.E.C.D.[2] definition which infers that wear occurs as a result of relative motion of the surfaces. Clearly some aspects of chemical wear are not covered. It has proved possible to identify several common mechanisms which contribute to wear, although they are rarely encountered in isolation. The main wear types, abrasion, adhesion, rolling contact fatigue and corrosion are supplemented by several minor types which can be considered hybrid mechanisms. The most common of these are fretting and erosion.

ABRASION

Abrasion accounts for some 50% of wear found in industrial equipment[1]. Although this type of wear is rarely catastrophic, the cumulative effect often results in loss of efficiency and necessitates component replacement.

Abrasion may be defined as:-

> "The removal of material from one of two surfaces in relative motion as a result of the presence of hard asperities on one of the contact surfaces or as a result of hard particles trapped between the surfaces or embedded in one of them[3]."

These particles may be foreign bodies or products from the surfaces. These two basic manifestations of abrasive wear are termed two body and three body situations. The former is caused when the abrasives rub against a second face and the latter when trapped between two moving surfaces.

The literature on abrasive wear may be divided into those that concentrate on two body and those which deal with three body wear. The larger volume of work has been with two body situations because it is more important as an industrial failure mechanism and also because testing equipment is simpler and the results more reproducable. The early research of Kruschov and Babichev[4] in two body wear found a direct proportionality between relative wear resistance and bulk hardness for pure metals and some annealed metals and a linear relationship for heat treated steels. Two main processes were identified when abrasive grains make contact with a wearing surface. These are the primary removal of metallic chips and plastic deformation to form grooves on the surface, without any removal of metal. Sedricks and Mulhearn[5] reviewed the effect of the angle which the cutting face of the abrasive made with the wearing surfaces. A critical angle was found to occur at which the mechanism changes from rubbing to a cutting action. The angle was also important when determining the likely embedding of particles in the surface. During cutting the particle is supported by the frictional force but during rubbing the abrasive is supported on the inclined contacting surfaces. It was also found that the critical angle at which rubbing changed to cutting depended on the materials under test and is influenced by the coefficient of friction between the abrasive and surface. Goddard and Wilman[6] theoretically calculated the effect of particle shape on the coefficient of friction and the type of abrasive mechanism which occurs.

The influence of hardness on the wear resistance has been examined by Richardson[7,8] who defined hard abrasives as those

whose hardness is greater than the contacting surface and soft when less than that surface. For hard abrasives the wear resistance is dependent on the hardness of the abrasive to a critical value above which the wear becomes independent of the abrasive hardness. This occurs at about 1.5 x the hardness of the metal surface.

Kruschov[9] & Richardson[7] found that work hardening prior to testing did not influence the wear resistance and both concluded that the surface work hardened to a critical value during abrasion until equilibrium wear occurred. For soft abrasives the running-in time takes much longer and it is doubtful whether the work hardening occurs to the same extent over all of the surface. The threshold at which soft abrasives will affect the the contacting surface occurs when the hardness is about 0.7 x the surface hardness. The wear rate increases with abrasive hardness up to the maximum critical size.

When considering heterogeneous materials, Kruschov[10] proposed that an additive effect occurred between the matrix and hard phases in the microstructure.

$$E = \alpha E_1 + \beta E_2$$

E = Relative wear resistance

α, β = Volume fractions

$E_1 E_2$ = Bulk wear resistance

Richardson[7] proposed modifications to the basic hypothesis to take account of the width of the abrasive grooves and the dimensions of the second phase particles. As the size of the abrasive scratches increases the hard phase becomes less effective. It was thought that carbides in particular as second phase particles work harden during abrasive wear. Richardson[8] found that for soft abrasives, heterogeneous materials were strongly influenced by the width of abrasive grooves in a similar way to hard abrasives.

Nathan and Jones[11], Avient Goddard and Wilman[12] and Kruschov and Babichev[4] have all shown that volumetric wear is directly proportional to the nominal load up to a critical value which is limited by deformation of the specimen and degradation of the particles. Nathan and Jones[11] also found that the critical load occurs at a lower value for small abrasives. Although the diameter of the wear scars does not depend strongly on the load, the number of contacting points increases linearly with the increase in load. Kruschov and Babichev[4] and others[11] found a small increase in volume wear with increases in speed. In both cases however, these increases were thought to be due to experimental variables.

The importance of grit size has been investigated by many workers. The dependence of wear on the abrasive particle size is an important characteristic of abrasion. It has been well established that the volume of wear increases rapidly with abrasive size from 1 to 70-80 μ and then increases at a much reduced rate with further increases in grit size. This critical size is apparent in both two and three body wear. Rabinowicz and Mutis[13] have shown that the critical size for three body wear is less than for two body wear, at about 50 μ and that the wear rate was a factor of 10 less than for two body[14]. This was not confirmed by Miller[15] who used diamond abrasives in contrast to silicon carbide used by Rabinowicz[13].

Rabinowicz[13] explained the transition effect to be due to the interference of the abrasive mechanism by the formation of large adhesive particles. Avient et al[12] concluded that clogging of the interstices between the finer abrasives by wear debris was responsible for the size effect. Clearly this explanation would not be relevant for three body wear.

Richardson[7] thought that the small particles were more prone to fracture than the large particles. This theory was first proposed by Mulhearn and Samuels[16]. Avient, Goddard and Wilman[12] thought that this characteristic grit size depended on the amount of abrasives embedded in the wearing surface. This was confirmed by Johnson[17] as he showed that the amount of pickup increased as the grit size decreased.

Larsen-Badse[18] found that fine grits may only have elastic interactions with surfaces whereas larger grits cause more cutting and plastic deformation. Sin, Saka and Suh[19] have recently shown that the size effect occurs for non metals in addition to the metallic case at roughly the same size. These investigators saw the transition to be due to the change in elastic/plastic deformation to plastic/cutting. Theoretically Kragelskii[20] found that these types of deformation occur at distinct ratios of track width to particle tip radius.

$w/r < 0.28$ - elastic

$0.28 < w/r < 0.87$ - plastic

$0.87 < w/r$ - cutting

Sin, Saka and Suh[19] were able to calculate w/r ratios for different particle sizes and found that the small particles have smaller ratios and they concluded that this ratio was responsible for the variation of wear due to grit size. Depending on the ratio w/r the surface will either deform or be cut. One of the variables affecting the ratio is the ductility of the surface. They also showed there to be a similar variation of coefficient of friction with grit size. This also occurred at roughly 70 μ and was found to be explained theoretically by w/r ratio considerations.

Moore[21] and Mutton and Watson[22] have attempted to explain the influence of the microstructure on the abrasion resistance of the ferrous metals. Mutton and Watson[22] conclude that increases in hardness due to alloy additions causes a change in ease of chip formation and transition from ploughing to cutting. The mechanism of groove formation is fundamentally different for two phase materials containing hard brittle phases, although no data was presented. Moore[21] found that for pearlitic steels containing over 10% vol. of pearlite the wear resistance and hardness are linear functions of pearlite volume. Moore[21] excluded materials in which properties other than those of the bulk material were influenced by second phases. Miller[15] investigated the abrasive size effect up to 70 μ using diamond abrasive. He concluded that the k value in the wear relationship was a value which related to the efficiency of cutting in abrasive wear. $(K = \frac{3VH}{LS})$

The relationship proposed by Kruschov[9] was:-

$E = b\,M$

E = Wear resistance
  = ^{1}/wear volume

M = Bulk hardness

b = Coefficient of proportionality

This related wear to hardness of the material. Subsequently Rabinowicz[23] derived the following expression:-

$$\frac{dv}{dl} = \frac{L \tan\theta}{\pi P}$$

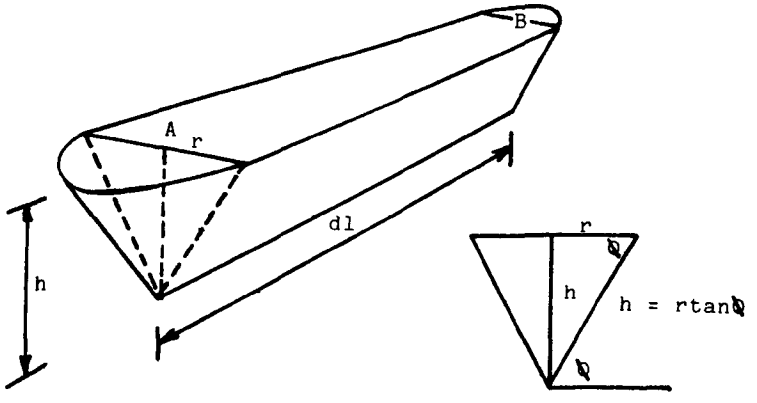

The load, $L = r^2 p$, where p = hardness of material.

$$\Longrightarrow \quad r^2 = \frac{L}{\pi p} \qquad \text{——————} \quad 1$$

The volume of material removed during motion from A to B, $dv = rh(dl)$

$$dv = r(r\tan\theta)dl \quad = r^2 \tan\theta \, dl$$

$$dv = \frac{L \tan\theta \, dl}{\pi} \qquad \text{— Substituting from 1}$$

$$\frac{dv}{dl} = \frac{L \tan\theta}{\pi p} \quad = \text{Wear rate}$$

$$\text{when } \frac{L \tan\theta}{\pi} \quad = K$$

The wear resistance, $E = Kp$

This value of K takes into account the impinging angle of particles onto the surface and the possibility that all the loaded particles do not cause the same volume of wear. Although Rabinowicz and Mutis[13] took only $\tan\theta$ to be variable, assuming that all the loaded grains produce wear, and referred to the $\tan\theta$ as the coefficient of abrasive wear. Miller[15] calculated from wear rates against load plots that:-

$$\frac{\Delta M}{\Delta W} = \text{Wear rate per unit load} = C\,K$$

The slope of the load/wear curves was a measure of the efficiency of cutting of abrasive particles. This was defined as the ratio of material plastically deformed to material worn away and was found to initially increase rapidly with abrasive size, increasing less rapidly at around 70μ. The reason for this behaviour was not proposed. Sin, Saka and Suh[19] determined K to be the ratio of work used to generate wear particles in the form of chips to the total work done, and showed the variation of K with size of abrasive to be due in part to the ratio of wear scar width to tip radii of abrading particle.

Mutton and Watson[22] found the lower wear resistance of certain steels to be due to the relative ease of chip formation which was related to fracture propensity, flow behaviour and morphology of second phases. These factors may also affect the value of K, the cutting efficiency.

EROSION

Erosion occurs when particles carried in a gas or liquid impinge on a solid and gradually remove material from its surface. Erosion is normally considered to be similar to abrasion as both processes involve hard particles impacting and sliding over a solid surface. Differences between the two however, are apparent as important features of erosion are the angle at which the particles impinge on the surface[24], the ductility and hardness of that surface[25] and the kinetic energy of the incident particles[26].

The mechanism of removal by erosion changes according to the impact angle. At low angles (15-30°), cutting is predominant. Under these conditions Eyre[26] indicated the use of high hardness as a precaution against wear. At angles approaching 90° different precautions may be necessary as deformation of the surface may occur with particles shattering on impact.

ADHESIVE WEAR

When two surfaces are in contact it has been shown that the real asperity contact area is 1×10^{-2} to 10^{-4} of the nominal area[27]. The resultant high pressures which develop in these areas are sufficient to deform the asperities to the extent that they are able to support the applied load, and may cause adhesion. As in any form of pressure welding, adhesion is favoured by clean surfaces, non oxidising conditions and by chemical and structural similarities.

When a junction fractures to transfer material from one surface to the other, or fractures at both surfaces to produce debris, wear occurs. Should the junction fracture at the original interface no wear occurs, although local plastic deformation and work hardening have both occurred.

Welsh[28] was one of the first to identify changes in wear behaviour due to thermal effects caused by variation in load and sliding speed. These transitions occur between periods of so called "severe" (metallic) and "mild" (oxidative) wear conditions. Wear in the oxidative regime, although classified under adhesive wear clearly separates the wearing surfaces. Wear occurs by the removal of oxide debris from an oxidised surface supported on a work hardened substrate[26].

CORROSIVE WEAR

Corrosive wear covers situations where chemical or electrochemical reactions of components with the environment dictate the wear process. Corrosion, although much of the time detrimental to wear, may work to improve wear behaviour. In some cases reaction with air to form oxides or hydroxides reduces wear, as found in severe to mild transitions, but can often have the opposite effect, for example in fretting.

Lubrication exerts a marked effect on corrosive wear. Burwell[29] separates the effect into two general types:-

1). It may protect the surfaces from the corroding environment, thus reducing the corrosive wear that would otherwise result.

2). The lubricant itself may react chemically with the surface, thus altering the type of compound and amount of wear that would otherwise result.

In addition to the intentional reactions of lubricant and additive it is clear that reactions due to chemical deterioration, decomposition and contamination of the lubricant can be detrimental.

SURFACE FATIGUE

The mechanism of fatigue caused by rolling contact is well known. This type of failure which is characterised by pitting or flaking of the surface, results in a relatively rapid deterioration of performance. Application of the Hertz equation for the elastic deformation of solid bodies to rolling contact has shown that the maximum shear stress occurs just below the contact surface. If fatigue cracks initiate they will do so in this high shear zone and generally run parallel to the surface. This eventually leads to the characteristic spalling of fragments of metal from the surface.

DELAMINATION

Delamination as proposed by Suh[30] is becoming more accepted as a mechanism of wear under sliding conditions. Subsurface cracks are thought to be formed by dislocation pile-up and subsequent formation of voids which may then coalesce to form cracks under the surface. Suh[30] holds that the mechanism can be used to explain fatigue, fretting and adhesive wear.

FRETTING

Fretting describes wear which often occurs when closely fitted parts are subject to low amplitude vibration. Although considered a basic wear mechanism by Waterhouse[31] fretting is often thought to amalgamate some of the main wear types.

The relative movement was thought by Moore[32] to break down the stable films on the surface. The freshly exposed surface would once again oxidise and be broken away. The generation

of large volumes of oxide debris in confined areas was then thought to accelerate abrasion between the components. The pressence of any lubricant was believed to reduce the scale of the damage, although MacPherson[33] reported that special lubricants were necessary to control the oxidation of the surface. It is often the case that the oxide completely seals the area from lubrication which can lead to excessive noise or eventual seizure.

MacPherson[33] saw two methods of combatting fretting:-

1). Prevention of relative vibration by modification of design to remove fretting sites.

2). Prevention of oxidation of the surface by a bulk change in material to a non-metallic (for example), by use of surface coatings or by control of the environment with specially formulated lubricants.

2.2 MATERIALS AND MANUFACTURE

CYLINDER LINERS

All cylinder liners and piston rings for marine engines are manufactured using cast iron. The basic material is grey cast iron with a pearlitic matrix, although the structure may be modified by alloying elements and casting technique.

The basic requirements of the materials used are:

1). Thermal stability.

2). High thermal conductivity.

3). Resistance to abrasive, adhesive and chemical wear.

4). Adequate mechanical properties.

5). Low cost.

6). Good castability and easy machining.

Grey cast iron gives a compromise of these requirements. Experience has shown that optimum mechanical properties are obtained from a fully pearlitic iron with a maximum of 5% free ferrite to at least grade 17 (BS 1452 - 1961). In highly stressed environments grade 23 cast iron is commonly used which may be hardened and tempered or be induction hardened. The mechanical properties are obtained by additions of tin or chromium which promotes the formation of pearlite. Phosphorus used initially up to 0.7% in large bore cylinders, forms a phosphide eutectic which is known to improve wear resistance under marginal lubrication conditions. Additions of 0.3% vanadium have been used to reduce the phosphorus content to around 0.3% which gives improved castability with no loss of wear resistance. The effect of the vanadium is to produce a dispersed phosphide/carbide complex and to reduce the iron's solubility in sulphuric acid. Additions of copper are sometimes made on the basis of corrosion resistance.

A typical composition range for a large marine engine cylinder is[31]:

Total carbon	2.7 - 3.5%
Silicon	0.7 - 1.4%
Manganese	0.4 - 0.6%
Sulphur	0.1% approx.
Phosphorus	0.1 - 0.3%
Vanadium	0.1 - 0.25%

The iron is cast into cylinder pots in either resin or CO_2 bonded sands. These pots are then machined to the required dimensions.

The surface of the finished cylinder is very important

during the early life of the engine. To avoid scuffing which is predominantly a running-in phenomena and therefore to achieve satisfactory long term performance, the surface should have:

1). Accurate dimensions.

2). Consistent finish over all the bore.

3). Grooves to help spread the oil from the lubricators over all the bore.

4). Freedom from embedded or loose particles and deformed layers.

There are two main finishing techniques and their application depends on the cylinder size. Large bore engines of about 1 m or greater diameter are turned with a single point round-nosed tool which gives a "wave turned" surface. A smoother surface is obtained by cross honing with diamond or silicon carbide embedded in rubber or cork, or a combination of the two, generally used on smaller bore cylinders which produces a plateau groove finish.

PISTON RINGS

Piston rings must satisfy certain requirements[34]:

1). A gas seal must be formed between the cylinder and bore at both high and low revs.

2). Allow correct amount of oil to pass to lubricate the upper cylinder.

3). Conduct heat away from the piston.

4). Withstand the mechanical and physical stresses without deformation.

5). Be resistant to corrosion.

The cast iron piston ring is again a compromise of all these requirements. Experience has shown that a grey iron with

flakes of "A type" graphite in the 3 - 5 size range, performs well in diesel engines. There should be a pearlitic matrix with less than 0.5% free ferrite and some hard phase. This phase may be of carbide, controlled by additions of chromium, molybdenum or vanadium up to about 0.5% and/or phosphide eutectic with phosphorus additions of between 0.3 to 0.5%. For better mechanical properties nodular irons may be used but some wear resistance may have to be sacrificed. The metallurgy of both ring and liner is closely linked to the casting process in particular to cooling rate for piston rings. There are two methods of manufacture in general use, these are, individually cast, and rings machined from pots of cast material. It is believed that for rings less than 200 mm dia., single casting produces an optimum microstructure while large bore rings, greater than 400 mm, are superior when pot cast[35]. Large bore diesel engine rings are pot cast usually by centrifugal casting. The rate of cooling is greater than for static pot casting with the result that rings of intermediate modulus are produced[34]. Additions of carbide stabilizing elements are made to suppress the formation of ferrite normally associated with more rapid cooling rates.

The rings are then finished to the required shape and profile. The shape of the ring is critical to maintain an even pressure on the liner surface when the engine is assembled. Large bore rings are formed to the correct profile after cooling on a mandrel . The smaller ones are normally cast with the required shape. The rings are accurately machined using sophisticated lathes before the gap is cut and the final profile is ground. Although rings are often coated to increase efficiency, liners are not coated at the manufacturing stage. The rings,

however, may have either long term or short term coatings applied during manufacture.

Coatings which retard corrosion during storage and assist during the running-in period of an engine are commonly applied. These may be oxide coatings which provide a mild abrasive action to ensure good conformity between ring and liner while providing good resistance to further oxidation during storage. A second type are diffusion treatments to a depth of 0.4 mm, e.g. Tuffriding and Sulfinuz. Soft coatings of manganese phosphate are also often used giving a low shear strength layer which has a granular appearance and holds the lubricant.

Running-in coatings of copper have been applied to the surface and have proved useful protection against scuffing. Soft electroplating of cadmium or tin whilst not having any wear resistant characteristics will aid running-in by melting and acting as emergency lubrication.

Long term coatings designed to last for the life of the component are still applied to cast iron rings. The most common coating of piston rings in marine service is electrodeposited chrome. It is intrinsically hard (800 - 900 Hv) and resistant to both abrasive and corrosive wear. The plated surface is usually treated by etching to produce irregularities on the surface which will retain oil. Other techniques are grit-blasting, phonograph finish and channel cracking. The thickness of the deposit varies up to 0.3 mm for large engine rings, and is sometimes applied to the flanks as well as the face to control the groove wear in the piston.

Plasma sprayed coating is a modern technique which has not been fully evaluated but it does offer the inherent advantage of being more porous than electrodeposited coatings.

2.3 CORROSION OF CAST IRON

The long standing belief that the fuel sulphur level influenced liner and ring wear in marine engines running on residual fuels, is now widely accepted[36, 37, 38, 39]. The mechanism of this interaction has been established beyond reasonable doubt to be due to the condensation of sulphuric acid from sulphur trioxide vapour from combustion, on to surfaces below the acid dew point. There is surprisingly little information available however, on the effect of the ensuing corrosion on the structure or properties of the ring and liner materials which are, for the most part, grey cast iron.

Recognising to some extent the heterogeneous nature of cast iron on corrosion potentials within the material, Cotti and Simonetti[38] explained the preferential corrosion of pearlite. Pearlite was identified as being negative with respect to the potential of graphite and therefore, in the presence of a suitable electrolyte, corroded preferentially. This view clearly fails to recognise the true complexity of the situation as pearlite itself has a two phase structure. Grey cast iron used for marine liners and rings has several constituent phases in different forms:-

- Graphite - Carbon
- Pearlite
  - Ferrite (α iron)
  - Cementite - Iron carbide (Fe_3C)
- Phosphide Eutectic
  - Ternary
    - Ferrite
    - Iron Phosphide (Fe_3P)
    - Iron Carbide (Fe_3C)
  - Pseudo Binary
    - Ferrite
    - Iron Phosphide
- Free Carbides - Iron carbide (and other Metallic Carbides)
- Others - Sulphides, Nitrides etc.

Each of the phases has an electrochemical potential which is dependent on the prevailing conditions.

Angus[40] has referred to the resistance of low alloy cast iron to acid attack by mineral acids. At low concentrations (less than 60%) these irons possess no useful resistance to attack. At higher concentrations and at room temperature an insoluble ferrous sulphate ($FeSO_4$) film forms on the surface and provides a barrier to further attack. The breakdown of this film which can be due to high temperature or mechanical removal will lead to an accelerated rate of acid attack. Maahn[41] found that the more concentrated the acid the higher the temperature at which the film broke down. For boiling H_2SO_4 the critical acid concentration was found to be 93%, but the presence of small volumes of organic impurities increased this concentration to 97%. Maahn[41] concluded that the presence of reducing impurities prevented the formation of a passive film. Under these conditions of high temperature and pH passivation is due to the formation of ferric sulphate ($Fe_2(SO_4)_3$).

The effect of various microconstituents in cast iron for use in corrosive environments has received very little attention. This is not really surprising when it is considered that cast iron is notoriously poor and has hardly any application for acid conditions. One notable exception is the use of grey cast iron pots to concentrate sulphuric acid by boiling, although here corrosion rates of 35 mm/year are normally tolerated. In contrast the effect of the microstructure of steel in corrosive environments has been of much greater interest. These two materials are similar enough for some qualitative information to be applicable to both.

That copper reduces corrosion in steels is well known, the mechanism, however, is not completely understood. It has been ascribed to the formation of copper or copper oxide on the metal surface acting as a barrier. When formed in acid environments however, copper is porous and does not afford the same protection[42]. Angus[40] attributes the effect of copper to the precipitation of sulphide ions from solution which tends to accelerate the corrosion of cast iron. Hoar and Havenhand[43] also refer to the beneficial formation of copper sulphide on steel surfaces which is insoluble in acid.

Hoar and Havenhand[43] found that steels with large carbide areas have more efficient cathodic reactions. They outline the conditions for efficient cathodic areas as:-

1). Electrically conducting.

2). Insoluble in acids.

3). Mechanically stable during corrosion.

It is clear therefore, that a phase which is not attacked in acid is more noble than other phases in the matrix and will be cathodic in corrosion reactions. Cementite in pearlite was believed to be too fine and during corrosion would exfoliate with the anodic iron. Hoar and Havenhand[43] concluded that massive carbides and phosphides may be expected to have a similar effect. Endo[44] has confirmed that high phosphorus contents stimulate acid attack of steel. Although within the normal compositional range for cast iron, Glantz and Maahn[45] found phosphorus to have very little effect in 96% concentrated sulphuric acid.

Manuel[46] investigated the influence of carbide structure on corrosion of steel. He recognised that corrosion products are largely insoluble and may therefore impart some protection against

further corrosion. If the deposit is porous or non-adherent, localised corrosion is likely to occur. Pearlitic steels were found to be superior to those which are heat treated to give spheroidal carbide precipitates. Radd and McGlasson[47] thought the orientation of pearlite to be significant. They found this to be due to the number of corrosion cells, (anodic/cathodic couples) per unit area, although massive carbides were found not to be susceptable to orientation.

LaQue[48] explained that graphite, which is insoluble in normal acid environments, is left as a residue as the cast iron matrix is dissolved. When the graphite network is packed with other insoluble phases such as carbides, phosphides and corrosion products, a layer may form on the surface which protects against further corrosion. In cast iron the graphite was also thought to act as an enlarged cathode which supplemented other cathodic reactions in the matrix. The balance of protection or corrosion was thought to be largely dependent on the environment. Turbulent or abrasive environments will reduce the protective capability and accelerate corrosion. The higher volume to surface area ratio of spheroidal graphite irons is believed to be the reason for their superiority in acid environments as this resulted in a smaller cathodic area[48].

Wesley, Copson and LaQue[49] have indicated the consequences of severe graphitic cast iron corrosion. When the ferrite matrix has been completely corroded a porous structure remains. This graphitised layer has very little strength and although showing no signs of degradation, may itself lead to failure. The surface area of the graphitised layer is large and is, therefore, an efficient cathode having noble electrode potentials (and low hydrogen overpotential).

Silicon containing irons of 14 to 18% have long been established as corrosion resistant irons and are standard for use with H_2SO_4. Graham et al[36] have shown that in concentrations normally encountered in cast irons, 1 to 3% silicon has an adverse effect on corrosion. The maximum effect was found at just over 2% Si and they recommended silicon levels below 1% for use in acid environments.

The corrosion resistance of the 14% silicon is due to the formation of a silica like oxide film. This is formed when the iron is leached from the surface leaving the cathodic silicon which forms a passive film when combined with oxygen. Graham et al[36] assumed that the lower silicon irons are not able to form protective films and at the critical composition, detrimentally influence the corrosion of cast iron.

2.4 MARINE DIESEL ENGINES

Diesel engines are widely used for propulsion in railway, automotive and marine applications. In addition, diesels are used as stationary engines supplementing national grid requirements. As might be expected a wide range of engines has developed to meet the needs of each application. Diesel engines may be loosely divided into four categories[50]:

Category	Slow Speed	Medium Speed	Med.High Speed	High Speed
Type	Crosshead	Trunk Piston	Trunk Piston	Trunk Piston
Cycle	2 stroke	2/4 stroke	2/4 stroke	2/4 stroke
Type of Aspiration	Pressure	Atmos./Press.	Atmos./Press.	Atmos./Press.
Engine Bhp	3000-48000	1000-20000	400-4000	> 800
R.P.M.	100 - 280	350 - 750	350 - 1800	1500 - 3000
Bore dia. (mm)	500 - 1050	254 - 520	200 - 280	100 - 178

Both slow and medium speed engines have found application in marine use.

Large slow speed engines are of a Crosshead design, with a bearing surface between the upper compression piston and the crankshaft. This Crosshead bearing may take the form of a second piston or slideway below the top piston. Its function is to ensure that the top piston does not tilt during the rotation of the crank. A gland or seal separates the cylinder from the Crosshead bearing. The lubrication of the upper cylinder is a total loss system. The oil is not circulated but the oil which is not burnt is collected when it drains to the bottom of the cylinder. The crankcase has a separate oil system.

Trunk piston engines are of conventional automobile design where the piston drives the crankshaft directly through a connecting rod. The lubricating system utilises a sump which continuously circulates oil round the cylinder and crankcase.

There has been an impressive increase in power output per cylinder of marine diesel engines since 1940 from 500 to 5000 bhp. This has been achieved mainly by improvements in pressure charging which has been made possible by significant development in materials, manufacture and design to overcome the mechanical and thermal stresses involved.

FUELS

The general requirements of a fuel for marine engine use are:-

1). Low initial boiling point.

2). High cetain number - short ignition delay.

3). Optimum viscosity.

4). Free from contamination.

5). No engine deposits after combustion.

6). Low cost.

The last requirement is often the overriding consideration and is the reason for the widespread use of residual fuels for marine engines. In fact there are no technical advantages in the use of residual fuels. The term residual fuel is used to describe the substance which remains after all useful fractions have been removed during refining of the crude oil. The residual component can amount to 10 to 40% of the refinery throughput and is usually sold as boiler fuel for less than the cost of the original crude oil. Not all marine engines operate on these residues; some use heavy distillate fuels called marine diesel which is more expensive, but does not have the problems associated with residual fuel. The quality of the residue is continually deteriorating due to improvements in distillation and particularly catalytic cracking techniques. One engine manufacturer[51] has found it necessary to specify an increase of 10 - 15° C in pre-injection fuel heating to compensate for deterioration in fuel viscosity. This trend in fuel deterioration is expected to continue into the 1980's with the prospect of reduced engine efficiency. Each fuel has different characteristics dependent on its area or origin. All the properties are important to engine operation[50]. The most significant for the purpose of this review is the sulphur content. The level of sulphur in residual fuels can be as high as 4% for Middle Eastern crudes, although some crudes notably the North African reserves, can contain down to 1.8% sulphur. In the early 1950's the majority of fuel was from Russia and North Africa, both low sulphur crudes. The increasing use of the vast Middle Eastern reserves has resulted in an increase of fuel sulphur levels since that time. It is well known that under certain conditions the sulphur can be converted to sulphuric acid in the combustion

chamber which gives rise to corrosion of rings and liners. These effects will be discussed in much greater detail in a later section.

LUBRICANTS

There are several general requirements of a cylinder lubricant

Primary - Control of wear, friction and surface damage.

Secondary - Scavenge heat, dirt and wear debris.

- Prevent corrosion.
- Transfer force and energy.
- Provide a gas seal.

The way in which these are tackled depends on the type of engine (crosshead or trunk piston) and also the properties of the fuel, particularly sulphur level.

LOW SPEED CROSSHEAD ENGINES

For the lubricant to be successful in the cylinder it must distribute itself over all the liner surface with sufficient alkalinity to ensure uniform protection against corrosion from the strong mineral acids in the cylinder. The alkalinity is measured by the total base number T.B.N. which is the equivalent in Mg of potassium hydroxide (KOH) present in 1g of oil, although calcium or barium based additives are most common. The analysis of lubrication by Hosie and Schrakamp[52] imagines that the piston spreads the droplets of oil fed into the cylinder very rapidly over the area above and below the supply points. The speed at which it is able to spread round the bore is much slower. They suggest that there may be sufficient time for the acid to completely neutralise the additives in the lubricant so that by the time the lubricant reaches the areas between the feed points it may be "chemically exhausted". Golothan[39] emphasises the need

for sufficiently high oil feed rates not only to ensure sufficient lubrication, but also sufficient additive levels over all the cylinder surface. The use of high feed rates to compensate for lower than adequate T.B.N., however, may lead to excessive deposits and piston ring sticking. It is quite common to find oil spreading grooves cut into the walls of the cylinder to assist in the distribution of the oil. It is generally accepted[38, 39, 37] that with current levels of sulphur in residual fuel, an oil with a T.B.N. of 60 - 70 is necessary for use in cylinders of crosshead engines. Cotti and Simonetti[38] point out however, that although the higher T.B.N. oils are capable of neutralising more acid and therefore result in a low wear rate, the high additive content may become incompatible with other engine factors. Cylinder lubricants also contain detergents to avoid deposits causing ring sticking etc., and dispersants to control the formation of sludge in the engine.

The crankcase system, separated from the cylinder by the crosshead seal, does not need such high alkalinity but does require resistance to water contamination to protect against bearing corrosion.

MEDIUM SPEED TRUNK PISTON ENGINES

Lubricants required for medium speed engines are different from crosshead lubricants. Some engine designs have separate oil feeds for cylinder and crankcase, but crankcase oils are often contaminated by oil drains from the cylinder. Many medium speed engines are not fitted with separate lubricators but depend entirely on splash lubrication. The lubricants therefore have to fulfil a dual function of crankcase and cylinder lubricant. In addition to efficient detergency and anti-oxidation properties,

the alkalinity control is especially important. The T.B.N. commences at 25 but rapidly falls to a steady equilibrium. Belcher[53] interprets this as a balance of the neutralisation of the additive and the condensation of the acid. The lubricant is consumed at a rate of 0.75% of fuel consumption and is replenished continuously with fresh oil of 20 - 30 T.B.N.

LUBRICATION

The lubricant in marine engine cylinders should fulfil several requirements:-

1). Provide an oil film to separate rings and liners over the whole length of the stroke.

2). Neutralise acid formed during combustion of residual fuels.

3). Remain stable to avoid the formation of products likely to contribute to wear.

The primary requirement is influenced by the speed, load and temperature conditions over the whole stroke. A useful indication of the influence of these variables on the lubrication of plane surfaces is given by the Stribeck Curve[54], which relates the Sommerfeld Number to the coefficient of friction (μ). (Fig. 1)

The Stribeck Curve may be divided into three areas. Boundary and hydrodynamic lubrication are the basic mechanisms and the transition area between the two is normally referred to as mixed lubrication.

The exact limits of boundary, mixed and hydrodynamic are rather vague. The literature suffers from a lack of an agreed definition of boundary lubrication. Lansdown and Hurricks[55]

describe boundary lubrication as

> "that type which occurs when the fluid film is insufficient to keep the solid bearing surfaces separated and interaction occurs between the asperities".

Boundary lubrication was thought to occur only where "asperities" are in contact.

Lubrication under these conditions does not depend on the bulk lubricant or material properties but on the surface and subsurface materials and the formation of molecular dimension films on the surfaces[27].

It is clear that the factors which promote the formation of a hydrodynamic lubrication film separating the surfaces are:-

1). High viscosity.

2). High sliding speed.

3). Low loads.

The conditions which are likely to produce boundary lubrication effects are opposite to those promoting hydrodynamic films. These are low viscosity, low speeds and high loads.

There have been numerous attempts to obtain information about lubrication in a running engine. The various approaches suggest a model which is supported by an elementary analysis of the Stribeck Curve.

Along the centre of the stroke the lubrication is predominantly hydrodynamic, i.e., the oil film thickness generated by

the "wedge" effect of the piston ring is greater than the asperity height. Hydrodynamic lubricant films are a result of pressure generated in the oil. This can be produced by a combination of wedge, squeeze and stretch effects (Fig 2). Friction may be attributed to the internal shear of the lubricant film. Towards Top Dead Centre (T.D.C.) and Bottom Dead Centre (B.D.C.) of the stroke the reduction in piston speed causes a decrease in the film thickness. At or just after T.D.C., where gas pressures and temperatures are at a maximum and the direction of ring travel changes, the reduction in film thickness can result in asperity contact. Friction is no longer caused by shear of the entrained film and is due to boundary contact (Fig 3).

2.5 OPERATING CONDITIONS

Successful operation of the marine diesel engine depends largly on the lubrication of the piston rings and cylinder liner. The model of lubrication outlined in the previous section is complicated in a marine engine by contamination from the air, fuel and wear debris. Without the correct maintenance of filters, air-borne abrasive particles can find their way into the combustion chamber. Particles of 1 μm are nearly always present in the atmosphere and particles of up to 200 um are not uncommon[56]. Abrasives resulting from the deposits remaining after incomplete combustion of poor quality fuels in addition to the debris produced by wear of the surfaces, can penetrate oil films and interfere with the efficiency of the lubricants in separating the moving surfaces. Particles generated between ring and liner were thought by Poppinga[57] to be in the range of 0.5 - 6 μm. In addition particles of less than 2 μm may be brought into the cylinder with the fuel as they are

normally outside the limit of fuel cleaning. Other products such as asphalt and carbonaceous matter can cause the formation of lacquers and carbon deposits which may result in excessive wear or even seizure through its effect on ring movement and lubrication. One further complication is that much of the abrasive, whether from combustion or wear, tends to be concentrated in the upper part of the cylinder where lubricant films are at their minimum thickness.

Although abrasive problems from the fuel can be reduced by filtration, vanadium in its organic form is completely soluble in oil. Vanadium contents of residual fuels are continually on the increase due to extensive "cracking" of the crude oil which concentrates the impurity in the residue. When reacted with sodium in the fuel from contamination with sea water, the product is extremely corrosive and can lead to catastrophic failure of valves in both 2 and 4 stroke designs. The effect can be minimised by temperature control of the susceptible areas of the engine.

Residual fuel has many characteristics which affect engine operation, at room temperature it is too viscous to use and has to be heated to around 90° C before injection. The presence of sulphur in the fuel leads to the formation of sulphur dioxide during combustion. Under certain conditions sulphur trioxide can form and condense as sulphuric acid which can corrode the liners and rings. The formation of this acid along with the presence of ash is one of the major factors influencing engine wear. In addition to the control of surface temperatures high enough to restrict the condensation, neutralising additives are incorporated into the cylinder lubricant. The high surface

temperatures involved can have a detrimental effect on lubricant viscosity.

In nearly all marine diesel engines which run on residual fuels the induction air is pressurised to 0.28 - 0.35 kg cm^{-2} to achieve high power outputs. For slow speed engines this raises the bmep to around 10 kg cm^{2} which can increase the power output by some 50% to 2500 - 4000 bhp per cylinder. Medium speed engines are pressurized from 1.8 - 2.1 kg cm^{-2} (around 16 - 18 kg cm^{-2} bmep) leading to outputs of 300 - 500 bhp per cylinder.

In addition to higher piston ring loads, modern engines have much higher thermal stresses imposed. Flame temperatures in excess of 1900^{o} C have been measured, while piston crown sub-surface temperatures have been measured up to 450^{o} C. Of the total amount of heat generated in the engine from combustion, 41% is used as work, 37% is lost through the heat contained in the exhaust gas, and 22% is dissipated by the cylinder components and oil system.

In summary, engines run on thick viscous residual fuels which contain most of the useless compounds from distillation. The combustion characteristics are far from ideal and often produce ash, deposits and potentially corrosive vapour. Poor fuels are counteracted by sophisticated lubricants but it is not always possible to achieve ideal lubrication over the whole of the liner surface. The lubricant, already working at its limits, has to contend with a wide size range of abrasives from fuel, air and wear debris in addition to the blow torch like effect of the combustion gases and high piston ring loads.

2.6 CORROSION USING RESIDUAL FUELS

Corrosion of cylinder liners and piston rings in engines running on residual fuels is a major feature of engine operation. The problem was first isolated in 1934 by Williams[58]. The theory was advanced that sulphuric acid bearing moisture was condensing on the cylinder walls causing corrosion at low temperatures. By 1938 Broeze and Gravesteyn[59] had concluded that contrary to popular belief, part of the fuel sulphur was oxidised to SO_3 during combustion. Some years later Cloud and Blackwood[60] reported that 60 - 90% of sulphur oxidised to SO_3, a figure which has not subsequently received much support. They did however, realise that SO_2 itself had little deleterious effect. The oxidation of SO_2, formed during combustion of sulphur containing fuels, to SO_3 has been suggested[61] as due to the direct reaction with atomic oxygen. Fursund[62] and Cotti and Simonetti[38] have shown the importance of vanadium pentoxide as a catalyst in the oxidation of SO_2 to SO_3. The proposed mechanism is:-

$$V_2O_5 + SO_2 \rightleftharpoons V_2O_4SO_3$$

$$V_2O_4SO_3 + \tfrac{1}{2}O_2 \rightleftharpoons V_2O_5 + SO_3$$

The importance of iron oxide as a catalyst has been demonstrated by Jenkinson[63], the reaction was thought to be:-

$$2Fe_2O_3 + 6SO_2 + 3O_2 \rightleftharpoons 2Fe_2(SO_4)3$$

$$2Fe_2(SO_4)3 \rightleftharpoons 2Fe_2O_3 + 6SO_3$$

Jenkinson[63] had reservations as to whether the latter reaction actually occurred. Both V_2O_5 and Fe_2O_3 are available in the combustion zone of the engine[38]. The tests he performed, however, demonstrated that at temperatures in excess of 700° C, further oxidation of $SO_2 \rightleftharpoons SO_3$ occurred rapidly. Laxton[64] showed that the percentage oxidation of $SO_2 \Longrightarrow SO_3$ increased as

the fuel sulphur content increased in the presence of excess oxygen (Fig. 4). Several authors[64, 61, 63] have referred to the importance of excess oxygen for the oxidation of sulphur to occur. Laxton[64] performed a series of tests in which he showed that with perfect mixing of the fuel and air, and stoichiometric conditions, no SO_3 was formed. He argued that products of incomplete combustion were either preferentially oxidised or any SO_3 which formed, was reduced back to SO_2.

Once the SO_3 has formed it will react with water vapour to form H_2SO_4 vapour. The reaction $SO_3 + H_2O \rightleftharpoons H_2SO_4$ will occur below 350° C[63], although the acid vapour does not itself cause serious corrosion problems. The acid will condense on any surface which is below the dew point. (Reverse of boiling point of a liquid).

Flint and Kear[65] found that the quantity of acid available for condensation increases with the difference in temperature between the dew point of the gas and the temperature of the surface and that the lower the surface temperature, the more dilute the acid(Fig. 5). The optimum conditions for acid condensation were found to be 25 to 40° C below the dew point, and concentration varied from 60 to 80% H_2SO_4.

The acid dew point is also dependent on pressure, Hoegh[66] calculated that at maximum cylinder pressure the dew point could be as high as 330° C. At this temperature acids of 95% concentration could condense. Golothan[36] has compiled a graph of acid dew point which takes into account cylinder pressure and SO_3 concentration through its dependence on fuel sulphur content (Fig. 6).

2.7 ENGINE WEAR

The mechanisms of wear which have been identified in marine diesel cylinders are abrasion, corrosion and scuffing[67,68,39]. The recent literature[67, 39] regards scuffing as the most detrimental form of wear, assuming that corrosion is controllable within tolerable limits. For the most part scuffing is regarded as a running-in phenomena which occurs before full fluid film lubrication has been achieved. Golothan[39], Langballe[69] and Wiborg[70] have all referred to an intermittent scuffing process which occurs during long term engine operation. (Fig. 7)

SCUFFING

Scuffing, which has been defined by the Institute of Mechanical Engineers (1957)[71] as:

"gross damage caused by the formation of local welds between the surfaces",

is not commonly encountered in practice[72]. When it occurs between liner and rings it often leads to increased gas blowby and oil consumption, which results in an appreciable loss of power.

The literature on marine diesel engine wear, in particular, is somewhat confused over what does and what does not constitute "scuffing". Identification depends largely on surface appearance. Neale[73] describes them as torn and smeared in the direction of motion in the cylinder. Rogers[74], on the other hand, describes scuffing as "dull vertical stripes" on the rings, while on liners, scuffing appears as "smooth bright stripes". These two examples illustrate the subjective nature of identification.

This has led to the wide use of the word scuffing to describe various types of surface damage not only on piston rings and cylinder liners, but also cams, tappets and gears. Out of

this confusion terms such as micro seizure , contact wear, frictional wear, and even micro-scuffing have appeared to describe scuffing type damage.

It is clear from the literature that very little is known about the mechanism of scuffing. Wiborg[70] as an example, describes scuffing as:

"a form of wear which is defined as the adhesion and successive shearing of junctions in metallic contact".

This much quoted view, proposed by Neale[73] in the early 1970's has not been significantly changed since. The large number of interacting factors, the dynamic nature of the process and the range of scuffing severity, appear to have confounded both experimental and theoretical research into the problem. A recent attempt by Shafia[75], however, concluded that in some cases adhesion plays no part in the process but proposed delamination as the mechanism responsible[29]. His results, however, far from indicating subsurface initiation of cracks, show plastic flow of the surface layers to form lamellæ, which are separated by extruded graphite from a flake structure. This type of plastic surface deformation was also recognised by Nadel and Eyre[67] who were able to identify transverse cracks in the flowed layers due to high surface stresses which could lead to delamination of the "plate-like" debris.

Aue[76] proposed that heat generated between the ring and liner surfaces by friction when the oil film breaks down, can cause local expansion of the surfaces. This in turn causes more contact and more heat to be generated. If the wear rate becomes greater than the surface expansion rate severe wear stops, if not scuffing will continue.

Neale[73] also believes that the generation of high local temperature plays an important role in the mechanism, whereas Nadel and Eyre[67] saw no indication of excessive surface heating in their examination of scuffed liner surfaces. In addition they could find no evidence of "white layer" formation on liners, although it is common on piston rings. Dyson[72] and others[68 73 70] however, identify the production of hard etch resistant phases on the surface of ferrous materials as characteristic of scuffing. These so called "white layers" are thought to play an influential part in severe wear. Wiborg et al[68] describe the layer itself as scuff-resistant, but prone to fracture and spalling from the surface. Due to its high hardness (up to 5 x bulk hardness) it can cause severe abrasion.

Although Rogers[24] has identified two different "white Layers" and Lazarendo[77] seven, these are likely to be different stages in the formation of a smaller number of types depending on both material and environment.

Phase transformation

1). Martensitic.

2). Austenitic - martensitic saturated with carbon and nigrogen.

3). Ferritic - austenitic.

4). Austenitic - martensitic and tempered martensite.

Phase formation

5). Ferritic - cementitic.

6). Chromium carbides.

7). Layers of precipitated non carbide forming elements (nickel).

(Lazarenko[77])

Dyson[72] acknowledges only one type, but sees its development passing through at least an austenitic phase at some stage.

There is sufficient contradictory evidence in the literature concerning scuffing of rings and liners to suggest that at least there is a progression through a range of scuffing severity and damage, but more important perhaps a number of separate mechanisms producing surfaces of similar appearance which are all identified as scuffed.

RUNNING-IN

The ring and liner are a unique bearing couple which has to perform under extremely arduous conditions. The eventual successful operation depends to a large extent on the lubrication conditions existing between the two surfaces.

In order to separate the ring and liner over the whole stroke with a hydrodynamic oil film, the ring has to have an optimum parabolic profile, the liner should be flat and smooth and an adequate supply of oil should be available over all the liner surface. The accommodation of the first two requisites is difficult (which means expensive), if not impossible to achieve during manufacture. It is fortunate therefore that the engine itself can be induced to do the job successfully.

Sreenath and Raman[78] found there to be two stages in the running-in of liner surfaces. While the engine is run at constant load and speed the asperities are mechanically removed as debris. When the load and speed are increased in steps, the remaining valleys are filled either by debris formed during the second stage or by production of surface films. Neither of the wear mechanisms were identified. Although running-in and long

term wear of liner and ring are synonymous, Sreenath and Raman[78] made no attempt to see how the piston rings changed during the liner running-in process.

Wakuri and Ono[79] examined this change in ring profile over the running-in period. They found that the ring profile is formed by the removal of metal from the ring edges, due to interaction with the liner, as the ring tilted during the stroke.

Neale[80] distinguished four effects contributing to the change in ring attitude to the liner:-

1). Piston tilt.

2). Thermal distortion of the piston.

3). Thermal and pressure distortion of the cylinder.

4). Groove bias (ring movement in the groove and deformation of the groove).

The combination of these effects results in the removal of material from the edges of the ring face to form a large upper arc and a smaller lower arc (Fig. 8).

Many authors[39, 79, 26] have stressed the vulnerability of the engine to the onset of abnormal wear during running-in. Due to the roughness of the original liner surface, which is necessary to shape the ring to the correct profile, metal to metal contact at asperities is inevitable. Wiborg et al[68] believed that once the oil film had been disrupted and rubbing destroyed any protective surface layers, adhesion could occur between the asperities. Adhesion is regarded by Eyre[26] as the predominant wear mechanism during running-in. It is also thought to occur during start up and load changes where surface contact occurs[80]. Measurements of oil film thicknesses in a 4-stroke diesel engine have been made by Moore and Hamilton[81] who found that up to a period of

27 hours running at low loads, metal to metal contact occurred between liner and ring, particularly on the compression and firing stroke just after T.D.C. At higher loads contact still occurred after 62 hours running.

Wakuri and Ono[79] found that if during this time excessive edge loading occurred, scuffing could be initiated. Once a scuff had occurred it was thought to produce large wear particles, which would break through the partially formed hydrodynamic oil film and abrade away the centre of the ring profile (Fig. 9).

There are several question marks against this proposed mechanism:

1). Scuffed surfaces appear smeared and torn[73, 74, 72] and are expected to produce flat plate-like debris, not large abrasive particles[67, 75].

2). When scuffing occurs it would be expected to affect both liner and ring.

3). There does not appear to be any reason why the ring should stop tilting to remove the edge loading condition and allow the centre of the ring to wear flat.

It is possible, however, that the generation of heat at the scuffed surface could influence the ring tilting conditions by distortion of the ring and/or piston groove. Their results clearly indicate, however, that a flat profile was formed on the ring which would reduce its effectiveness to form a hydrodynamic wedge. The factors which influenced the onset of abnormal wear were found to be:

1). Availability of lubricant on the surface.

2). Spreadability of lubricant.

3). Original ring profile.

The first, they identified to be a characteristic of the liner topography. They concluded that lubricant dispersed over the liner surface encouraged both squeeze and wedge hydrodynamic effects, which separated the ring and liner, avoiding scuffing. It is possible that the presence of dispersed lubricant would contaminate the surfaces to avoid substantial adhesion between the ring and liner and reduce the possibility of widespread scuffing.

Spreadability of the lubricant was thought to govern the rate at which the oil film recovered after rupture. At high temperatures alkaline oil additives were found to reduce spreadability. Other Japanese workers[82] have found this to be due to the formation of sludge. The original ring profile was found to be important in that by using either tapered or barrelled rings, the likelihood of critical edge loading could be reduced.

Severe abnormal wear during running-in is rare, normally if an engine is prone to scuffing, it is detected during development and can be eliminated by changes in design. Abnormal wear is not, however, confined to running-in. Neale[73] estimated that about 4% of scuffing incidents occurred after running-in. Langballe[69] plotted frequent liner wear measurements taken over an 18 month span to identify a series of high wear periods (4 mm/1000 h) interspersed by spells of low wear (0.1 mm/1000 h) in some cylinders. The average wear rate over a period of discontinuous wear was found to be within acceptable limits (0.27 mm/1000 h) and would be missed were it not for semi-

continuous monitoring. The abnormal wear periods he found to coincide with increases in piston ring zone temperatures from 120 - 150° C up to 250 - 300° C. Langballe[69] did not clearly identify whether the high temperatures were the results or the cause of the high wear rates.

This work was continued by Wiborg, Erikson and Tjaernes[68] who were able to identify a simultaneous increase in wear and temperature. Gas blowby was thought to cause the destruction of the oil film which resulted in a higher wear rate.

Neale[73] refers to the fact that large bore engines were not considered to suffer from scuffing, contrary to the work at Det Norske Veritas[68]. He does, however, recognise that if fairly high rates of wear are acceptable then occasional scuffing problems may not be noticed. The occurrence of the discontinuous abnormal wear in the form of scuffing and self-healing may be more widespread than traditionally believed in the long term wear behaviour of rings and liners.

LONG TERM WEAR

For engines with acceptable wear rates Nadel and Eyre[67], in their survey of a large number of liners, found evidence of abrasion and corrosion. Abrasion was thought to be responsible for normal mechanical wear, although corrosion could indirectly lead to intensification of abrasion. This interaction of corrosion and abrasion has also been referred to by Cotti and Simonetti[38] and McConnel and Nathan[83].

McConnel and Nathan[83] thought that corrosion controlled wear because it weakens the matrix making possible the production of increased quantities of the abrasive material. Cotti and Simonetti[38] put less emphasis on the importance of corrosion in the mechanism.

".....Mechanical friction between the surfaces of piston ring and cylinder liner causes detachments of the matter resulting from corrosion, thus increasing the quantity of abrasive products and the roughness of the surface and consequently wear".

Fursund[62] on the other hand, thought abrasion to be dominant, due to the removal of corrosion products which exposed fresh material to attack by the acid.

Nadel and Eyre[67] identified the positions on a liner of a low wear rate engine where the mechanisms of wear occurred. Abrasion, they judged to predominate at the top and bottom of the stroke, but more severe at the top where hard phases stood in relief above the matrix. This was thought to be due to a differential wear mechanism. Abrasion at the bottom of the stroke was found not to have removed all the original machining marks. At the mid position they found no abrasion evidence, although corrosion in the form of widespread etching of the material structure was identified.

Boerlage and Gravesteyn[59] were able to measure the effect that fuel sulphur content has on cylinder liner wear. Below about 1.0% sulphur in the fuel has only a very limited effect. Wear increases rapidly however, at higher sulphur levels (Fig.10)

The effect of sulphur on ring wear has been shown by Graham et al[36] using a small four stroke engine, running on residual fuel (Fig. 11). The piston ring wear rate, with a 1.95% sulphur fuel, was found to be five times greater than for a 0.1% low sulphur fuel under the same test procedure. These results do not separate the corrosive effect from other effects induced by sulphur in the fuel. Du Jue[84], using a 80 mm bore

crosshead engine, which he found to correlate very well with wear of large marine engines, investigated the effect of additives on ring wear. From his results it is possible to see the effect of corrosion in the cylinder on the wear of the top ring (Fig. 12). As the alkalinity in the oil increases, the amount of acid available for corrosion decreases, which results in a rapid decrease in top ring radial wear. Du Jue[84] also achieved results similar to Boerlage and Gravesteyn[59] but over a larger sulphur range and including quantitative wear rates (Fig. 13).

WEAR IN DIFFERENT POSITIONS

Golothan[39] found maximum wear to occur at, or just below, the top of ring travel, the lowest wear around the middle of the cylinder and a small increase in wear at the bottom of ring travel. The maximum wear at T.D.C. he thought to be due to a combination of corrosion and wear arising from the breakdown of the oil film due to high gas pressures and high cylinder temperatures which led to oil films with low viscosity.

Dent[85] saw the two mechanisms of abrasion and corrosion combining to give a wear profile with two peaks. A peak at, or just below T.D.C. due to a predominantly abrasive mechanism, and an increase in wear at the middle of the stroke, due predominantly to the action of acid. The minimum wear was thought to occur at B.D.C. (Fig. 14). This view appears to be confirmed by the evidence presented by Nadel and Eyre[67].

Dent[85] considered the abrasion to be directly related to the pressure in the cylinder which is maximum just below T.D.C. and gradually declines to B.D.C. This seems to be rather

simplistic view as the load on the abrasive is not from the gas pressure directly, but through the piston ring which is separated from the liner by an oil film of variable thickness. It is more likely that it is the oil film thickness which governs abrasive damage. When the oil film is thinnest the range of abrasive particle sizes which can cause damage is greater than when the oil film is at its maximum. Neale[80] has shown that the oil film thickness typically reaches a minimum value just after T.D.C. but increases sharply through the centre of the stroke to decrease again just after B.D.C. The analysis takes into account gas pressure, temperature, piston speed and ring geometry (Fig. 3).

From this it might be expected that abrasive wear is maximum just after T.D.C., minimum along the centre of the stroke but increases slightly just before B.D.C. Cotti and Simonetti[38] also relate maximum pressure with maximum mechanical wear but found that the position of greatest wear did not coincide with the highest gas pressure (Fig. 15). It should be emphasised however, that the postion of minimum oil film thickness does not necessarily occur at maximum pressure but is determined by the fluid dynamics of ring lubrication and is likely to vary from engine to engine. Cotti and Simonetti[38] were forced to conclude that the peak in cylinder wear just below T.D.C. was due to the dominance of a corrosive mechanism.

An aspect of abrasive wear in engines which has received no attention in the literature is the importance of the distribution of abrasive particles over the liner surface. It is likely that there would be a higher concentration of abrasive debris around the position of maximum wear which may coincide

with the minimum oil film thickness. The generation of debris at this point would tend to accelerate abrasive damage. The distribution of abrasives from induction and combustion may also be important.

Work by Price et al and reported by Dent[85] has theoretically predicted a profile of corrosion potential down the liner (Fig. 14). The probability of maximum acid corrosive effect, taking into account concentration and volume effects, was found to be just above the mid-stroke position. Cotti and Simonetti[38] were able to plot corrosion potential down the liner surface for a 3% sulphur residual fuel (Fig. 15).

Over a range of engine cooling conditions which gave maximum cylinder liner temperatures of 150° C to 225° C, the greatest corrosion potential for each condition was in the top third of the stroke. This corrosion peak was thought to be responsible for the increase in wear towards the top of the stroke. The possibility that acid formed on the cooler areas of the liner could be transported by the action of the ring to cause corrosion in other areas was forwarded by Golothan[39].

Hosie and Schrakamp[52] reported that one of the main functions of the lubricant was to transport neutralising additive to ensure uniform protection against corrosive attack. Due to the rate of chemical neutralisation of the lubricant additive, they found that by the time the lubricant had reached some areas of the cylinder liner it could be chemically exhausted. Corrosion of these areas would then occur.

It has not been possible from examination of worn components to identify areas of maximum corrosive potential owing to the superimpcsed effect of abrasion, which often obscures corrosive

damage. Dent[85] has argued that the balance between corrosion and abrasion over the whole liner, but particularly along the centre of the stroke, is so fine that one could easily be shifted to appear dominant over the other. The balance was thought to vary not only over the liner surface but also during the life of the liner and rings.

In spite of the fact that it is the wear of the piston ring which is the cause for most concern[37], very little attention has been given to the wear mechanisms which occur on the rings of engines running on residual fuels. Eyre, Dent and Dale[86], based on examination of rings taken from marine engines, found evidence of scuffing and abrasion. They did not discount the possiblity that corrosion occurred but thought that because rings are subject to abrasive conditions at top and bottom of the stroke, any evidence would be masked by abrasion. That ring wear increases in corrosive environments has been established[37, 86], but evidence of corrosion on the ring rubbing face is rare. McConnell and Nathan[83] found that although the ring surfaces were heavily abraded, irregularities within the grooves were evidence of corrosive action.

It is clear from the literature that the prediction of corrosive action is inaccurate. This is due in part to variation in cooling conditions, fuel sulphur levels, lubricant supply and T.B.N. and engine loads, which can and do vary from engine to engine and cylinder to cylinder over a period of time. All these variables either directly or indirectly affect corrosive attack.

The evaluation of worn components is made difficult by the complex interaction of abrasion and corrosion which can produce surfaces which appear to have been affected by only one mechanism.

3. EXPERIMENTAL

3.1 CORROSION TESTS

Originally this test was designed to examine the neutralising characteristics of lubricants in an acid environment containing ground cast iron particles. It has been used, however, to evaluate corrosion of several ferrous materials under acidified conditions with standard lubricants. Cast iron specimens, sealed in a reaction flask, are reacted in a controlled acid environment to enable determination of reaction rate and examination of corrosion effects.

EQUIPMENT

A conical glass flask modified to provide a side arm with a replaceable self-sealing PTFE/Rubber Septum was connected to a pressure transducer through a gas tight joint held by two springs (Fig. 16). A three-way valve was incorporated between the transducer and flask to allow the system to be brought to atmospheric pressure as and when required. The flask was immersed in a stirred water bath, maintained at a constant temperature, which sat on a magnetic stirrer to couple with the specimens inside the flask. Gas pressure in the flask was continuously recorded on a chart recorder connected to the pressure transducer.

PROCEDURE

Two series of tests have been run on the equipment; firstly to examine three different grey cast irons at different temperatures. Secondly, five ferrous metals were evaluated for identical test conditions. Differences in procedure are discussed where they are applicable.

FIRST SERIES

Cast iron samples were cut and ground on each face to a 600# finish on wet abrasive papers to a finished size of 3 x 0.4 x 0.4 cm. Analysis and microstructures of the specimens are given in Table 17 and Fig. 18 . Each specimen was degreased and weighed before it was placed in a clean conical flask with a 10 g sample of lubricant A. A 70 T.B.N. oil with a viscosity of 17.0Cs was used for the tests. After sealing the joint with silicone grease, the flask was immersed in the water bath and left for the temperature to stabilize. During this time the specimen was rotated via a magnetic stirrer at a slow speed. Once the system had attained the bath temperature, 0.44 ml of 40% sulphuric acid was injected slowly through the self-sealing septum into the oil. Acid volume was determined as just sufficient to neutralise the basicity of the lubricant. Gas samples were syringed through the septum at intervals throughout the test and analysed for hydrogen in a gas chromatrograph. When the transduer sensed no further increase in gas reaction pressure, and the hydrogen content showed no further increase, the tests were stopped. Tests were repeated for each of the three cast irons at 40, 60, 80 and 100° C.

SECOND SERIES

Three different grey cast irons and two 0.8% C steels, one of which was normalised and the other in a hardened condition, were examined at a temperature of 60° C. Acid conditions were as for the previous cast iron tests, although the oil used had a 25 T.B.N. with a viscosity of 14.45 Cs. In the second series only the final hydrogen content was measured when the reaction pressure reached a maximum. Each of the test conditions

was repeated to obtain reproducible results.

When the corrosion reactions were complete, pressure was reduced and the metal specimens removed. These were degreased using white spirit and acetone before ultrasonic cleaning in warm water to remove any remaining reaction products. Finally the specimens were re-weighed and stored in a dessicator prior to further examination. Surfaces of the corroded specimens were examined in an electron microscope, E.P.M.A. was used to examine selected areas in more detail.

3.2 RECIPROCATING WEAR RIG

A reciprocating wear rig has been designed and manufactured in which both abrasive and corrosive wear mechanisms can be produced (Fig.19 a+b). Essentially, the rig reciprocated a flat plate under a loaded pin. The plate was fastened to the base of a stainless steel bath by two brass screws through holes at either end of the specimen (Fig. 20). This bath was fixed to a cast iron platform which reciprocated on two guides acting as bearing surfaces, lubricated through grease nipples in the platform. Reciprocation was achieved by linking one end of the platform to a rotating spindle with a connecting rod. The rod was fixed by screws which clamped through the centre of ballraces housed at either end of the rod which were free to rotate. The amplitude of reciprocation was selected by positioning the connecting rod in one of several positions at different radii from the centre of the spindle. This spindle was driven by a variable speed 1½ h.p. Kopp motor geared to give a speed range of 8.3 to 70 r.p.m.

A pin specimen, fixed in a lever arm, was normal to the

plate surface (Fig. 20). As this pin was fixed one third the distance along the arm from the pivoted end, which allowed both vertical and horizontal movement, a 3:1 advantage of the suspended load was gained at the pin/plate interface. Horizontal movement of the arm was restricted by a force post which was deformed elastically by transmitted forces resulting from the friction interaction between pin and plate. Friction force was measured in only one direction, movement in the other direction was damped by an adjustable stop. Horizontal deflection of the force post and vertical displacement of the arm representing combined wear of the pin and plate materials were measured by low voltage displacement transducers.

Lubricant was circulated through the stainless steel bath from an insulated glass reservoir by a peristaltic pump delivering up to 94 ml min^{-1}, depending on oil viscosity (Fig. 21). An in line mixing unit was included in the system which was designed to break up acid droplets in the lubricant stream. This consisted of a P.T.F.E. covered magnetic couple inside a sealed circular glass container with an inlet at the bottom and outlet at the top (Fig. 22), which was driven externally by a rotating magnetic head.

Lubricant temperature was closely controlled from two heat sources. Reservoir oil temperature was controlled from a thermocouple implanted in the tube which measured the temperature just before entering the bath. Bath and plate specimens were heated by three cartridge heaters located in the platform, controlled by a thermocouple between the bath and platform, maintaining oil at the required temperature inside the bath. This temperature was monitored by a thermocouple in the oil

which was displayed as a digital output and, after amplification, recorded one of three chart channels for the whole of the test. Two other channels on this chart recorded the amplified force and displacement signals from the two rig transducers.

SPECIMEN PREPARATION

Pin and plate specimens were machined from standard cast irons in addition to piston rings and cylinder liner components used in the Abingdon B1 test engine[87]. 25 mm curved lengths cut from the ring radius were milled to straight square sections. One end of the pin was turned to 1 mm diameter for a length of 3 mm using a 1 mm radius round nosed tool. After the specimens had been cut to length, they were ground to the final surface finish and length in a jig using new 300# wet abrasive papers so that abrasive grooves ran parallel to one of the sides of the pin. The specimens were then thoroughly cleaned in an ultrasonic bath, degreased and stored in a dessicator until required. Plate material was cut from the wall of a cylinder liner and milled roughly to shape. Holes were accurately drilled at each end of the plate with the aid of a jig. Finally the surfaces were ground using a freshly prepared wheel on a horizontal grinding machine. The lay of the final surface to be tested was orientated so that the grooves were 45° to the intended direction of rubbing.

CALIBRATION

Before testing commenced the two transducers measuring the vertical arm displacement and deflection of the force post were calibrated over the linear portion of their output. Amplification was set for each signal to give a known displacement

on the chart recorder from which measurements of wear and frictional force could be taken after the test. These amplification settings were checked periodically through the test programme to maintain reproducibility. Kopp motor variable speed settings were callibrated against the final spindle speeds using a stroboscope. All the thermocouples were checked against each other over the range of intended temperature use. The lever arm was balanced with counterbalance weights to give zero load on the pin when only the load pan was suspended from the arm.

TEST PROCEDURE

At the beginning of a test cycle a prepared flat plate specimen was clamped into the stainless steel bath using two brass screws. Inside the bath, specimen and thermocouples were coated in protective lacquer and allowed to dry. The pin, clamped into a pin holder was fixed into the lever arm so that the grinding grooves ran transverse to the direction of sliding. Lacquer was also used to coat the sides of the pin. The lever arm was then brought down between the friction post and stop so that pin and plate specimens were in contact. Using the threaded adjustable stop, the arm was raised so that there was a 0.5 - 1.0 mm gap between the pin and plate before the load was suspended from the end of the lever arm. It was sometimes necessary to adjust the postion of the vertical displacement transducer, although the specimen length was controlled within fine limits because the transducer position did not coincide with the pin position. This meant that the transducer output varied with elastic deformation of the lever arm resulting from the large suspended loads.

300 ml of fresh lubricant was preheated to 80° C before being pumped through the system to fill the oil bath. Once a constant bath temperature of 80° C had been maintained for thirty minutes, the Kopp motor was started and the pin lowered onto the plate specimen. A gap of 1 mm was left between the vertical arm stop and the arm to avoid excessive damage if the pin fractured. During the time taken for the bath temperature to reach equilibrium the chart recorder was allowed to warm up and was set to run at 10 mm min^{-1}. Both the in-line mixing unit and oil reservoir stirrer were started at this time which then ran throughout the test. Wear and friction transducer outputs and bath temperature were continuously monitored on the three channel chart recorder. Tests were allowed to run under set conditions for several hours to allow steady state wear to stabilize between the specimens. This time was determined as the maximum time for the surfaces to run-in which was monitored by the change in friction and wear over the length of the test.

In the tests where acid was added, the run-in condition was allowed to occur before the environment was changed. Acid was added when the pin had been raised from the specimen and the motor stopped. After the peristaltic pump was switched off, 6 ml of 20% H_2SO_4 were slowly added to the reservoir whilst being continuously stirred. Before the motor was started, the pin was lowered onto the plate lubricated by oil remaining in the bath, and the pump turned on, to reciculate the acidified lubricant. Tests were then run for the desired time, before the specimens were removed.

In order to remove the specimens from the rig as quickly

as possible, the following procedure was followed. Before stopping the motor, the vertical displacement transducer support was removed and the pin lifted from the plate with the vertical stop adjustor. The peristaltic pump was reversed to remove the oil in the bath which was then flushed with 70 T.B.N. oil to neutralise the remaining acid. When the motor was switched off, pin and plate specimens were removed and thoroughly cleaned. The worn specimens were stored under a 70 T.B.N. additive oil until they were examined.

After each test the bath and tubing were flushed with white spirit and acetone before re-use to remove all traces of oil and debris.

EXAMINATION OF WORN SURFACES

Before wear surfaces were examined they were ultrasonicly cleaned in white spirit and then alcohol, to remove all traces of oil. The main tool for surface examination was scanning electron microscopy (S.E.M.) which allows a depth of focus superior to optical examination. Both pin and plate specimens were examined in the microscope before sectioning. In addition to routine surface examination areas of interest were analysed using energy dispersive X-ray analysis (E.P.M.A.).

Films formed on the specimen surface in unacidified conditions using base oils have been examined by both wavelength dispersive X-ray analysis and X-ray photoelectron spectroscopy (XPS) or E.S.C.A. For the XPS analysis small sections of wear track were carefully removed from the specimens and comparisons made with similar size areas cut from the same plate away from the wear track. Several taper sections were made of pin and plate to examine surface and

subsurface effects. The angle of section was $11\frac{1}{2}^{o}$ to the surface which introduces a factor of 5x when linear measurements are made.

3.3 PETTER TESTS

EQUIPMENT

Two fuels, one a distillate type containing 0.1% S and the other doped to contain 3.5% sulphur have been run in a converted Petter AV-1 single cylinder diesel engine. Conversion of the engine included provision of a second piston in a separate cylinder above the normal piston. The bottom piston acts as a crosshead bearing with the top one as the working piston. A spacing block between the upper and lower cylinder was designed to include trays to collect oil drains from the upper cylinder. This enabled a radioactive top piston ring to be used so that oil samples containing radioactive debris could be collected at different time intervals.

A brake was connected to the engine output to allow loads to be applied. Various thermocouples were used to monitor the cooling water and crankcase oil temperatures.

PROCEDURE

Two periods of 144 hours were run on the engine, changing only fuel sulphur level. Each test began with new rings and cylinder liners which were run in for the first 24 hours of the test under standard conditions. The converted engine (Petter RA-3) had already completed several hundred hours running and was itself considered to be running under equilibrium conditions. Running-in of the new liner and rings was according to conditions set out in Table 23. After 24 hours, the upper cylinders were dismantled in order to take replicas of the ring and liners. When reassembled, the engine was run

under the normal test conditions outlined in Table 24. Oil trays were removed and the drains collected at intervals during the test (Table 25). Two sets of trays were available so that each could be completely cleaned while the other was in the engine.

At the end of the test period, replicas of the rings and liners were made and profile traces of the liner taken. An S.E.M. examination was carried out on the second rings and sections of the liner taken from the top, middle and bottom of the stroke for both tests along with coated replicas taken before the test and after 24 hours running. Collected oil samples were comprehensively analysed by three techniques;

1). Radioactive detection.

2). Ferrography.

3). Chemical analysis.

4. RESULTS

4.1 CORROSION TESTS

FIRST SERIES

Three grey cast irons of different compositions were exposed to a mixture of additive lubricant and sulphuric acid in a sealed container. The hydrogen content of the reaction gas, measured at intervals throughout the test has been plotted against the time of the sample for different temperatures (Fig. 26). For all the irons the rate of acid attack increased with temperature although the degree of corrosion decreased. The rate of acid neutralisation by the alkaline additions in the oil must also have increased to have an overriding effect as temperature was increased to 100° C.

The total amount of corrosion on each of the three irons was similar through the range of temperatures (Fig. 27). Sample B, the high copper iron, was marginally inferior but the difference was small compared to the effect of temperature.

Examination of the corroded surfaces of the three specimens revealed identical features although the scale of the effects depended on their microstructure. The original surface of the corrosion specimens type B showed evidence of graphite flakes through the grinding marks (Fig. 28). Areas on the specimens surface were identified where corrosion was centred around graphite flakes (Fig. 29). Corrosion of the pearlitic matrix had left unsupported cementite wafers where the ferrite lamellae had been removed (Fig. 30). It was clear that the unsupported cementite wafers did not extend to the original surface level, they are either broken off by the stirring action inside the reaction flask or during the cleaning procedure. Phosphide

eutectic appeared to be unattacked by the acid. Fig. 31 shows one such area which is confirmed as a phosphide by an X-ray dot image (Fig. 32). Even after ultrasonic cleaning of the specimens, areas of a sulphur based deposit were found (Figs. 33 and 34). Straight sections through the surface of type A and C confirmed that the phosphide eutectic was unattacked and remained at the original surface level of the specimen (Figs. 35 and 36).

SECOND SERIES

The total amount of corrosion on five irons with significant variation in composition and structure is given for a single temperature in Table 37 . Microstructures and analyses for the irons are shown in Fig. 18 and Table 17 respectively. Total corrosion of the petter cylinder liner material was found to be over seven times greater than that of the normalised and heat treated 0.8% C steels but corrosion on the two grey cast irons, although similar, was only twice that of the steels.

Stimulation of corrosion by graphite flakes was seen clearly on the petter material surface (Fig. 38). In addition, the lack of attack on the phosphide eutectic was evident (Figs. 39 and 40). Fig. 39 also shows evidence of a film formed on some of the specimen surface. Although bulk phosphide eutectic appeared unattacked, the internal structure of the phase was corroded (Fig 41).

Areas of the surface of type E grey cast iron were covered by a surface film but this was not as widespread on type D. This film appeared to be formed only on the ferrous areas and did not cover the graphite flakes. More severe corrosion was found in these unprotected areas (Fig. 42). The corrosion

of the low copper iron (type E) was more uniform and clearly showed the cementite wafers remaining from corrosion of the pearlite on the surface (Fig. 43).

Corrosion on both the steel surfaces was influenced by surface films. In the case of the martensitic structure corrosion formed pits in the surface and no discernable structure was revealed (Fig. 44). The surface of the fully pearlitic steel also appeared to be covered by a film (Fig. 45).

4.2 WEAR RIG

The results of the work from the reciprocating wear rig have been divided into three sections:

Wear Results

Friction Behaviour

Wear Surfaces

WEAR RESULTS

The vertical movement of the lever arm on the wear rig (Fig. 19) as measured by a displacement transducer was recorded along with both temperature and frictional force using a three channel chart recorder for the duration of the test. A section of this chart is shown in Fig. 46 . As the rate of change of wear was small, it proved impossible to separate running-in portions of the wear from equilibrium wear behaviour. Accordingly both wear and frictional force were plotted for the test duration on graphs with a much compressed time scale using values taken from the original chart (Fig. 47).

The running-in and equilibrium wear portions were then easily identified so that equilibrium wear rates could be calculated. These wear rates, calculated as a total volume of material removed from both pin and plate expressed in mm^3 per mm

of relative sliding of pin over plate are shown in Fig. 48 for several unacidified conditions.

The change in wear rate over the range of loads tested was similar in all cases. The curves exhibit a roughly exponential increase in wear rate as the load increased up to 150 kg (191 kg mm^{-2} pressure). At loads in excess of 150 kg, plastic deformation and eventual fracture along the graphite flakes of the grey cast iron pin occurred before equilibreum wear behaviour could be established.

Two lubricants, a fully formulated additive marine diesel lubricant and a non-additive base oil, which was later used in acidified tests, were compared. Differences between the oils, although negligible at the lower test loads were quite marked at the other extreme of load conditions, where an increased dependence on boundary lubrication properties would be expected.

A comparison can also be made to determine the effect of oil type on the wear rate of alloy cast iron plate at a higher speed of 45 mm^{-1} and at 80° C. In this case wear rates for 120 kg load are available which show a reduced equilibrium wear rate for the test using the additive oil.

Comparison was made between a grey cast iron and an alloy containing hard phase, worn against the same pin material with identical oil, speed and temperature conditions. The alloy cast iron proved to be superior over the whole range of loads.

A lower wear rate was found when the oil bath temperature was reduced form 90° to 80° C for the alloy plate material using base oil.

When all the unacidified wear results are compared at a load of 120 kg (153 kg mm^{-2} pressure) and the results calculated

as a percentage of the worst wear condition, the effect of the variables can be identified more clearly (Table 49). The worst set of conditions were a mean speed of 43 mms^{-1} at 90° C using the base oil and a plain grey cast iron plate. At a lower temperature and mean speed of 80° C and 7.8 mms^{-1} the wear was improved by 29% for the same material although the fully pearlitic (steel) plate, for identical conditions had a higher percentage wear. The best plate material for these conditions was an alloy cast iron which was marginally superior to the cast iron with no bulk hard phase content. The disadvantage of plain grey cast iron was offset by the use of additive oil at 80° C and a mean speed of 7.8 mms^{-1} when compared to an alloy cast iron plate using a base oil lubricant.

With only 25% of the worst wear condition, the lowest wear was for an alloy cast iron plate at a speed of 43 mms^{-1} and 80° C using the base oil. An increase in temperature to 90° C produced a higher wear of 45% of the worst condition.

Wear rig results showed that the design and test procedure were sufficiently sensitive to measure the modification in wear rate corresponding to small changes in operating conditions.

For acidified test conditions a load of 120 kg (153 kg mm^{-2} pressure) was adopted in addition to the use of base oil throughout. This oil was selected to isolate the mechanism of metallic corrosion from the competing reaction of the lubricant alkaline additives with the acid. Several tests were run to determine the acid conditions necessary to achieve the type of damage found on marine diesel liners. Additions of 2% of total oil volume of 20% sulphuric acid were made to the oil reservoir after a period of running-in and equilibrium wear had elapsed.

When the acid was added the wear rapidly increased for a number of passes before a reduction occurred to a wear rate less than the unacidified equlibrium rate (Fig. 50). Coincidental with this changing wear rate, was an immediate increase and subsequent reduction in friction (Fig. 50).

FRICTION RESULTS

The frictional force between the pin and plate, transmitted through the lever arm acts against an elastically deformpost. Movement of this post was monitored by an L.V.D.T. In this way the frictional force could be monitored along the stroke length. Although a continuous record of this force was retained on a test chart (Fig. 46), a storage oscilloscope was also used to retain some of the force traces over the length of one pass. The stored traces could then be transferred to chart paper at a slow enough speed to ensure that the response of the recorder was not responsible for losing any relevant information (Fig. 51).

Although no two traces gave identical friction responses, despite close control of surface preparation, they all showed two main levels of friction. A maximum friction force was encountered at the end of the stroke while a minimum force occured along the centre. In most cases an intermediate force was found at the beginning of the stroke. The apparently different forces at each end were a consequence of the rig design. When friction was measured by an additional pillar on the opposite side of the lever arm, similar levels of friction were found at each end of the stroke (Fig. 52). The friction force measured between the pin and plate of unlubricated tests run at room temperature on the same rig did not show a similar

increase at the end of the stroke (Fig. 53).

The calculated end and mid-stroke friction coefficients which correspond to the maximum and minimum forces along the stroke for base and additive oils are given in Fig 54 .

The coefficient of friction was calculated by the simple formula:-

$\mu = \frac{F}{L}$ where μ = coefficient of friction

F = frictional force

L = normal load

End-stroke coefficient of friction was found to be greater for the base oil than for the additive lubricant but mid-stroke friction for both oils was similar. It was found that while the frictional force increased as the normal load increased the coefficient of friction decreased. Confirmation of this reduction in the friction coefficient as the load increased is clearly demonstrated in Fig. 54 . Friction force was measured, after a period of stabilisation, as the load was incrementally increased from 15 to 105 kg in the same test using a base oil lubricant. This feature was also found for a limited number of unlubricated tests which were run at room temperature (Fig. 55)

Addition of acid to the system to simulate the corrosive effect of condensed sulphuric acid on marine cylinder liners and piston rings modified the friction response over the stroke. An initial increase in friction at the end of the stroke as the acidified lubricant entered the oil bath may have been due to a change in the oil viscosity (Fig. 50). A small increase in mid-stroke friction also occurred. Friction at the end of the track subsequently reduced to a level similar to that along the middle of the stroke over a period of around 40 minutes running

(approximately 650 passes). This end stroke friction slowly increased again after a further 40 minutes running, and after several hours reached levels similar to those before acid had been added.

A series of oscilloscope traces, taken from a typical test give a clear picture of changes which occurred as acid was added to the system (Fig 56). The peaks at the end of the stroke decreased while the centre of the stroke appeared unaffected. As the test proceeded the end stroke friction was found to decrease below the mid point level but finally showed signs of increasing again.

WORN SURFACES

In the unacidified tests there was very little difference between the tests run at high and low loads. At low magnification all the plate surfaces appeared rough, with parallel grooves running the length of the track (Fig 57). Examination at higher magnification revealed that on a micro scale the plate surfaces were very smooth (Fig 58). Fig 58 also showed evidence of cracking on the surface of the plain grey cast iron plate material which was later found to be the result of the original graphite flake structure. Sections taken through the track showed the graphite to have been closed up by the deformation on the surface (Fig 59). This effect could be identified, to a lesser extent, away from the track resulting from the original griding operation (Fig 60)

The pin wear surfaces also contained grooves (Fig 61), but on a finer scale these surfaces were very smooth and showed evidence of a differential wear mechanism on the constituent phases (Fig 62). In the

tests where alloy cast iron plate material was used, which contained a significant volume of hard phase, no evidence of differential wear could be identified. This may have been due to a difference in abrasive wear intensity on the pin and plate material. The length of the track on the plate was 27 times the diameter of the pin. On each pass, therefore, the pin had a sliding distance of 27 mm, whereas each point on the track had a sliding distance of only 1 mm.

When using base oil as the lubricant for the tests, a film developed on the surface of the plate which was not formed when the additive oil was used. This film, which had a dark grey appearance, when examined optically, was restricted to the wear track. Fig. 63 shows the deposit on the surface between the grooves of the original machining marks.

Although no quantitative analysis was available from X.P.S., it was possible to compare qualitative information from two areas of similar size; one cut from the wear track and the other from the same plate specimen but away from the track (Fig. 64). Before any removal of the surface layers by ion beam thinning both surfaces contained carbon and oxygen in approximately equal amounts (Fig. 65). The presence of carbon and oxygen would be expected to be relatively high on surfaces which have been exposed to atmosphere. It is necessary to remove this masking layer before the real surface can be examined. After 30 minutes etching of the surface, the oxygen levels of the specimen without the deposit had reduced significantly, although the carbon had risen slightly. On the specimen with the deposit, oxygen had increased while carbon decreased

(Fig 66). Finally after 45 minutes etching of each sample it was clear that the deposit contained larger percentages of oxygen and iron than the clean surface (Fig 67). Increases in etching time beyond 45 minutes did not result in any further change in the levels of the elements. It can be inferred, therefore, that the deposit was based on iron oxide.

Use of non-alkaline base oils for the tests meant that it would be possible to use less severe corrosion conditions to achieve the same scale of damage as in a marine engine. This, coupled with the lack of information on the volume and concentration of acid which condenses in the marine engine, meant that the method for determination of the corrosion potential in the rig had to be by trial and error. Before the rig conditions were finally determined, several tests produced surfaces which did not resemble marine engine liner wear (Fig 68). Outside the track, however, pure corrosion effects were identified similar to those produced in the corrosion rig (Fig 69). The conditions which were eventually found to result in the type of surface damage identified either by direct examination of worn engine components[85] or evaluation of replicas taken from in-service engines (Fig 70), were 2% by volume of the oil system of 0.2M sulphuric acid. These acid conditions, combined with the abrasive wear achieved on the rig produced areas on the specimens which were identical to the type of wear described as corrosion damage in marine diesel engines operating on residual fuels[85].

When the surfaces of the plain grey iron plate were examined at the end of an acidified test the centre of the wear

track was covered by a deposit. Fig 71 shows this deposit at the end of the stroke. In areas where the film was incomplete the lamellar appearance of the corroded pearlitic matrix was clear (Fig 72). Although the plate surfaces were flat, particularly where areas of deposit existed, there was very little evidence of abrasion. The conformity grooves on the pin and plate surfaces were still obvious on a macro-scale but the unsupported carbide wafers of the original pearlite, produced by corrosion, had not been affected by mechanical wear. Surfaces such as those shown in Fig 73 were identified towards the side of the track and away from the deposit which were indistinguishable from worn surfaces of marine liners. Corrosion damage was centred around the graphite flakes which were clearly visible on these surfaces. Closer examination revealed the pearlitic structure of the matrix material (Fig 74).

For the acidified tests using cast iron plate material, containing phosphorus as an alloying addition, the appearance of the worn plate surface was different to that of the unalloyed plate tested under the same conditions. Islands of a relatively unattacked phase were present on the surface (Fig 75). These phases were found to be rich in phosphorus and identified as phosphide eutectic. The corrosion damage to the remainder of the surface was more severe. This severe corrosion did not, however, extend over all the surface and some areas of the specimen were covered by a film (Fig 76).

The level of phosphide eutectic appeared to be slightly above the level of the corroded matrix. This effect was thought to be due to a difference in the combined wear rate

(corrosive and abrasive) between the hard phase and matrix material. Although the matrix appeared to be more corroded than the hard phase, some corrosion had occured on the phosphide eutectic to reveal its internal structure (Fig 77).

Pin surfaces from acidified tests showed similar features running against either alloyed or unalloyed plate materials. Films were present on the surface but were confined to areas which ran against regions of deposit on the plate. Outside these areas both pearlite and hard phosphide eutectic islands were apparent on the surface (Figs 79 and 80). There was no evidence of abrasion on the corroded matrix areas, although abrasive marks were apparent on the phosphide islands.

Abrasion on the pin at some time during its life had been more severe than on the plate. At the end of the tests, however, no evidence of recent abrasion could be identified in corroded areas of the surface.

4.3 PETTER TESTS

Several methods of examination and monitoring of the Petter RA3 engine tests were employed to extract the maximum volume of information from the tests. Direct examination of liner and ring surfaces after the running-in period using plastic film replicas and complete examination of worn surfaces at the end of the test enabled information about the wear mechanisms to be obtained. Identification of the position around the liner was relative to the single oil feed hole. The positions 0, 90, 180, 270 were measured round the bore from above with 0^{o} at the oil hole.

After 24 hours running-in there were slight differences between the two liners. Wear around liner A was uniform and had modified the original X-honed surface at the top of the stroke to a plateau finish separated by channels. Small areas where all evidence of honing had been removed and others with hardly any wear could also be found. In the centre of the stroke less wear had occurred, much of the original honing remained, but some areas had been worn to a plateau appearance. At the bottom of the stroke the surface consisted of mainly original honing with small flattened areas and only evidence of abrasion could be identified.

The surface of liner B differed around the bore. At 0^{o}, 90^{o}, and 270^{o} the surfaces were similar to those of liner A with the exception that a small number of etched phosphide eutectic areas were evident over the top 1.5 cm of the stroke. At 180^{o} to the oil hole, over the top of the stroke, almost all evidence of honing had been removed. A picture of increased wear continued down the bore in this position. Two mechanisms of wear were identified; corrosion and abrasion. Some abrasive grooves were more severe at 180^{o} and appeared to emanate from the remains of honing marks near the top of the stroke.

At the end of the run-in period the fuel for the high sulphur test (H.S.) was changed to a 3.5 % sulphur "doped" distillate fuel.

Examination of the surfaces after 144 hours showed a slight increase in wear on the low sulphur (L.S.) liner B but a large increase in wear on H.S. liner A. Compared to the difference in the wear between the two tests, the L.S. test was considered to be similar around all the bore. Using

the low sulphur fuel, wear had increased at the top and middle of the bore, most of the surface now appeared as plateaux separated by heavy diagonal honing marks (Fig 81). There was evidence of phosphide eutectic particularly at the top of the stroke where it was only lightly etched (Fig 82). At the bottom of the stroke there was hardly any increase in wear except for a small area around the oil hole (Fig 83).

All the surface showed evidence of abrasive wear which included some wide abrasive grooves over the top and middle of the stroke (>5 μ) (Fig 84). The majority of the abrasion grooves were of 1μ or less in width. Although corrosion was evident at the top and down to the middle of the bore, it was not as severe as in the high sulphur test.

On the H.S. liner two different areas of wear were identified. Although the mechanisms were similar, the severity of corrosion and abrasion was greater at 180^{o} to the oil feed hole. At the top of the stroke the surface appeared stained (Fig 85), but closer examination showed corrosion to have revealed both the phosphide and pearlitic matrix structure (Figs 86 and 87). The surface showed evidence of a pitting type of damage from which particles appeared to have been removed (Fig 88). Although some honing marks remained, most of the original surface had been removed. Evidence of corrosion on phosphide eutectic and pearlite was also available in the middle and bottom of the stroke (Figs 89 and 90 respectively). In small areas at the bottom of the stroke, corrosion had attacked the matrix around graphite flakes (Fig 91).

Abrasion at the top of the stroke had resulted in both fine and heavy abrasive damage (Fig 92). The same range of

damage was also evident in the middle but only fine abrasive grooves were visible at the bottom of the stroke. Wear did not appear as severe on the opposite side of the H.S. liner although evidence of both corrosion and abrasion was available (Fig. 93). Some of the original honing remained at the top (Fig. 94) and middle (Fig. 95), although wear at the bottom appeared to be slight and in vertical bands on the liner (Fig. 96). In this position of the liner, the extent of wear was only slightly worse than that of the low sulphur test.

Examination of the second ring surface showed a much higher wear on the H.S. test (Fig. 97) in comparison to the rings from the L.S. test (Fig. 98). The top rings were not available for examination as they were radioactive. The ring from the H.S. test had worn over the whole ring face, whereas wear had only occurred over 60% of the L.S. test ring. Evidence of abrasion was apparent although corrosion was predominant in some areas (Fig. 99). Etched phosphide eutectic and pearlite were present on both rings (L.S. Fig. 100), but were more deeply etched and widespread on the H.S. ring (H.S. Fig 101).

Examination of corroded areas with the aid of stereo pairs showed that the phosphide hard phase was at a level above that of the general matrix. The greatest height of the phase above the matrix was found at the top and middle of H.S. test at 180^{o} to the oil hole. Taper sections through the phases in this area has shown them to be up to0.4u above the surface (Fig. 102).

The microstructure of the Petter cylinder liner and rings was not typical of materials for use with high sulphur content fuels (Figs. 103 and 104 respectively). The material,

basically a grey cast iron with a pearlitic matrix, had an almost complete network of phosphide eutectic. The graphite itself was undercooled and associated with ferrite. This graphite structure was probably caused by a rapid cooling rate as a result of the relatively small liner and ring section thickness. The high phosphorus content was probably designed to extend the freezing range and to improve the fluidity of the iron for the thin sections. This could also be caused if the melt had been super heated during casting also to improve fluidity.

Liner profile measurements taken at the end of the test has enabled liner wear rates to be calculated along the length of the stroke (Fig. 105).

An average of all the individual rates down the liner gives a rough indication of the overall wear rate. For both tests this value is 0.02 mm/1000 hrs. If it is assumed that this diametric wear is the average over all the liner surface it is possible to crudely calculate that this represents a wear rate of around 3 mg/hr. As was seen from direct examination, however, the wear is not uniform over all the bore of the acidified test, which will mean that this estimate may be on the low side for the H.S. liner wear.

The total wear on the top ring of these engines was measured by the radioactive debris in the oil drain samples. A total of ten samples were taken which enabled the change in wear rate to be plotted for the length of the test (Fig. 106). The first sample taken at the end of running-in shows that the wear in the L.S. test was marginally higher on the top ring. During the test subsequently run on high sulphur fuel, the wear rate gradually increased from 0.35 mg/hr to a maximum of

16 mg/hr just before the end of the test. The total top ring wear of the L.S. test continued at a uniform 0.15 - 0.3 mg/hr for the duration of the test.

Chemical separation of the iron sulphates due to direct reaction of sulphuric acid on the liner and ring surface from the calcium sulphate, the product of neutralisation of the acid by the lubricant overbasing, gives an indication of the amount of acid which has caused corrosion. Sufficient experience has been gained by the industrial sponsor to estimate the amount of corrosion directly from this type of analysis with an accuracy of $\pm$20%. These results are shown in Fig. 106 . It is clear that the increase in wear on the top ring is not directly attributable to an increase in corrosion of the rings and liner. Direct dissolution of the metal surfaces produced a combined wear rate of up to 1 mg/hr with a mean value of 0.4 mg/hr. The maximum rate of corrosion did not coincide with maximum ring wear.

Engine oil drains have also been analysed by ferrography. The average size of the debris particles for the two tests are similar, 1.3μm and 1.0μm for the low and high sulphur tests respectively (Fig. 107). Abrasive particle density on the ferrographic slides can be related to the volume of debris in the oil samples (Fig. 108). For the L.S. test the production of debris was constant which indicated equilibrium wear. Particle volume in the H.S. test increased from 50 hours running to the end of the test which caused a stimulation of the mechanism producing the debris. The time scale for the increase in debris coincided with the increase in top ring wear.

5. DISCUSSION

5.1 INTRODUCTION

The literature on marine engine wear refers to three fundamental wear mechanisms; abrasion, corrosion, and adhesion. Of these, abrasion and corrosion are believed to account for the majority of wear during normal engine operation. Adhesion is usually thought to be associated with the "running-in" process and during abnormal periods of high wear rate which occur through extended engine use.

That abrasion and corrosion interact to cause normal cylinder wear has been widely referred to although agreement on the mechanism of the interdependence is lacking. A wear rig has been used to simulate a corrosive wear mechanism to complement the work on dry wear carried out by Dent[85]. This work was aimed at improving the basic understanding of the mechanism with particular reference to acid interaction with the constituent phases of grey cast iron.

This avenue of study culminated with a rig, designed and built to incorporate the two wear mechanisms in a lubricated environment. The first use of this rig was to investigate nominally pure abrasion in a lubricated environment prior to the introduction of a corrosive element. In the final series of tests on the rig, particular attention was paid to balancing the severity of the mechanisms to obtain wear surfaces similar to those encountered on cylinder components during normal marine engine operation.

In addition to this approach there was involvement in the specification of parameters for a small test engine including provision of monitoring facilities to obtain a

maximum amount of information relating to the interaction of abrasion and corrosion. Although some of the analysis work was conducted elsewhere, examination and interpretation of the ring and liner surfaces and replicas was performed by the author to give a complete picture of the wearing process. Results from the various sources have been collated to form the basis for the engine test discussion.

5.2 CORROSION TESTS

As the corrosion tests were designed to simulate only the mechanism of corrosion and not the engine environment, the temperature and acid conditions are not entirely representative of those encountered inside marine engines. Cylinder temperatures are usually in the order of 250° C for highly rated engines, although surface temperatures at the top of the stroke may be appreciably higher. Acid concentration is known to depend on a number of variables which may cause acid to condense at up to 80% concentration under the worst conditions[65]. Good correlation was found between rig and engine corrosion effects which indicated that these differences in temperature and acid conditions were overcome by the test. This validates the rig approach and means that various materials can be compared to establish the important metallurgical factors. As the quantitative results relate only to the rig conditions, they are useful only when comparisons are made with other results in the series. Results for the three grey cast irons of the first series of tests, shows no significant variation despite considerable differences in their microstructures. Although samples A and B have similar flake distributions (C.E.V. 3.41 and 3.79),

Fig. 18 shows sample A to have a large volume of phosphide eutectic. The literature reports that phosporus accelerates corrosion in steels[43, 46] but in cast iron, Glantz and Maahn[45] found it to have an insignificant effect within the normal compositional range. It is this latter view which is corroborated by the results from the corrosion rig. Sample B also contained a high proportion of copper (0.9%) which has been referred to as imparting a degree of protection against mineral acid attack[40, 45]. The benefits of copper have not been substantiated by these tests but it is possible that it may be effective outside the rig temperature range.

Cast iron C had a much smaller graphite structure than A or B and contained a small volume of hard phase (carbides and phosphides). No significant difference was found between the amounts of corrosion on this and the iron with a larger flake size. This effect was also identified in the second series of tests with samples D and E using a different additive lubricant. Results from the two series are not comparable however, due to this difference in lubricant. Table 37 illustrates the difference in the amount of corrosion between a fully pearlitic grey cast iron, samples F and G, and 0.8%C steel. From the corrosion of sample F, which was only 60% of that experienced with cast iron E, it was clear that the presence of graphite and not its distribution played an important role during corrosion. Heat treatment of the pearlitic steel to a fully martensitic structure in which the cementite was evenly distributed, only slightly reduced the corrosion for sample G. This difference was equivalent to the variation in corrosion between sample D and E. Sample

H was included as it was the cylinder liner material of the Petter AV1 test engine discussed in a later section and corrosion was four times greater than for the other grey cast irons. This result was thought to be due to the effect of free ferrite associated with undercooled graphite and this is discussed in more detail below. This structure is typically caused by the fast cooling rates induced in thin sections during casting but may also be due to alloying additions of Ti or Zr.

Corrosion effects on the surface of each of the cast irons was similar and Fig 29 is an example of the way in which corrosion centred around the graphite flakes on the surface. A thin film was also apparent, which protected large areas of the specimen. In addition to the areas around the flakes, other regions of corrosion were thought to have been caused by the removal of the film by turbulence in the corrosion vessel. Stimulation of corrosion by graphite was also clearly apparent on the surface of sample H (Fig 38). This corrosion could have been due to a combination of effects. McConnel and Nathan[83] suggested that the graphite, being porous, acted like a sponge for the acid which was thought to subsequently cause sub-surface attack of the areas surrounding the flakes. They did not speculate as to the effect of the neutralising additives carried in the lubricant which may also be present in the graphite cavities. Alkaline additives in the oil are likely to be rapidly exhausted however, and not easily replaced.

Graphite is frequently referred to as being strongly cathodic with respect to ferrite[49]. Its efficiency is due

not only to its large surface area to volume ratio but also to its noble electrochemical potential. Areas of ferrite surrounding the graphite would be rapidly dissolved in the presence of a suitable electrolyte such as sulphuric acid. Another possible mechanism involves the sulphate film which is a product of reaction of sulphuric acid and iron and has been demonstrated to be protective but only loosely adherent[87]. The film does not appear to form on graphite but leaves an interface where the edges of the film come into contact with the carbon. If acid undermined the protective film it could cause it to exfoliate by the generation of corrosion products underneath, corrosion of surrounding matrix would then ensue. As corrosion concentrates on the ferritic lamellae of the pearlite, carbide wafers also may not be covered by a film. A possible combination of these mechanisms could be catastrophic as the ratio of anodic and cathodic sites changes in favour of more severe corrosion.

Corrosion effects on the pearlite are to preferentially remove ferrite from between the cementite lamellae (Fig 30). This mechanism leaves unsupported wafers of iron carbide on the surface which are easily removed by turbulence or specimen cleaning after a test. Fig 35 shows the original surface level and the way in which the matrix receded although the cementite itself was not attacked by the acid. Bulk iron carbides are cathodic with respect to ferrite[43, 48] but cementite lamellae of pearlite tend to exfoliate as ferrite is dissolved and are not, therefore, as effective as massive carbides in the structure[43]. Graphite was thought by LaQue[48] to be a more efficient cathode and overwhelm the

effect of the cementite.

Other areas of the surface appeared to be unaffected by corrosion. Fig 31 shows one such area, shown by E.P.M.A. to be partly phosphide eutectic although the upper half of the phase was thought to be an unattacked iron carbide. It was clear from the sections taken normal to the surface, (Fig 35), that phosphide eutectic was not attacked by the acid in the corrosion rig. The original surface level for both samples A and C was clearly defined although pearlite had been removed. Corrosion of pearlite leaving phosphide eutectic standing proud was also found by McConnel and Nathan[83] in their laboratory work at room temperature. Fursund[62], on the other hand, found the phase to be more severely corroded than the pearlitic matrix on the surface of a marine engine running with residual fuel. He was able to reproduce the effect at high temperatures using concentrated acid in the laboratory. It is possible, therefore, that the action of acid at high temperatures on cast irons microconstituents may change; this is a view which has the support of at least one major engine manufacturer[88]. Even at low temperatures, some corrosion of phosphide eutectic occurs. The phase can be of two forms, pseudo binary (Fe_3P and α) and ternary eutectic (Fe_3P, Fe_3C and α). In both cases the eutectic contains pools of ferrite which are likely to be leached out by acid attack. This effect can be seen on the surface of corrosion sample H which revealed the internal structure of the phase in a way similar to a metallographic etch (Fig 41).

A white deposit was easily distinguishable from the

other surface films, (Fig 33) and was identified by E.P.M.A. as a sulphur containing compound (Fig 34). This was probably calcium sulphate which is the product of neutralisation of sulphuric acid and calcium based additives in the oil. After testing, large areas of the specimen were covered by the deposit most of which was removed by cleaning in an ultrasonic bath.

Examination of surfaces from the second series of tests using the alternative lubricant, revealed the reason for the major variation in corrosion behaviour. Surfaces of samples D and E showed graphite stimulation of corrosion, (Fig 42) and although both samples showed evidence of surface films, they were more widespread on sample D but in both cases did not cover graphite flakes on the surface. In contrast the steel surfaces were almost completely covered by films (Figs 44, 45). It is thought, therefore, that the presence of graphite strongly contributed to the difference in corrosion between the materials. Corrosion pits formed on the surface of the martensitic steel could be seen on sample G but there was no evidence of a differential corrosion mechanism.

The inferior corrosion performance of sample H was mainly due to the association of graphite with free ferrite in the structure. Fig 38 clearly illustrates this effect and comparison with the microstructure shown in Fig 103 shows free ferrite to be the affected area. Intense corrosion around the graphite flakes results from the electrochemical effect of closely coupling the cathodic carbon to the anodic iron. There may also have been a contribution

from phosphide eutectic which was present as almost a complete network and was certainly outside the normal compositional range referred to by Glantz and Maahn[45]. Hoar and Havenhand[43] thought that iron phosphide had a similar effect to iron carbide and although they were considering much lower concentrations for steels, it is reasonable to conclude that it would be significantly cathodic in such large volumes for the rig test conditions.

Fig 41 shows an area of the surface of sample H in which both iron phosphide and wafers of iron carbide stand above the level of the remaining surface. The structure of this material in the light of the corrosion rig results was a very poor combination from the point of view of corrosion. This was borne out to some extent by engine test results in which this material was used for the cylinder liners (Section 5.5)

5.3 WEAR RIG DESIGN

The mechanisms of corrosion and abrasion have been isolated from studies of cylinder liners, piston rings and also replicas of similar surfaces from marine engines operating on residual fuels. Abrasion of grey cast iron has been previously been studied by Dent[85] and corrosion is covered by the present investigation. The next step towards understanding the complex interaction of these mechanisms was to combine the two in a single wear rig.

In order that a corrosive media could be introduced in a similar way to the corrosion rig, it was necessary to run the tests in a liquid environment. The use of a lubricant as a carrier also made the environment more closely reproduce

the abrasion mechanism. It was thought that this would also eliminate the overscaling of abrasion which was a feature of Dent's work[85]. A flat pin specimen of piston ring material was used in place of the single point diamond abrasive to enable both surfaces to wear. Examination of worn cylinder liners and piston rings has shown that the maximum wear occurs at, or just below the top dead centre of the stroke (TDC). This position coincides with the minimum oil film thickness occurring on the expansion stroke. It is impossible to define exactly the conditions of lubrication in this area because the proportions of boundary and hydrodynamic lubrication are not fixed. For controlled simulative tests however, the same variation in conditions cannot be tolerated and a single lubrication mechanism should be employed. As hydrodynamic lubrication introduces a gap between the surfaces, which would reduce abrasive wear, the test was defined to achieve a boundary lubrication condition.

Examination of the Sommerfeld Number[89] indicates the conditions likely to promote boundary lubrication:

$$Z = \frac{\mu N}{P}$$

Z = generalised Sommerfeld Number

μ = dynamic viscosity

N = speed

P = load per unit projected area

Small values of Z lead to these conditions which can be achieved with a minimum speed and maximum load. In boundary lubrication the bulk viscosity does not play any part, but for a mixed system the hydrodynamic component would be minimised by a low oil viscosity. This may be achieved

by careful temperature control. Too high a temperature may lead to disorientation of the boundary films and even breakdown of the lubricant. In view of the speed requirements, a reciprocating test offers the best conditions as at the end of the stroke the speed reaches a zero value which is where boundary lubrication is most likely to occur.

The test involves, therefore, two specimens, representing the piston ring and cylinder liner materials which are reciprocated relative to each other under a normal load, with lubricated conditions and at elevated temperatures. The design requirements were:

(a) Reciprocating specimen

(b) Accessable specimens

(c) Provision of an oil bath

(d) Control of: (1) Load
(2) Speed
(3) Temperature

(e) Measurement of: (1) Wear
(2) Friction
(3) Temperature

(f) Continuous operation

(g) Enable acidification of oil bath

In the initial design the pin was held in a fixed gantry over the oil bath and loaded from above (Fig 109). The pin fixture was free to move vertically in the gantry through an accurately machined bronze bush insert. Wear was monitored by a transducer measuring the vertical displacement of the pin and friction was obtained by a similar device measuring the transmitted tangential force through the gantry.

After a few passes from new, the loaded pin began to rock in the gantry bearing at the end of each stroke. This caused friction in the sleeve which in turn prevented vertical movement of the pin and reduced the effective pressure at the specimen interface. In addition, the inertial forces of the large loads rocking from side to side caused a level of background movement which masked the small transducer signals relating to frictional force and wear. This problem is a feature of many gantry systems, although the noise may only be significant when the design is used in conjunction with lubricated tests where transducer outputs are relatively small.

These problems were solved using an arm fixed at one end and loaded at the other, with the pin specimen fixed one third of the way along the lever (Fig 19). The disadvantages of an arc of mobility in both vertical and horizontal directions were minor due to the small movements in those arcs (0.5^{o} horizontal and 0.1^{o} vertical movement maximum). As the wear transducer support moved in the same horizontal arc as the lever, interference between force and wear signals was minimised. Torsional bending of the lever, induced by forces acting at the end of the pin caused some reaction of the wear transducer but this effect was small and could be accounted for.

In an attempt to separate wear of pin and plate materials, a conical pin with a taper of 30^{o} was evaluated. Measurement of the pin diameter was made at intervals throughout the test but were of little value. Increases in pin diameter with wear meant that pressures at the surface reduced

throughout testing. New material was constantly being run-in at the edges of the track and the test had to be interrupted for measurements of the pin diameter to be made. A 1 mm diameter parallel shouldered pin did not allow separation of wear but it was simple to manufacture and produced the required pressures with only moderate suspended loads. As the metallurgies of pin and plate material were fundamentally similar, no natural characteristics could be isolated to indicate the individual wear rates from debris analysis. Expensive techniques such as Thin Layer Activation to separate wear could not be justified. The overall objective of the research, to investigate the interaction of corrosion and abrasion, was not seriously jeopardised by the decision to adopt the measurement of combined wear. Use of the same pin material throughout the tests meant that this wear could be used as a valid basis for comparison of plate material wear.

Measurement of friction force was found to give a non symmetrical friction curve over the stroke length. Friction force was transmitted through the lever which moved to deform a force pillar. As the pin reached the end of the stroke, the lever could not return to the neutral position until the pin began its movement in the opposite direction (Fig 110). A similar effect worked in reverse at the other end of the stroke. Friction was not measured until the pin movement was sufficient to move the arm from the stop position to a contact with the pillar. The consequence of this was that the friction profile started after the beginning of one pass from right to left and ended at a position at the start

PAGE
MISSING
IN
ORIGINAL

an oil in which there were no alkaline additives competing for reaction with the acid. This was considered justified as it was the acid attack on the metal, rather than the neutralisation of the acid by the oil, which was important.

Previous work with the corrosion rig had led to the conclusion that to be most effective acid had to be in the form of a fine emulsion rather than large droplets in the lubricant. This was achieved in the wear rig by adopting a circulating system in which the acid droplets were broken up by a specially designed mixing unit before being pumped into the oil bath (Fig.22). In order to increase the volume of acid in the system, to prolong the period of corrosion, the capacity of the oil system was enlarged to incorporate a heated reservoir making the total oil volume up to 300 ml.

Friction and wear outputs were found to be extremely sensitive to bath temperature variation of $\pm$ 1^{o} C, this was thought to be due to changes in oil viscosity over this range. To improve this it was necessary to modify the temperature control system. Repositioning of the control thermocouple to between the bath and base plate reduced some of the control lag but the main problem had caused the inclusion of an external oil reservoir. Heaters in the base no longer controlled bulk oil temperature and it was necessary to position a further thermocouple in the oil line just before entry into the bath, to control heating of the oil reservoir (Fig 21). This ensured that the oil entering the bath was the same temperature as the bath and specimens and allowed for variation in ambient conditions.

When these modifications had been made, control of

temperature was excellent with no significant deviation from the set point. These stable conditions allowed more accurate measurement of both friction and wear throughout the tests.

5.4 RECIPROCATING WEAR RIG TESTS

Wear, plotted throughout the test followed a similar pattern for all the unacidified tests (Fig 47). An initial high wear gradually reduced over a number of hours to a lower equilibrium rate. During the running-in stage surfaces are conditioned from the original ground finish to a smoother surface which is more suitable for lubrication.

This running-in phenomena has been studied by Sreenath and Raman[78] who identified two stages in the process. The first was thought to be rapid removal of the surface peaks by deformation and severe mechanical wear. During the second stage the remaining valleys were filled in by debris or films generated on the surface.

Initially, the test wear rate was high because large asperities were removed from both surfaces, but this gradually reduced as the interaction between the asperities became less frequent and less severe. When running-in changed to equilibrium wear there was no further improvement in surface roughness. Wear continued through slight asperity interaction and debris, carried in the lubricant which was trapped between the counterfaces. These mechanisms are thought to combine to prevent any further smoothing of the surfaces.

Tests were run for up to 24 hours to identify any further changes in wear behaviour. Deviation from a running-in and equilibrium wear pattern only occurred during the early stages of equilibrium wear for high loads. After a

period of normal running-in and equilibrium wear, the rate was found to increase which culminated in fracture of the pin. The fractures appeared to have initiated around the edges of the pin at points along graphite flakes. Although the resulting fracture of material from the pin should not have changed the real area of contact between the specimens, deformation of the surfaces to maintain that the area and disruption of lubrication between the surfaces, rapidly increased the wear rate. The tests did not recover from this change in the wear process. Apart from this exception, equilibrium wear was representative of the long term wear behaviour for the test conditions.

The time taken for the specimens to complete the running-in process varied from test to test, despite close control of specimen preparation. These variations were thought to be caused by minute differences in topography and metallurgy. As the reproducibility of the equilibrium wear rate was acceptable, variation in running-in behaviour did not appear to significantly influence equilibrium wear conditions.

In addition to changes in wear which occurred during running-in, friction between the pin and plate also varied (Fig 47). The high initial frictional force was a result of deformation and mechanical interlocking of the surface grooves. As the surface became smoother, the proportion of metallic friction reduced and lubrication became more stable.

Although conditions on the rig were arranged to provide boundary lubrication between the pin and plate, it is clear from some of the friction results that this was not fulfilled over all of the wear track. The friction recorded from an

oscilloscope for one pass during equilibrium wear, shows a decrease along the middle of the stroke (Fig 51). For identical speed conditions, an unlubricated test where metal to metal contact occurs over the whole stroke, showed no such variation in friction (Fig 53). This was borne out by Bowden and Tabor[27] who showed that the coefficient of friction was independant of speed for true boundary lubrication.

Values for the coefficient of friction in boundary lubrication are usually quoted in the range of 0.05 to 0.2μ, whilst hydrodynamic friction, 0.001 to 0.03 μ, is much lower. The range of friction coefficient for the lubricated tests is 0.11 to 0.20 μ and is within this boundary range. Variation of friction with changes in speed, however, is indicative of a hydrodynamic component in the lubrication regime. Although boundary lubrication may be approached at the end of the stroke, most of the track seems to have been operating in a mixed lubrication regime.

Oxide based films on the wear surface of specimens run in base oil were a result of the oils' additive make-up. The decision to standardise on a base oil for the tests was taken to simplify the introduction of acid at a later stage. Lubricant additive packages are carefully balanced and addition to, or subtraction of components could cause problems. Although it was only the alkaline additives which were likely to interfere with acidification, the base oil which was chosen contained none of the normal additives. In retrospect this decision was badly founded and led to complications caused by oxide films. One of the important components of an additive package is the anti-oxidant. When aerated oils are

subject to moderate temperatures without these additives, molecular chains can produce free radicals which combine with oxygen. Oil then becomes a carrier of oxygen which may result in production of surface films and even breakdown of the oil. Takuchi[90] showed that oxidised lubricants could transport oxygen to wear surfaces and react only with the metal of the sliding surface to form oxides. He was able to show by electron diffraction that these oxides were a combination of Fe_2O_3 and Fe_3O_4 when formed on grey cast iron. Use of an oil designed for an application such as crosshead crankcases which have a similar viscosity and no alkaline additives could have proved to be a better solution to the problem.

Differences in the physical properties of base and additive oils make it difficult to assess the influence of this film. Although the wear performance of the additive oil was superior to that of the base oil, it cannot be interpreted as indicative of the detrimental effect of the film. Both the friction and wear performance of the formulated oil would be expected to be superior to the unformulated alternative because of its higher viscosity, 17 Cs against 13 Cs, and the influence of its boundary additives. The effect of these factors is evident in the difference in the end stroke friction for the two lubricants (Fig 54).

Surfaces of specimens after running-in, although rough on a macro scale (Fig 57), were very smooth on a micro scale (Fig 58). Features apparent on the plate surface at high magnification were remains of the original grinding marks at 45° to the direction of pin movement, fine parallel abrasive grooves running the length of the track and, on the surface

of the plates lubricated with additive oil, randomly orientated cracks. These were later found to be the result of surface deformation which had closed up the original graphite structure (Fig 59). On the surface of the base oil specimens these cracks were obscured by the deposit referred to above.

Some pins showed evidence of a differential abrasion rate between the matrix and phosphide eutectic, (Fig 62), which was similar to effects seen by Dent[85] in his review of worn liner surfaces. Pure abrasion effects on the phosphide eutectic could be separated from the combined effect of corrosion and abrasion on both the rig specimens and marine engine liners, as only the corrosive environment revealed the phosphides internal structure. No evidence of this type of wear could be identified on plate surfaces containing phosphide eutectic. As with ring wear in an engine, the pin wear rate was greater than the plate. This was clear from the original grinding evidence remaining on the surface of the specimens (Fig 61). This wear may be mainly attributed to the difference in the sliding distance of the components, although the effect of traversing the conditions at the ends of the stroke on each pass should not be ignored. It is likely that the wear rate on the plate was insufficient to produce visible signs of a differential wear mechanism.

Wear rates for unacidified tests on the reciprocating wear rig, (Fig 48), showed that the conditions that led to an increase in wear rate were lower oil viscosity, and lower sliding speeds or higher loads. Small increases in the oil temperature also caused a higher equilibrium wear rate. As the temperature of an oil increases, its kinematic viscosity

decreases. The characteristics of this change are classified by the oils viscosity index.

In mixed lubrication it is thought to be the summation of all hydrodynamic effects over the surface which controls the proportion of solid contact and indirectly, the amount of wear. An increase in hydrodynamic lubrication results in less solid contact as more of the load is supported by hydrodynamic pressure within the oil film. It is possible to show theoretically that the hydrodynamic pressure between two relatively moving surfaces is a function of viscosity, speed and variation of the film thickness in the direction of sliding[32].

$$\text{Hydrodynamic pressure} = 6uU\frac{dh}{dx} \qquad (4 : 1)$$

u = absolute oil viscosity

U = relative velocity

h = distance between surfaces

x = direction of sliding

This, however, does not indicate a relationship between pressure and film thickness. For a measure of the effectiveness of lubrication it is necessary to refer to the generalised form of the Sommerfeld Number which is defined as:-

$$So = \frac{uU}{pL}$$

U = relative velocity

u = absolute oil viscosity

p = pressure stresses

L = length of the bearing

After assuming Newtonian behaviour, the Sommerfeld Number becomes:-

$$So = \frac{\text{viscosity x speed}}{\text{load}} \qquad (4 : 2)$$

As the rig results and Generalised Sommerfeld Number indicate, increases to the viscosity or speed improve lubrication. Reference to (4 : 1) shows that these effects increase the hydrodynamic pressure which is likely to decrease the proportion of solid contact and lead to a lower wear rate. Increasing the load reduces the lubrication effectiveness. Providing the surfaces remain rigid, load does not alter the generation of hydrodynamic pressure (4 : 1). Increased solid contact to accommodate the load change can then lead to a higher wear rate.

Wear curves for all the tests using a base oil are of similar shape and display an exponential increase in wear rate with load (Fig 48). Reduction in the Sommerfeld Number, brought about by increases in load, indicate more support through solid contact and therefore more severe boundary conditions. Tests run with additive oil, however, were less sensitive to load changes than those run with base oil. Although there is no positive evidence to indicate the reason for this behaviour, it is thought to be related to the effect of additives on the solid contact between the specimens.

All oils exhibit some tendency to form thin absorbed surface films, but formulated oils contain additives whose molecules are intended to adhere to the surface. The action of these molecular layers is to lubricate and protect surfaces which come into contact under marginal lubrication conditions. It is thought, therefore, that the difference between the two lubricants was due to the relative stability of the films under extreme boundary conditions. Evidence to support this was found in the coefficients of friction for

the two oils (Fig 54). At the end of the stroke, where the Sommerfeld Number, (4 : 2), indicates a large proportion of solid contact, the oil with boundary additives had a lower coefficient of friction. In the middle of the stroke, similar friction coefficients were found for the two oils which would be consistent with a lower proportion of solid contact and less dependance on boundary films.

These films should not be confused with visible films formed on the surface of tests run with base oil. Although the results did not indicate the effects of the oxide films on wear, they did show an interaction with the coefficient of friction. Under normal metal to metal contact, Bowden and Tabor[27] showed that the coefficient of friction is independant of load. These results demonstrated Amontons second law of friction which holds only when the real area of contact increases proportionally with the load.

Comparison of the friction results (Fig 54), with those of Bowden and Tabor[27] shows that the additive oil falls within the range of their results and for the number of results available, must be considered to be following Amontons laws. More significant variation of friction coefficient with load was found with the base oil, particularly if the results from the test in which load was increased on the same specimen are included. It is clear that the oxide based deposit on the wear track was responsible for this deviation, as the additive oil test, which contained no evidence of such a film, conformed with the friction laws. There is insufficient evidence for the mechanism to be specified, although it is thought that the film causes a deviation from

the proportionality of the real area of contact with load.

Bowden and Tabor[27] indicated two instances of deviation, thin metallic films with low shear strength were found to reduce the frictional force, whilst the load was supported by the harder substrate. In addition it was argued that anisotopic solids with a plate like structure would be able to shear easily if a tangential force were applied but withstand large pressures normal to the lamellae. An obvious example of this latter material is graphite.

If the deviation of the rig results was due to graphite films, both additive and base oils would have identical friction/load characteristics. This is assuming, however, no effect from the lubricant additives or viscosity. Another possibility is that the oxide film behaves like a thin metallic film at the high test loads. Whitehead[91] found that over a load range of 10^{-2} to 10^{-3} g, a transition in friction behaviour occurred for an oxide film on polished copper from low to high coefficients of friction. This transition was found to be due to rupturing of the oxide film at the higher loads. At no time was a decrease in friction coefficient found for increasing load. Although the result bears no real comparison with the test rig conditions, it does serve to indicate the nature of oxides which are in general, hard and brittle. The third possibility is that the film is a complex mixture of oxide and graphite which combined to reduce the frictional force as the load increases. Savage[92] found that decontaminated graphite had a relatively large coefficient of friction and it was only when lubricated by absorbed contaminants that it became an effective lubricant.

He identified water vapour, certain organic vapours, and oxygen as able to lubricate graphite but not hydrogen or nitrogen.

Although compositional analysis of the base oil surface film indicated that it was based on iron oxide, carbon was also detected, but in a lower concentration than away from the wear track (Fig 67). Sections taken through one of the lubricated tracks (Fig 59), shows how the compressive stresses have closed up the graphite flakes. This would extrude graphite on to the surface in the same way as Eyre et al[112, 118] found for dry wear of grey cast irons.

Samuels and Craig[93] pointed out that similar effects could be produced by grinding of cast iron surfaces on SiC paper. Fig 60 shows that while carbon depletion of the sub-surface zone was apparent after grinding of the specimens, the depth of the effect was less than beneath the wear track itself. This indicates that graphite was extruded on to the surface during the test and had not all been removed by the original grinding operation.

A combination of graphite and oxidative effects would account for the difference in friction response of the two oils. When graphite is in a flake form in the matrix of cast iron, it is sealed from the environment. During wear, the graphite would be extruded under the lubricant, and the additive oil could limit contamination. The base oil, however, would not restrict the adsorbtion of oxygen.

Friction results for the dry wear tests (Fig 55), indicated a more pronounced decrease in coefficient of friction as load was increased than for lubricated tests.

In the dry wear instance, it is completely open to the atmosphere and supply of water vapour and oxygen would not be limited. Before this proposed mechanism can be accepted however, much more work is necessary.

In summary, the mechanism of abrasion in a lubricated environment has been reproduced. Although the severity and extent of abrasion effects were less than found in marine engines, the mechanism of differential abrasion was identified as similar to effects in marine engine cylinder wear. The significance of these friction and wear results was that they proved the reciprocating rig and test procedure was sensitive enough to respond to small changes in conditions. As a whole, therefore, the test was shown a good, but not perfect, basis for the second stage of the work which was to simulate abrasion and corrosion mechanisms simultaneously.

In order to establish acid conditions in the wear rig, to 2% of oil volume of 0.2M sulphuric acid, it was necessary to complete a number of tests. Wear and friction curves for the acidified portion of one of the final tests using an alloy cast iron plate (Fig 50), shows the effects of acidification.

All tests were run-in under unacidified conditions. Although addition of acid caused a rapid increase in friction at the ends of the stroke, mid-stroke friction was hardly affected (Fig 50). This effect was not thought to be a result of oil performance such as viscosity or breakdown of boundary lubrication films between the pin and plate, these would have had more significant effects on mid-stroke

friction. Before an explanation of this effect can be discussed, the remainder of the results have to be considered.

After initially increasing at the end of the stroke, friction gradually reduced to the same, or similar level as the mid-stroke friction. Although at this point, friction no longer varied with speed, it was not indicative of initiation of true boundary contact. As the end of the stroke represented true boundary conditions, breakdown in mixed lubrication would cause an increase of mid-stroke friction to the same level as that at the end. Whatever mechanism was responsible for these friction effects it appears to be concentrated at the limits of the stroke. This mechanism is believed to be preferential corrosion around the ends of the track.

Concentration of corrosion in these regions may be explained by a conditioning of the surface as a result of increased boundary contact and change in sliding direction. This may have taken the form of a reduction of oxide film thickness and continuity under unacidified conditions which allowed preferential corrosion to occur. When acid entered the bath it could quickly undermine the load supporting contact area which would produce a rapid increase in friction force as deformation occurred to re-establish the area of contact. An increase in wear rate would be expected in these regions which did occur immediately after acid was added (Fig 50). There is evidence to show that this was confined to the ends of the stroke (Fig 111). After an initial increase in wear, a gradual reduction occurred to a very low level.

Examination of the plate specimens at the end of testing indicated that corrosion was more severe at the side of the track than on the track itself (Fig 112). Clearly the wear track was subject to an effect which not only limited corrosion but also led to a decrease in friction force and wear rate. That friction and wear are directly related can be seen from the way in which the onset of a low wear rate occurred at the same time as the end-stroke friction attained its maximum value.

Compacted corrosion products on the track seems to be the most likely cause of these effects. Although iron sulphate is a passive film, it is normally only loosely adherent and offers no real protection against corrosion[87]. This can be confirmed by the more severe trackside corrosion. Under conditions prevailing between the specimens, however, it may be formed, or become, adherent and protective. A parallel of wear conditions causing non-equilibrium phenomena may be drawn with oxidation of specimens run in base oils. Here, oxide was formed on the wear track and not to the same extent on the remainder of the specimen. A deposit of this type would reduce wear by limiting further corrosion but may also perform as an effective solid lubricant to reduce the end stroke friction force. When the acid was neutralised by the reaction with the surrounding metal surface, the wear rate and friction would be expected to return to their original levels. These effects could be identified on both friction and wear curves.

Before final conditions for acidification were determined, several tests produced wear surfaces which bore no

resemblance to marine engine wear. The plate surface of one such test run at 120 Kg load 43 mms^{-1} mean speed and 1% of acid shows a curious plateau effect (Fig 68). Examination of the side of the track, (Fig 69), showed that corrosion had occurred and was centred around the graphite flakes. This was clear evidence that graphite stimulated attack of the matrix and that corrosion could be simulated in the wear rig. It was decided to increase abrasion, by reducing the speed, and at the same time increase corrosion to produce a more uniform effect. These changes produced a balance of conditions to obtain worn surfaces in which effects were similar to some areas of marine engine wear (Fig 73).

From a rough original ground plate specimen (Fig 113), where graphite was almost completely obscured, a smooth surface was produced in which graphite flakes were clearly visible. The plain grey cast iron plate surface contained no evidence of plastic deformation, but showed areas of corrosion centred around graphite flakes (Fig 73). In these areas, a pearlitic structure was evident. This area of wear from the centre of the track, also contained large areas of a dark deposit (Fig 71). The pin surface for this test also showed evidence of a deposit along its diameter in the direction of sliding. At the edges, corresponding to the sides of the track, wear had produced areas of phosphide eutectic standing above the surface (Fig 79). This differential wear effect in a corrosive environment, leaving protruding phosphide eutectic has been identified on marine liners[83, 67] as well as on replicas taken from engines (Fig 70). Fursund[62], in his review of cylinder liner

wear however, found the opposite to be true, phosphide eutectic lay below the surrounding pearlite. Although his evidence is not conclusive, a similar effect of preferential corrosion of both phosphide eutectic and cementite has been identified by an engine manufacturer[88]. This was found to occur at high temperatures, above that used in this investigation.

Cast iron used in the rig tests did not contain bulk carbides but the effect of corrosion on cementite could be evaluated from the effects of corrosion on pearlite (Fig 79). Although there was no evidence of abrasion, some of the carbide wafers were fractured and were observed lying on the surface. It is clear that in the absence of ferrite in the pearlite, unsupported cementite has little strength and can easily become detached. It was likely that the pin specimen of this test could only make contact over a band along the middle of the track and on the protruding phosphide phases at the edges.

On the surface of the pins run against a phosphoric grey cast iron plate specimen, phosphide eutectic was again seen standing above the matrix (Fig 78). Corrosion had leached the ferrite out of the eutectic structure. Areas similar to these are often found on corroded marine engine liners and examples are contained in Dent's review[85].

In the centre of the plate track, wear had also left eutectic standing above the matrix (Fig 77). Comparison of such areas with replicas taken from marine diesel liners (Fig 70), indicates that the rig has successfully simulated the mechanisms of both abrasion and corrosion, and combined

them to reproduce effects identified in marine engines[67]. From an originally rough ground cast iron specimen, flat etched surfaces were produced on which graphite flakes, pearlite and phosphide eutectic were visible. A differential wear mechanism was also reproduced which caused etched phosphide eutectic to protrude above the matrix and leave cementite wafers unsupported on the surface. All these effects are found on diesel engine liners which have been run with high sulphur residual fuels. As Nadel and Eyre[67] point out however, these features are confined to certain areas of the liner.

Although condensation of corrosive acid occurs over a fairly narrow band of conditions in an engine[38], it may be subject to transport up and down the stroke by the scraping action of the rings. Acid would then be available to corrode the ring and liner surface over the whole stroke. However, conditions only allow evidence of corrosion in the form of etched surfaces, to be seen on the liner over a short section of the stroke. This is usually the middle portion, where the oil film thickness is a maximum, the abrasive wear rate is very low and a corrosive wear mechanism appears to predominate. McConnel and Nathan[83] have found evidence of corrosion, in the form of irregular acid attack in deep abrasion grooves, on the piston ring and at the top of the stroke where abrasion was observed to predominate.

Clearly, interaction of corrosion and abrasion varies over the length of the stroke according to the conditions. Present test conditions allow only the mid-stroke interaction to be reproduced. It would be feasible however, to increase

abrasion by modification to the test in order to investigate the interaction nearer the top of the stroke.

There are also limitations with the rig for simulation of mid-stroke wear effects. Whilst good correlation exists between areas of the specimens and marine cylinder liners, the extents of the effects were dissimilar. Corroded surfaces of the types shown in Fig 73 occurred only over relatively small areas which was thought to be due to the corrosion protection afforded by surface deposits. These would not have remained on the surface had abrasion been more severe. Despite pressure and speed conditions similar to T.D.C., wear rig abrasion effects were less than are encountered in marine engines. Consideration of the significant differences between rig and engine conditions is necessary to understand the reasons for, and possible remedies to, this situation.

Lubrication conditions in the rig were flooded over the whole track length which did not result in the partial or total oil starvation sometimes found at T.D.C. in marine engines. This may cause collapse of lubrication[39] and lead to intensification of wear. Temperatures in the rig were modest compared to average surface temperatures near T.D.C. which may be up to 250^{o} C for a highly rated engine[50] and have significant effects on oil properties. Pin and plate were fixed on the rig, which continuously reciprocated the the same areas of the specimens against each other producing very smooth conforming surfaces which were able to support effective lubrication. Surfaces in an engine cylinder rarely become as smooth as these which may be attributed to a

combination of the nature of ring and liner contact and three body abrasive effects. Changes in areas of contact between rings and liner can be caused by several factors:

1) Ring tilting at the ends of each stroke
2) Rotation of rings in piston grooves
3) Thermal expansion and contraction of cylinder components
4) Tilting of the piston

One effect of these movements would be that a groove formed on one of these surfaces on one pass would be unlikely to be in contact on the next pass, with the asperity on the mating surface which caused that damage. Ring and liner surfaces would be continually changing and reach an equilibrium roughness in excess of that produced on the rig specimens surface. It is also possible that in a marine engine the effects of air-borne abrasive particles, combustion products and debris from the wear surface are more important in preventing the formation of smooth surfaces. They can also significantly affect abrasive wear of the ring and liner, particularly over the top of the stroke to produce more severe abrasive conditions than were encountered in the wear rig test.

5.5 PETTER ENGINE TESTS

Although the worn surfaces of the two liners after 24 hours running-in appeared to be slightly different, this was not considered to be significant compared to differences between the liners at the end of the test. Dissimilarities of this magnitude are expected during running-in which accommodates minor component variations resulting from

manufacture and assembly.

Etched phosphide eutectic was present near T.D.C. of liner B which was due to acid formation. The combination of low suphur fuel and low T.B.N. oil should have ensured that corrosion was minimal and similar for both tests. Two possible causes of acid condensation were either low cylinder temperature or fuel contamination but precautions were taken to avoid both these occurrences. This corrosion was not thought to have materially influenced running-in, as abrasion and wear on most of the remaining liner surfaces from the two tests were similar.

At the end of 144 hours, the observed wear on both liners had increased but was more severe on liner A which had been run on high sulphur fuel (H.S.). Profile measurements at the end of the test show both liners to have experienced similar wear rates (Fig 105). This anomaly was thought to be due to too few measurements to accurately assess wear around these non-uniform surfaces. Wear measurement of liner A may not have included the more severe wear at 180^{o} to the oil hole which would underestimate total wear. As wear of liner B was more uniform, this was thought to give the most accurate result. This wear rate of 0.05 mm/1000 hours, although based on a short period, compares well with low speed marine diesel cylinder liners which have acceptable rates of up to 0.1 mm/1000 hours.

Examination of the L.S. liner surface revealed evidence of corrosion near T.D.C. (Fig 82), but this was not widespread. Fine abrasion appeared to be the predominant wear mechanism but some coarse abrasion was also visible (Fig 84). This

originated from honing marks where debris may have collected and ran down the liner from near the top of the stroke. It was thought that this was linked to the minimum oil film thickness which would occur just below T.D.C. on the combustion stroke[81]. Over the middle of the liner, abrasion had resulted in a smooth surface which formed plateaux between the remaining honing marks (Fig 81). This is considered to be a good lubrication surface as the plateaux are able to support hydrodynamic oil films while the grooves distribute and hold lubricant on the surface.

Wear near B.D.C. had not increased significantly beyond that observed at the end of the run-in stage. Smoothing of the original honing had occurred vertically in narrow bands (Fig 83), which was indicative of effective lubrication over the whole stroke which maintained an oil film thickness in excess of the liner asperities.

On the second ring, only 60% of the available surface had worn in the L.S. test (Fig 98). A reduction in gas pressure and temperature down the ring pack would result in an increased film thickness between the second ring and liner and less wear would result. Rather surprisingly however, the surface of the second ring was extremely smooth and even showed some evidence of corrosion (Fig 100). Under normal conditions, piston rings become abraded[62, 83]. It is not clear whether this wear was normal for the modified Petter engine, using similar conditions, as rings from other tests were not available for comparison. The situation was thought to be due to hydrodynamic lubrication over the whole stroke, which prevented ring and liner contact.

Two zones of wear severity were identified on the high sulphur test liner. From the remaining evidence of honing it was possible to estimate that wear at 0^{o}, 90^{o} and 270^{o} to the oil hole was only slightly more severe than that on the low sulphur test liner (Fig 94). Corrosion was, however, more evident over most of the stroke. This corrosion had not caused a large increase in liner wear in these areas. Localised regions were produce at the bottom of the stroke in which phosphide eutectic, pearlite and areas around graphite were deeply etched (Fig 90). These surfaces were almost free from abrasion and were very similar to effects produced in the corrosion rig.

At 180^{o} to the oil hole, corrosion and abrasion were found to be more severe (Figs 86 + 87). As liner temperatures monitored around the bore indicated no change at 180^{o}, the reason for intensified corrosion was thought to be insufficient oil alkalinity. Movement of the piston rapidly spreads oil and alkaline additives, in a narrow band above and below the oil supply point. Spreading of this oil around the bore occurs at a much slower rate and when it reaches the opposite side of the bore it may be chemically exhausted[52]. As the low sulphur test indicated no variation in lubricant availability around the bore, it was probable that the oil had insufficient alkalinity to control acid condensation in this position.

Acid levels may have been much higher in this test than other engines run at identical temperatures but with residual fuels. Burtenshaw and Lilly[37] pointed out that sulphur which is added to a base fuel as light molecules may not burn

or condense in the same way as sulphur in its natural state in residual fuels. As a result the volume of acid may not be respresentative of that encountered in marine engines using residual fuels.

On the test liner, nearly all evidence of honing had been removed from the upper part of the stroke (Fig 85). Wear at the bottom of the liner was not as severe although both corrosion and abrasion were evident (Fig 90). A differential wear mechanism caused phosphide eutectic to be left standing above the matrix in the upper part of the cylinder and the eutectic itself was deeply etched (Fig 87). Examination of the matrix did not show severe corrosion although some evidence of slight pearlitic corrosion was visible.

Fine abrasion had caused the phosphide eutectic surface to appear polished (Fig 89), but the effect of large hard abrasives could also be observed (Fig 92). As particles passed over phosphide phases the abrasive groove width diminished with only a slight depression remaining on the other side of the phosphide. Plastic deformation would result in work hardening of the phase. Large abrasives would be broken into smaller particles which would not protrude through the oil film to cause such severe abrasion of the matrix.

These worn surfaces do not resemble those of marine liners surveyed by Dent[85] or Nadel and Eyre[67]. This is thought to be due to a number of contributory factors. Corrosion appears to be much more extensive and its effects more severe on the experimental liners and rings than on marine engine surfaces. This may be partly due to unrepresentative fuel and to an unsuitable lubricant, but its effects were

exaggerated by the liner material which other corrosion tests have shown to be unsuitable for corrosive environments. The corrosive effects were also extensive because of the lack of abrasion which appeared to be a result of efficient lubrication. Abrasion has been shown to be more severe in marine engines, particularly near T.D.C. and also on the piston rings. More severe abrasion in the tests would also have tended to obscure corrosive effects around the top of the stroke and on the rings.

Analysis of radioactive debris in the oil drains showed that both tests had similar top ring wear rates during the running-in period (Fig 106). Wear of the rings did not appear to have been affected by engine dismantling and reassembly. For the 0.18% sulphur fuel, wear continued at a similar rate for the duration of the test. For the other test, when fuel sulphur was increased to 3.5% after running-in, wear of the top ring increased to over 15 mg/hr after 130 hours, and was sixty times greater than that of the L.S. test.

Chemical analysis of the oil indicated that corrosion reached a peak of 1 mg/hr after 80 hours and did not accelerate over the range of maximum ring wear. This intensification of ring wear, therefore, was not directly due to an increase in metal corrosion. Ferrography indicated that the increase coincided with stimulation of particle production by corrosion resulting from use of high sulphur fuel (Fig 108). These particles may have been produced by a number of mechanisms:-

1). Products of combustion and cylinder deposits.

2). Products of corrosion.

3). Particles released as a result of wear.

Burtenshaw and Lilly[37] have shown that an increase in abrasion as a result of severe corrosion was not a result of abrasives generated during combustion. Although they suggested that the increase might have been due to wear debris released as a result of corrosion, they concluded that it was caused by detached fragments of cylinder deposits resulting from the use of residual fuels. This mechanism is not likely to have a serious effect in the Petter engine tests as distillate fuel has less tendency to form such deposits[38].

Calcium sulphate, a by-product of neutralisation of sulphuric acid by calcium based alkaline oil additives, was found to be soft (1.5 Moh's degrees) and does not cause abrasion[38]. Ferrous sulphate which is produced by reaction of sulphuric acid with ferrous surfaces, was thought by McConnel and Nathan[83] to be oxidised through heat produced by combustion in an engine to ferric oxide, Fe_2O_3. There are two forms of this oxide, α and γ , which have a hardness of 500 to 600 Hv. and upto 900 Hv. respectively. The extent to which these occured in an engine was not identified. They[83] also found evidence to show that corrosion could weaken the cast iron matrix and allow removal of metal by abrasion. This was thought to be partly responsible for the increase in oil drain particles for the Petter test run with high sulphur fuel.

Although it has been suggested[83] that corrosion released large particles from the wear surface by subsurface attack, none of these authors appreciated the significance of preferential corrosion of ferrite in cast iron. Cementite lamellae on the surface of a pearlitic cast iron liner would be continuously exposed. These unsupported carbide lamellae

can then be removed either by abrasion or pressure waves generated in the oil by piston ring movement.

As the cast iron matrix receded, phosphide eutectic islands are left standing above the surface. In many cases the phosphides are interconnected by a subsurface network, especially when phosphorus content is above 0.5%. Some of the unconnected phosphide may have been released by corrosion of the matrix. Areas were identified on the liner surface, where small particles appeared to have been removed (Fig 88). Photographic stereo pairs indicated these areas to be depressions, but it is possible to obtain the same information from interpretation of the electron beam shadowing. Particles removed are likely to be phosphide eutectic as phases of similar size and distribution remained on the liner surface. Fracture of phosphide eutectic occurred for other particles to break away from the surface to cause deep abrasive grooves down the liner (Fig 92). This process may have been accelerated by corrosion of ferrite from the eutectic which had weakened its structure.

Particle concentration in the oil, which increased as a result of these corrosion induced effects, would cause an intensification of abrasion. There was no evidence, however, to suggest that this caused the increase in top ring wear after 100 hours, which was established by radioactive debris analysis.

The rate of lamellar cementite debris production would remain constant throughout the test providing corrosion was uniform. Phosphide eutectic fracture and release of debris would increase as corrosion of the matrix proceeded but

evidence for this was not sufficiently extensive to account for the rapid increase in top ring wear.

Although the evidence was not conclusive, it is thought that the protruding eutectic contributed directly to abrasion of the piston ring. Corrosion and abrasion are known to cause the matrix to recede leaving hard phosphide eutectic standing proud of the surface. As the area of this phase has been measured to be 10% of the surface, it would not be able to support a hydrodynamic film between itself and the rings. When the protruding phase approached the oil film thickness between the ring and matrix, wear of both phosphide and ring would increase as a result of interaction with oil suspended abrasives. Equilibrium would be achieved when wear of the protruding phosphide was the same rate as the receding matrix. This would cause a large increase in wear rate of the top ring for the reasons previously discussed.

A combination of released cementite and phosphide eutectic would explain the increase in particle density in addition to the increase in ring wear at the beginning of the high sulphur test. When corrosion had caused sufficient wear of the liner and ring matrix, contact between the components would result in a rapid increase in ring wear identified from radioactive debris after 100 hours running. Evidence to support this proposed mechanism can be found in the polished nature of the phosphide eutectic surfaces compared to the matrix (Fig 89). In addition, it was clear that abrasion was more severe on these phases. As no evidence of abrasion to fracture and plough particles of iron phosphide was visible, (Fig 92), the necessary force must have come from direct ring

contact.

The final evidence comes from the lack of abrasion on the second ring surface which suggests that the measured increase in wear and debris was confined to the top ring. This ring would first make contact with the protruding phase and experience the highest wear rate.

Unfortunatley this ring was not available for examination as it was still radioactive at the end of the test. It would be necessary to complete this examination at sometime in the future to establish the mechanism.

5.6 ENGINE WEAR

Examination of surfaces from corrosion and wear rig tests in addition to those from the Petter engine has established a greater understanding of the interaction of corrosion and abrasion in marine diesel engines. Corrosion acting as a single mechanism produces rough surfaces on which differential corrosion preferentially dissolves any ferritic phases. This leaves phases of phosphide eutectic and bulk carbides standing above the matrix surface.

Corrosion effects occur over the engine stroke where acid is able to condense and is deposited as a result of acid distribution by the piston rings. As oil films are thinner around T.D.C., the volume of alkaline additives that are held in the oil is less than over the centre of the stroke. Acid which is swept to these areas[39] is likely to cause more severe corrosive than elsewhere on the liner surface. Abrasion varies over the engine stroke, depending on the oil film thickness separating ring and liner. It is most severe just after T.D.C.[85] on the liner but is apparent over the

whole piston ring rubbing face. Because lightly etched surfaces, associated with corrosion over the centre of the stroke[67], are not present in the severely abraded areas, it does not establish conclusively that no corrosion occurs. McConnel and Nathan[83] have seen evidence of corrosion in the form of irregularities in deep abrasive grooves over the upper part of the stroke and on the piston rings. This shows that acid attack cannot be discounted in these areas. Corrosion of the ring faces and upper part of the engine stroke, where abrasion is normally most severe, may be difficult to identify unless examined directly in an S.E.M.

Relatively smooth surfaces are produced over the centre of the engine stroke where oil film thicknesses are maximum and abrasives carried in the oil do not result in the type of damage associated with T.D.C. These conditions therefore produce more obvious evidence of corrosion in the form of etched smooth surfaces.

There appears to be, therefore, two areas of the liner surface where the mechanism of corrosion/abrasion interaction may be completely different. In areas where abrasion predominates over corrosion, the surface would be removed by mechanical wear as soon as it was weakened by corrosion. Corrosion has been shown to dissolve ferrite from both phosphide eutectic and pearlite which would make the phases less resistant to mechanical wear. This combined effect would produce more hard abrasive particles of iron phosphide and cementite than abrasion or corrosion could, acting on their own. As bulk metallic carbides are less susceptible to corrosion, they may be more effective against abrasion than

phosphide eutectic in this type of environment. Over the centre of the stroke, abrasion is not as severe and does not result in wear of the constituent hard phases to the same extent. Abrasives suspended in the oil or the hydrodynamic oil pressure shock wave are thought to cause fracture of the uncorroded cementite lamellae. Corrosive effects are very even because abrasion continually "polishes" the surface to prevent the effects which cause concentrated attack. As was found in the Petter engine tests, uncorroded phases which protrude on the surface may be released into the lubricant by corrosion along with smaller cementite lamella. This debris could then intensify abrasion in other areas of the liner and on also the ring. The height of phases above the matrix is thought to be essentially governed by abrasion. A point has to be reached where the wear rate of the hard phase matches that of the receding matrix. It is clear that as the oil film thickness separating the protruding phase and ring decreases, more abrasives in the oil are able to cause wear of, not only the hard phase but also the rings. If, as was thought to be the case in the Petter tests, the abrasives in the oil are not able to control the height of the hard phase, direct interaction with the ring would occur. This would then cause a rapid increase in the ring wear rate but would not increase liner wear to the same extent.

Any question of the benefits of corrosion has to be considered in the light of all areas of wear interaction. Corrosion and abrasion over the mid-stroke, produce a hard phase network above the liner surface which would first make contact with the ring to protect the liner matrix in the event of lubrication failure. This corroded surface may

also hold and distribute lubricant effectively, but in addition to stimulation of abrasion in other areas of the liner, corrosion causes wear of the matrix over the centre of the stroke. This in turn can cause intensification of abrasion by undermining and subsequent release of bulk hard phase particles and more severe abrasion of the ring if direct contact is made through the oil film. Corrosion in marine engine cylinders, therefore, is thought to be detrimental to engine operation. In fact measurements of engine liner wear show that corrosion effects are reduced using low sulphur distillate fuels or highly alkaline lubricants[37] and liner and ring wear is reduced.

There are four components of marine engine operation which can influence the corrosive problem:

1). Marine fuels.

2). Marine lubricants.

3). Engine design.

4). Ring and liner materials.

The main reason for the use of residual fuels in marine diesel engines is that they are inexpensive compared to alternative fuels[88]. This is likely to continue to be the case, as burning the fuels at sea is the simplest and cheapest way for refineries to dispose of pollutant contaminants concentrated in refinery residues. Golothan[89] thought it possible that as shipping costs increased, the proportional cost of fuel would become insignificant so that improved fuels could be adopted. This has not occurred during the elapsed ten years as fuel costs have escalated at a similar rate to shipping costs. At the present time, however,

increased maintenance costs resulting from use of residual fuel does not outweigh the cost of superior, low sulphur distillate fuel[90]. Removal of the offending sulphur from the fuel would increase its cost and defeat the object of using the fuel in the first place.

High sulphur residual fuels can only be tolerated in marine engines with the use of alkaline anti-corrosive cylinder lubricants. It is usual to employ 70 T.B.N. oils but up to 100 T.B.N.[91] are often used. Improvements in this area may lie in increasing oil spreadability within the cylinder to ensure even protection against acid condensation. Benefits may also be gained by matching oil T.B.N. with fuel sulphur, but this is not always possible.

It is feasible to limit acid condensation by temperature control of the liner surface. Temperatures above the acid dew point over the whole stroke would have to exceed 180° C at T.D.C.[39] which could result in ring sticking and oil breakdown. Laxton[64] has shown that with perfect mixing of fuel and air, sulphur containing fuels can be combusted to restrict acid deposition by limiting the volume of SO_3 which formed. A reduction in acid vapour, formed in marine diesel engines, may be achieved therefore, by improvements to combustion chamber design.

Grey cast iron is almost universally used as a cylinder liner and piston ring material for marine engines. It has proved itself to have a good compromise of properties, its metallic matrix has a dispersion of beneficial hard phases such as phosphides and metallic carbides and the presence of graphite flakes can act as a solid lubricant. It is prone,

however, to corrosive attack by mineral acids which tends to release its hard phase particles from the surface. Over the last few years, phosphorus has been reduced from 0.6 to 0.2% and replaced by 0.1 to 0.25% vanadium. This has improved casting soundness but has also resulted in improved performance in corrosive environments[32]. This is thought to be due to the reduction of phosphide eutectic which has been shown to be weakened by corrosion.

Analysis of engine wear suggests that it is necessary to design ring materials which are more abrasion resistant and liners, more resistant to corrosion to achieve benefits in engine wear. Ideally this should be achieved without sacrificing any benefits of cast iron in resistance to scuffing and pure abrasion. Harder ring material were evaluated by Burtenshaw and Lilly[37] and found to be beneficial. Hard chromium plating has also been used with some success but problems may be experienced in scuffing situations. Although the corrosion rig showed steel to be superior to cast iron, it has poor tribological properties and is difficult to manufacture. Where steel is used as a liner material it is often chromium plated to improve its wear resistance. Austenitic cast iron liners are beneficial for corrosive environments but are softer than conventional types and are prone to higher abrasion and scuffing[34]. Chromium plate is often used to refurbish liners and is more corrosion resistant than cast iron, but problems have occurred as a result of poor lubricant wettability. This may be improved by special finishes such as channel cracking or grit blasting which benefit lubricant distribution. In the future it is

possible that a deposited ceramic layer may prove to be beneficial for all aspects of wear.

In view of the foregoing grey cast iron is unlikely to be superceded in the foreseeable future by a substantially different material. Small modifications may be possible to control corrosion/abrasion effects. Elimination or reduction of phosphide eutectic in favour of metallic carbides or a finer pearlitic structure, to reduce the size of released cementite lamella may also bring about future improvements.

6. CONCLUSIONS

1) A laboratory test rig has successfully reproduced the mechanisms of abrasion and corrosion encountered in some marine engine environments. The severity of the individual mechanisms have been balanced to reproduce worn surfaces similar to phenomena found over large areas of marine liners.

2) Films were formed during rig testing in worn areas which were not formed under more equilibrium conditions. These non-equilibrium films were found to be more stable during wear than would be expected from their equilibrium properties.

3) The heterogeneous structure of grey cast iron promotes corrosion of its internal phases in moderately concentrated sulphuric acid conditions. This was due to a number of effects:

a) Electrochemical differences caused ferritic phases to dissolve in preference to all other major cast iron constituents.

b) Corrosion was accelerated around cathodic phases by the formation of relatively stable protective films on the cast iron surface.

4) Engine tests showed that the introduction of a corrosive environment led to a greater intensification of top ring wear than could be directly attributed to the corrosive effects. This increase is thought to be caused by stimulation of abrasive wear by particles released

from surfaces weakened by corrosion.

5) The mechanism of interaction of abrasion and corrosion has been found to be due to mechanical removal of hard debris from surfaces weakened by selective corrosion of ferritic phases. Subsequent release of particles is thought to lead to an intensification of abrasive effects. Two sources of abrasive were identified.

a) Wear of lamellar pearlite released cementite into the lubricant environment.

b) Attack of the phosphide eutectic is selective, the iron phosphide is not attacked whilst the ferrite is removed. The resulting weakening of the structure combined with the removal of the surrounding matrix, led to fracture and production of iron phosphide debris.

6) Several materials with more homogeneous structures were found to have superior corrosion resistance to grey cast iron but these are unlikely to be adopted as piston ring materials for marine engines as their other significant properties are inferior.

7) Ring and liner materials which have evolved for use in predominantly abrasive conditions do not necessarily have optimum properties for use in corrosive environments.

7. SUGGESTIONS FOR FURTHER WORK.

There are several areas which it is felt that the work presented in this thesis may be beneficially continued. One obvious limitation of the reciprocating rig is its inability to simulate severe abrasive conditions in lubricated environments. Although modifications to the design in order to reduce the conformity of the pin and plate specimens during running-in would be expected to increase abrasion, it may also be necessary to introduce foreign abrasives into the oil system. Rather than use debris collected from engine ports which may have been previously degraded by wear, it is thought that size graded particles such as silicon carbides would be more suitable. The size of the grit should be selected to produce damage similar to engine bore abrasion.

An increase in abrasion would enable wear nearer to T.D.C. to be simulated in the test rig. This is an area which deserves particular attention as the mechanism of removal of debris from surfaces weakened by corrosion is more severe at the top of the stroke. This is likely to be the most critical area of engine wear in corrosive environments. In addition to increasing abrasion, it may also be advantageous to revert to an additive lubricant to reduce the possibility of oxide formation on the wear surface. Increasing abrasion in isolation is likely to have the effect however, of controlling the formation and stability of surface films.

In order to increase and control the period of corrosion in the rig, a total loss oil system would be an advantage in which oil and acid were continuously fed into the specimen bath to be pumped out and discarded.

With the present rig it would be useful to evaluate a number of material effects. As it seems likely that grey cast iron will be utilised for some time for marine ring and liners, one of the most interesting areas for continued investigation would be the influence of microstructure. Some of the more important variables would be the volume of phosphide eutectic, pearlite spacing and morphology and graphite distribution and flake size in lubricated corrosive enviornments.

The wear rig is able to reproduce the severity of wear identified over large areas of marine engine surfaces. Significant industrial benefits may now be available with the careful control of the rig parameters outlined above. Wear rates on the rig and from engines have not been correlated in this study but if these could be obtained and useful correlations existed, the information gained from these studies would be more directly relevant to ring and liner manufacture.

In view of the present interest in the development of lower friction lubricants for energy reduction in engines, the rigs ability to separate lubricants on the basis of their frictional performance may also be valuable.

8) ACKNOWLEDGEMENTS

Sincere thanks are due to Professor C. Bodsworth and his staff in the Department of Metallurgy for providing facilities and assistance throughout this project. As supervisor, Dr. T.S. Eyre has always been constructive in discussion and his contribution to the work and general assistance are greatly appreciated.

The work has been jointly sponsored by the Science Research Council and Esso Research Abingdon, under the C.A.S.E. scheme. Dr. R. Price, Dr. C. Clarke and the technicians of Marine Lubricants at Esso have been very helpful during the periods of work on their site where the engine and corrosion rig tests were performed.

The time and effort of Mrs. M. Dale is appreciated for the typing of this thesis.

Finally, special thanks go to the author's family for their continued support and encouragement during his time at Brunel University.

9. REFERENCES

1. EYRE, T. S. Trib.Int., (1978), 11, 91 - 96.

2. O.E.C.D. Research Group on Wear of Engineering Materials.

3. SCHILLING, A. Automobile Lubrication, Scientific Publications, (1971), Ch. 7, 2 - 21.

4. KRUSCHOV, M. M., BABICHEV, M. Research on Wear of Metals, (1960), Ch. 8.

5. SEDRICKS, A. J., MULHEARN, T. O. Wear, (1963), 6, 457 - 466.

6. GODDARD, J., WILMAN, M. Wear, (1962), 5, 114 - 135.

7. RICHARDSON, R. D. C. Wear, (1967), 10, 291 - 309.

8. RICHARDSON, R. D. C. Wear, (1968), 11, 245 - 275.

9. KRUSCHOV, M. M. Wear, (1974), 28, 69 - 88.

10. KRUSCHOV, M. M. Proc.Int.Conf. on Lub. and Wear. Inst.Mech.Eng. London (1957).

11. NATHAN, G. K., JONES, W. J. D. Wear (1966), 9, 300 - 309.

12. AVIENT, V. W. E., GODDARD, J. and WILMAN, H. Proc.Roy.Soc.A. (London), (1960), 258, 159 - 180.

13. RABINOWICZ, E., MUTIS, A. Wear, (1965), 8, 381 - 390.

14. RABINOWICZ, E., PUNN, L. A., and RUSSEL, P. G. Wear, (1961), 4, 345 - 355.

15. MILLER, N. E. Wear, (1980), 58, 249 - 259.

16. MULHEARN, T. O., SAMUELS, L. E. Wear, (1962), 5, 478 - 498.

17. JOHNSON, R. W. Wear, (1960), 16, 351 - 358.

18. LARSON-BADSE, J. Wear, (1968), 11, 213 - 222.

19. SIN, H., SAKA, N. and SUH, N. P. Wear, (1979), 55, 163 - 190.

20. KRAGELSKII, I. V. Friction and Wear, Butterworth, London (1965).

21. MOORE, M. A. Wear, (1974), 28, 59 - 68.

22. MUTTON, P. J., WATSON, J. D. Wear, (1978), 48, 385 - 398.

23 RABINOWICZ, E. Lub.Engineering, (1977), 33, 378 - 381.

24. HEAD, W. J., HARR, M. E. Wear (1970), 15, 1 - 46.

25. SHELDON, G. L. Trans.Am.Soc.Mech.Engrs., (1970), 92, 619 - 626.

26. EYRE, T. S. Trib.Int., (1976), 9, 203 - 212.

27. BOWDEN, F. P., TABOR, D. The Friction and Lubrication of Solids, Oxford, (1950).

28. WELSH, N. C. Phil.Trans.Roy.Soc., (1965), 257, 31 - 70.

29. BURWELL, J. T. Wear, (1957/58), 1, 119 - 141.

30. SUH, N. P. Wear, (1973), 25, 111 - 124.

31. WATERHOUSE, R. B. Fretting Corrosion, Pergamon Press, (1972).

32. MOORE, D. F. Principles and Application of Tribology. Pergamon Press, (1975).

33. MACPHERSON, P. B. Trib.Int., (1978), 11, 6.

34. TAYLOR, B. J., EYRE, T. S. Trib.Int., (1979), 12, 79 - 81.

35. SUNDEN, H., SCHAUB, R. Trib.Int., (1969), 2, 3 - 12.

36. GRAHAM, R. et al, Foundary Trade Journal, (1960), 30, 805 - 811.

37. BURTENSHAW, R. P., LILLY, L. R. C. Trans.Inst.Mar.E., (1972), 84, 389 - 410.

38. COTTI, E., SIMONETTI, G. Inst.Mar.E., (1969), 46, 15 - 53.

39. GOLOTHAN, D. W. Ind.Lub. and Trib., (1978), 30, 72 - 77, 30, 128 - 133.

40. ANGUS, H. T. Cast Iron, Butterworth, London, (1960). 2nd Ed. (1976).

41. MAAHN, E. Brit.Corros.J., (1966), 1, 350 - 354.

C.D.A. Copper in Cast Iron, (1946), London.

43. HOAR, T. P., HAVENHAND, D. J.Iron and Steel Inst., (1936), 133, 239 - 289.

44. ENDO, H. Science Reports of Tohoku Univ., (1928), 17, 1245.

45. GLANTZ, G., MAAHN, E. Dansk Kemi, (1964), 45, 41.

46. MANUEL, R. W. Corrosion, (1947), 3, 415 - 431.

47. RADD, F. J., McGLASSON, R. L. Pet.Trans. A.I.M.E., (1954), 201, 73 - 78.

48. LaQUE, F. L. Corrosion, (1958), 14, 55 - 62.

49. WESLEY, W. A., COPSON, H. R., and LaQUE, F. L. Metals and Alloys, (1936), 7, 325 - 329.

50. CLARKE, G. H. Marine Diesel Lubrication, (1970). Burmah-Castrol Pub.

51. ANON. The Motor Ship, (1978), 59, 59 - 60.

52. HOSIE, R. M., SHRAKAMP, J. W. A. The Motor Ship, (1968), 49, 149 - 152.

53. BELCHER, P. R. The Motor Ship, (1971), 52, 396 - 398.

54. STRIBECK, R. V.D.I. - Zeitschrift (1902), 46, 1432 - 1463.

55. LANSDOWN, A. R., HURRICKS, P. L. Trans.I.Mar.E., (1973), 85, 157 - 168.

56. WATSON, C. E., HANLY, F. J., and BURCHELL, R. W. S.A.E.Trans., (1955), 63, 717 - 728.

57. POPPINGA, R. Amer.Soc.Lub.E., (1949).

58. WILLIAMS, C. G. Inst. of Automobile Eng. (1940).

59. BOERLAGE, G. D., GRAVESTEYN, B. J. J. The Motor Ship, (1932), 13, 171 - 173.

60. CLOUD, G. H., BLACKWOOD, A. J. Trans.Soc. Automotive Eng., (1943), 51, 408 - 414.

61 MACFARLANE, J. J. J.Inst. Fuel, (1962), 35, 502 - 505.

62. FURSUND, K. Wear, (1957/58), 1, 104 - 118.

63. JENKINSON, J. R. The Mechanism of Corrosion by Fuel Impurities, Butterworth, London, (1963), 443 - 450.

64. LAXTON, J. W. Ibid. (1963), 228 - 237.

65. FLINT, D., KEAR, R. W. J.Appl,Chem., (1951), 1, 388 - 393.

66. HOEGH, C. Cylinder Wear in Diesel Engines, Aschenough, Oslo, (1942).

67. NADEL, J., EYRE, T. S. Trib.Int., (1978), 11, 267 - 271.

68. WIBORG, T., ERIKSON, J., and TJAERNES, A. Støperitidende, (1974), 40, 71 - 81.

69. LANGBALLE, M. European Ship Building, (1969), 4, 58 - 70.

70. WIBORG, T. J. of Ship Repair and Maintenance, (1978), , 29 - 32.

71. Definitions, Symbols and Units, I.Mech.E.Proc. Lub. Wear, (1957).

72. DYSON, A. Treatise on Material Science and Technology, (1979), 13, 175 - 216.

73. NEALE, M. J. Proc.Instn.Mech.Engrs., (1970), 185, 21 - 32.

74. ROGERS, M. D. Tribology, (1969), 2, 123 - 127.

75. SHAFIA, M. A. Ph.D. Thesis, Brunel University, (1980).

76. AUE, G. K. Proc.Int.Cong. of Comb.Engines, (1973), paper 15, 367.

77. LAZARENKO, N. I. Izdatel Stvo AN SSSR, (1957), 1, 70 - 94. (In Russian).

78. SREENATH, A. V. S., RAMAN, N. Trib.Int., (1976), 9, 55 - 62.

79. WAKURI, Y., ONO, S. Bull. of J.S.M.E. (1973), 2, 47 - 58.

80. NEALE, M. J. A survey of information from Research on Piston Rings and its Application to Design (1973).

81. MOORE, S. L., HAMILTON, G. M. Proc.Instn.Mech.E. (1980), 194, 373 - 381.

82. WAKURI, Y., YANO, T., MITSUTAKE, S. and ONO, J. Bull. of J.S.M.E., (1964), 7, 615 - 624.

83. McCONNEL, G., NATHAN, W. S. Wear, (1962), 5, 43 - 45.

84. DuJUE, J. Proc.Int.Symp. on Marine Eng., Tokyo, (1973), 5E, 25 - 35.

85. DENT, N. P. Ph.D. Thesis, Brunel University, (1980).

86. EYRE, T. S., DENT, N. P. and DALE, P. E. A.S.L.E.-A.S.M.E. Lub. Conf. New Orleans, (1981).

87. MacDONALD, A. G. Private Communication.

88. SULZER BROS. Private Communication.

89. SOMMERFELD, A. Z.Math.Physik, (1904), 50, 97.

90. TAKEUCHI, E. Wear, (1970), 15, 201 - 208.

91. WHITEHEAD, J. R. Proc.Roy.Soc., (1950), A201, 109.

92. SAVAGE, R. H. J.Appl.Phys., (1948), 19, 1.

93. SAMUELS, L. E., CRAIG, J. V. J. Iron and Steel Inst., (1965), 162, 75 - 77.

94. SYASSEN, O. The Motor Ship, (1979), 60, 83 - 84.

95. GOLOTHAN, D. W. Trans.I.Mar.E., (1972), 84, 13.

96. HANSEN, R. K. The Motor Ship, (1979), 60, 82.

97. ANON. The Motor Ship, (1975), 56, 101 - 104.

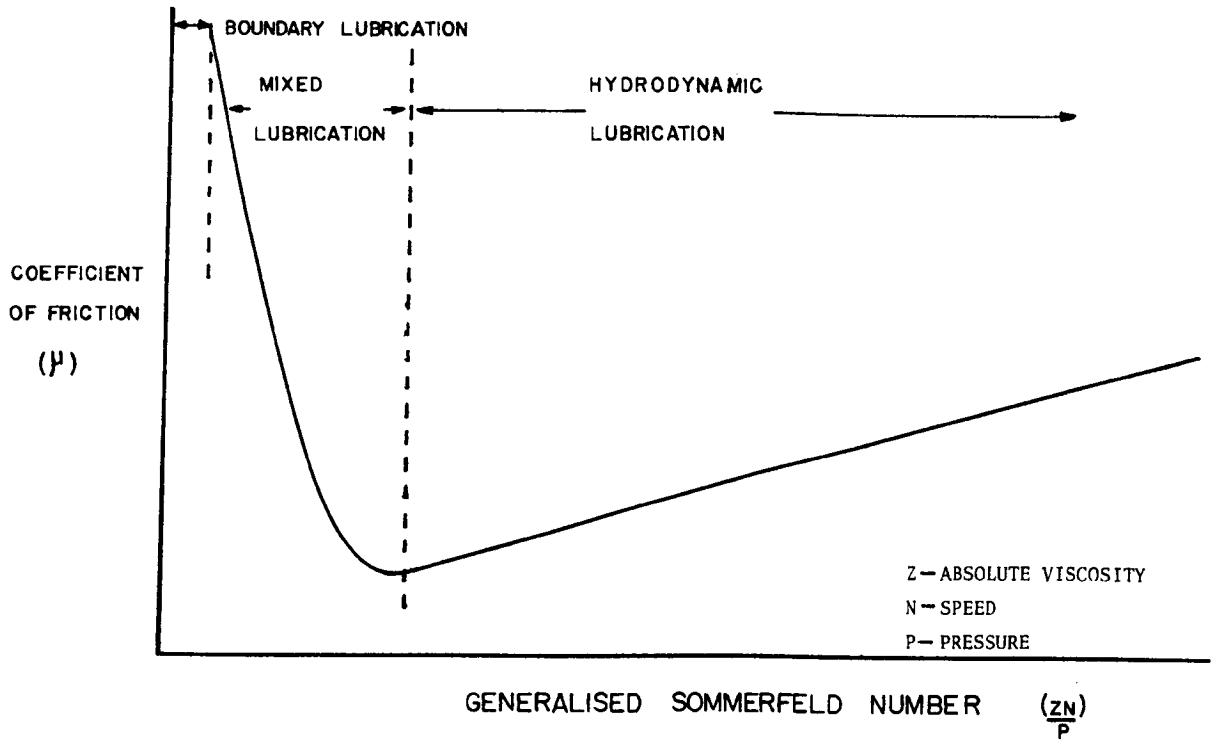

FIG. 1 Stribeck Curve.

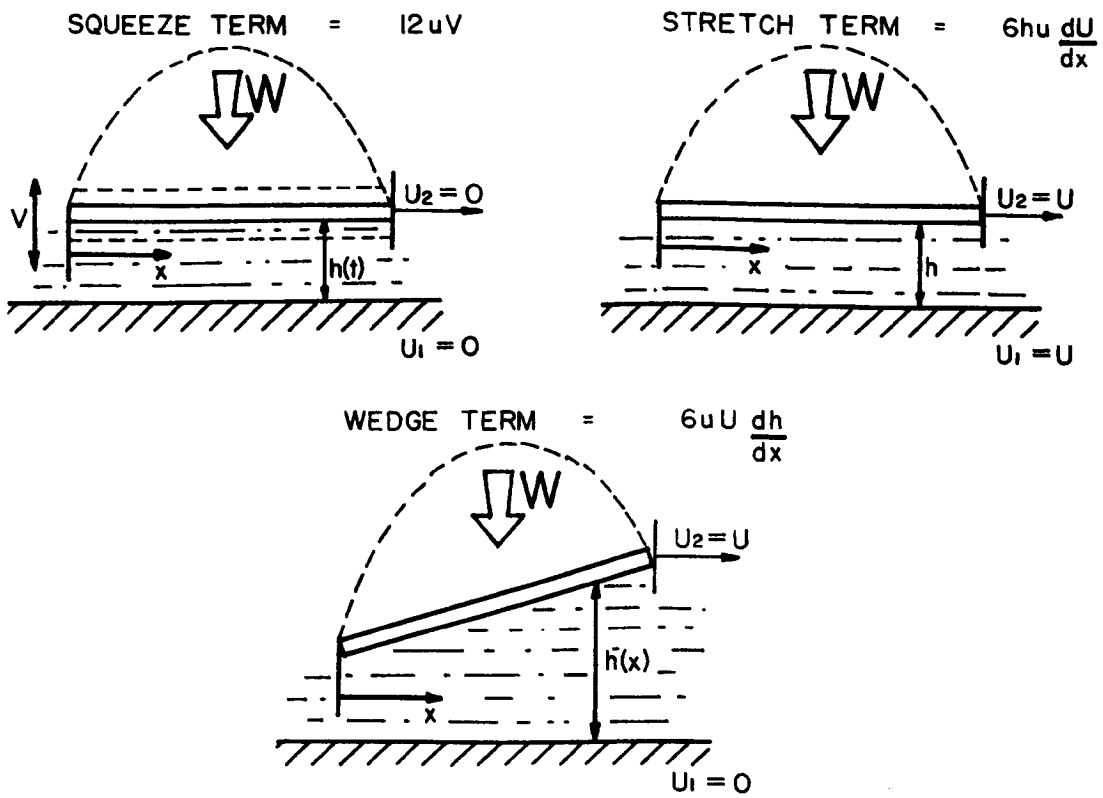

FIG. 2 Factors leading to the generation of hydrodynamic pressures in an oil film.

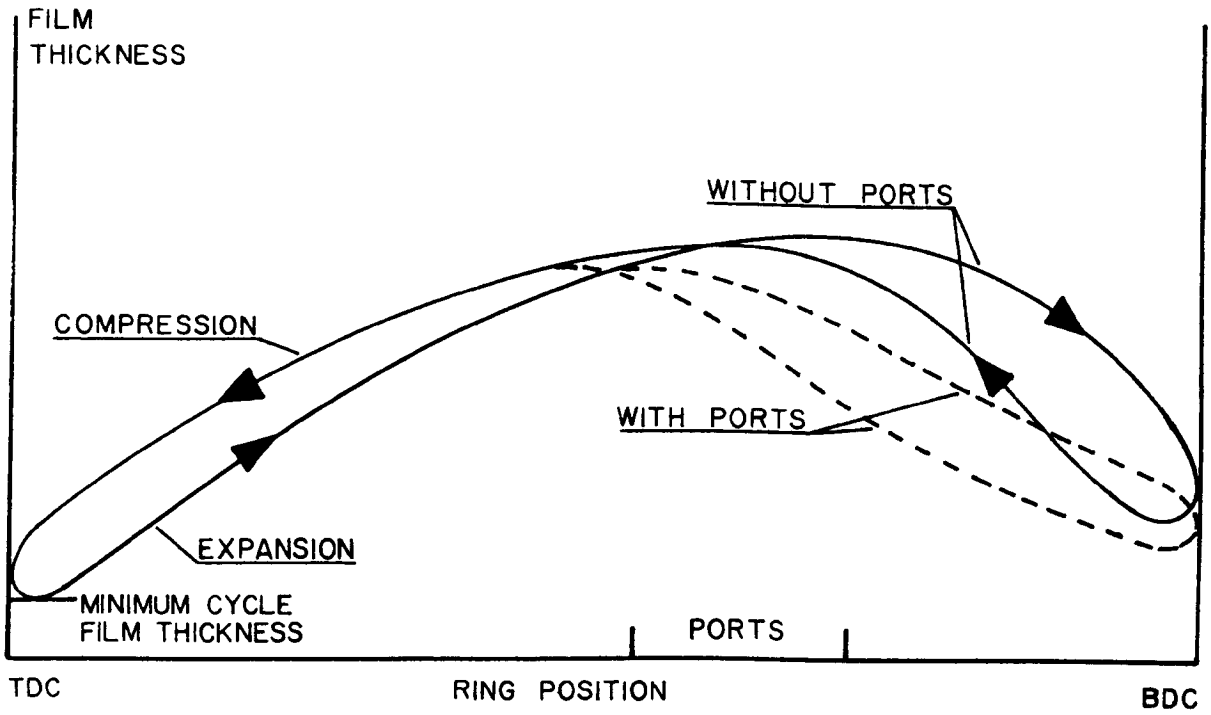

FIG. 3 Variation in oil film thickness over the stroke.

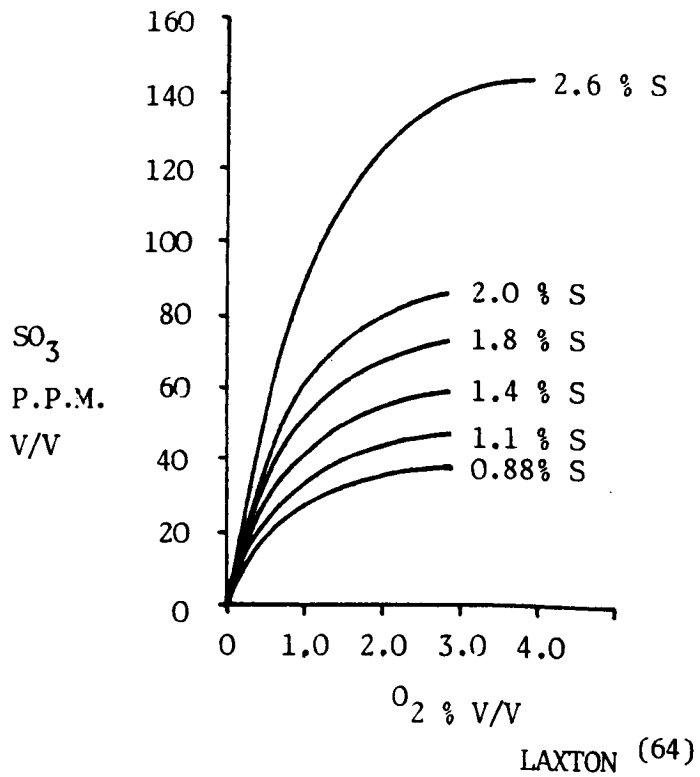

FIG. 4 Increase in SO_3 as fuel sulphur increases in the presence of excess oxygen.

CONCENTRATION OF SO_3 % VOLUME	DEW POINT °C ATMOSPHERIC PRESSURE
0.0016	116
0.0024	135
0.0036	149
0.0056	163
0.0088	177
0.0184	191
0.0560	205

FLINT, KEAR (65)

FIG. 5 Effect of SO_3 concentration on acid dew point.

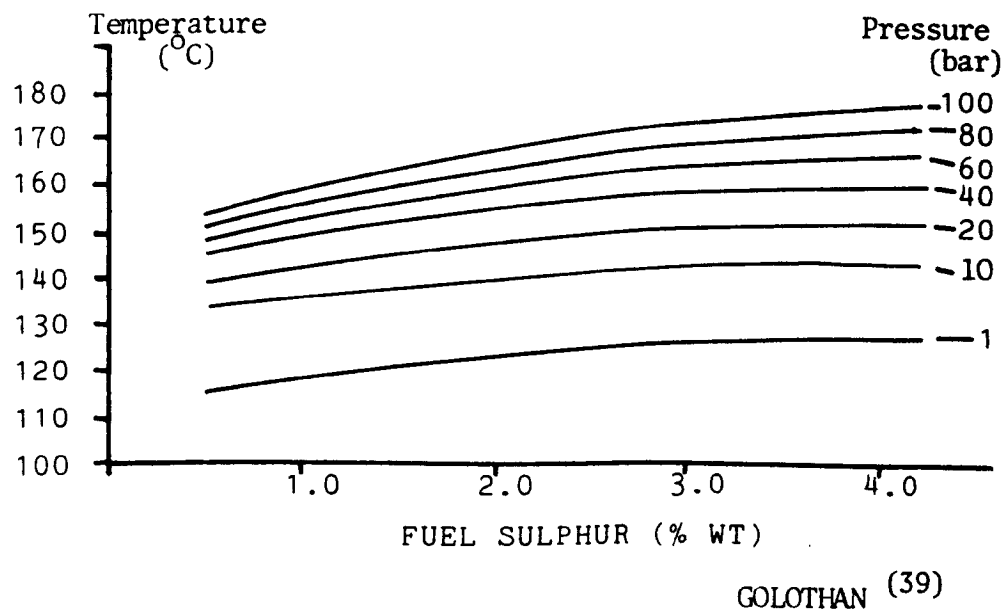

GOLOTHAN (39)

FIG. 6 Effect of cylinder pressure and fuel sulphur content on acid dew point.

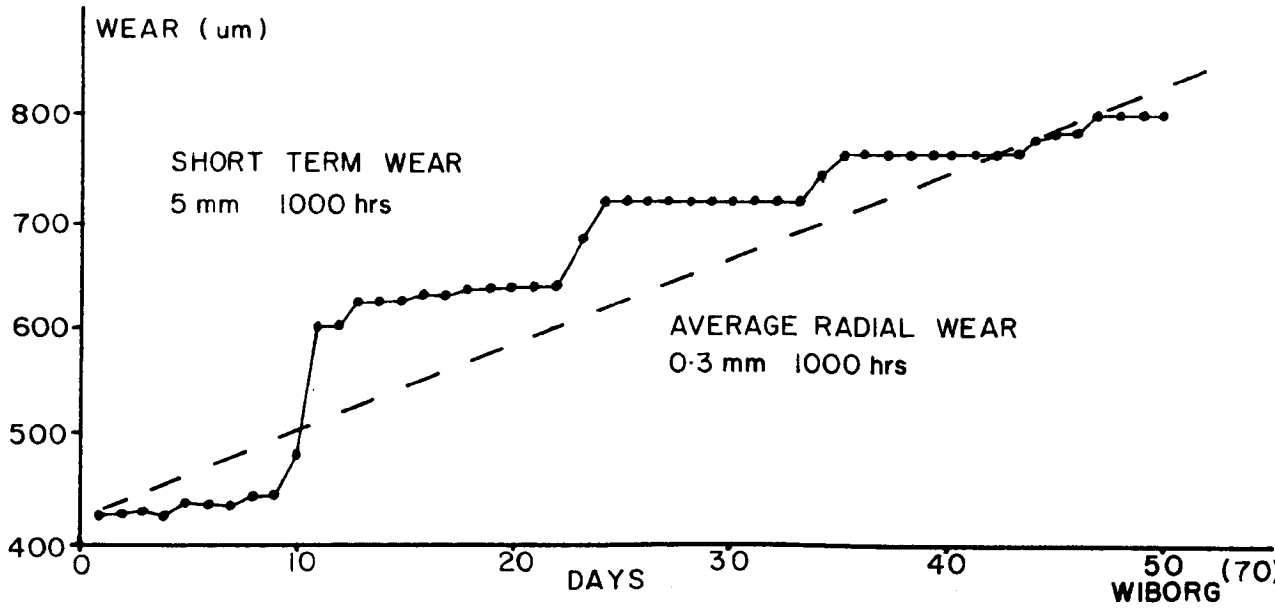

FIG. 7 Intermittent short term high wear rate periods in long term engine wear.

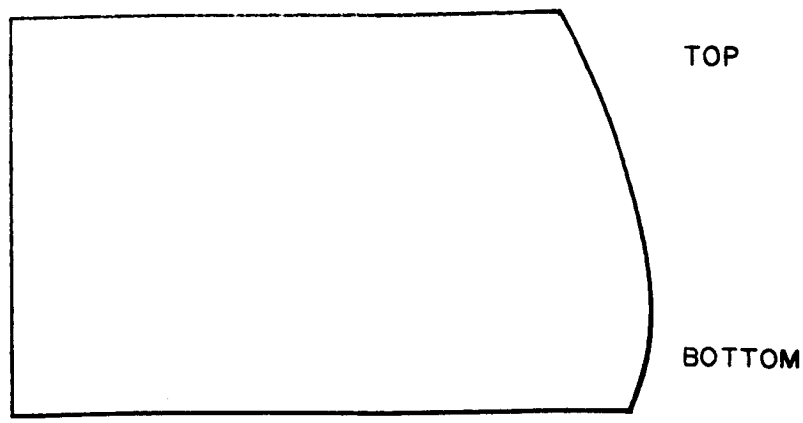

FIG. 8 Typical profile of worn piston ring.

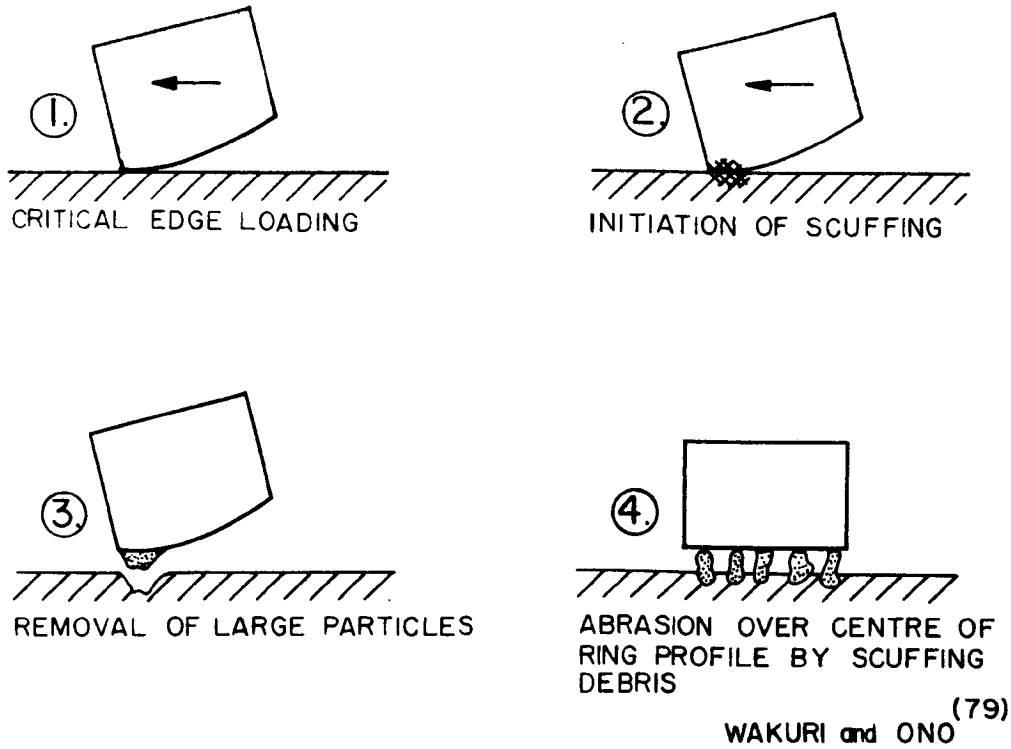

FIG. 9 Proposed mechanism to account for ring scuffing.

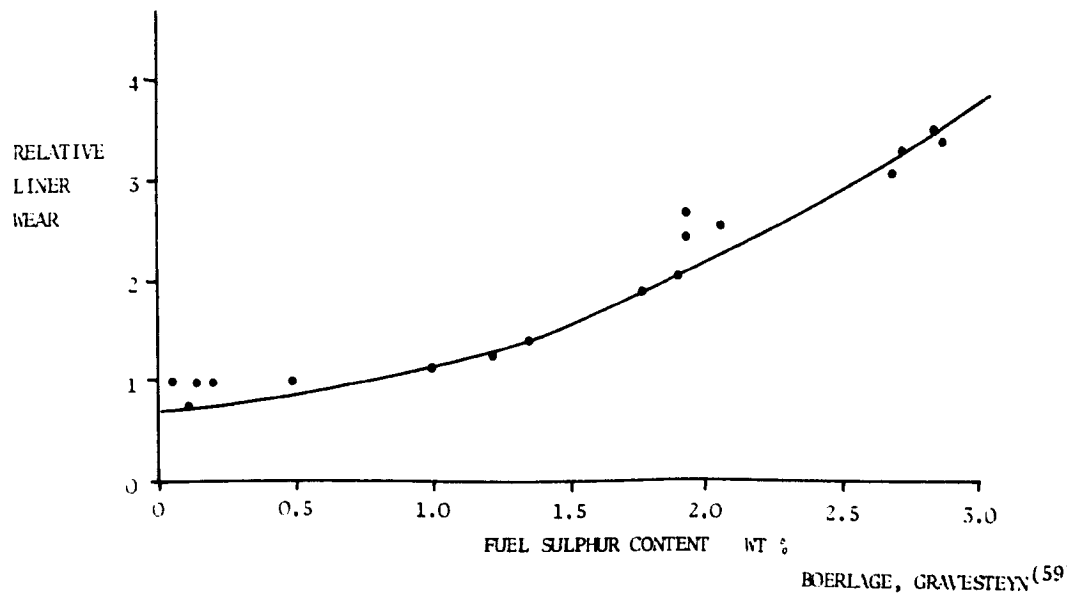

FIG. 10 Influence of fuel sulphur on liner wear.

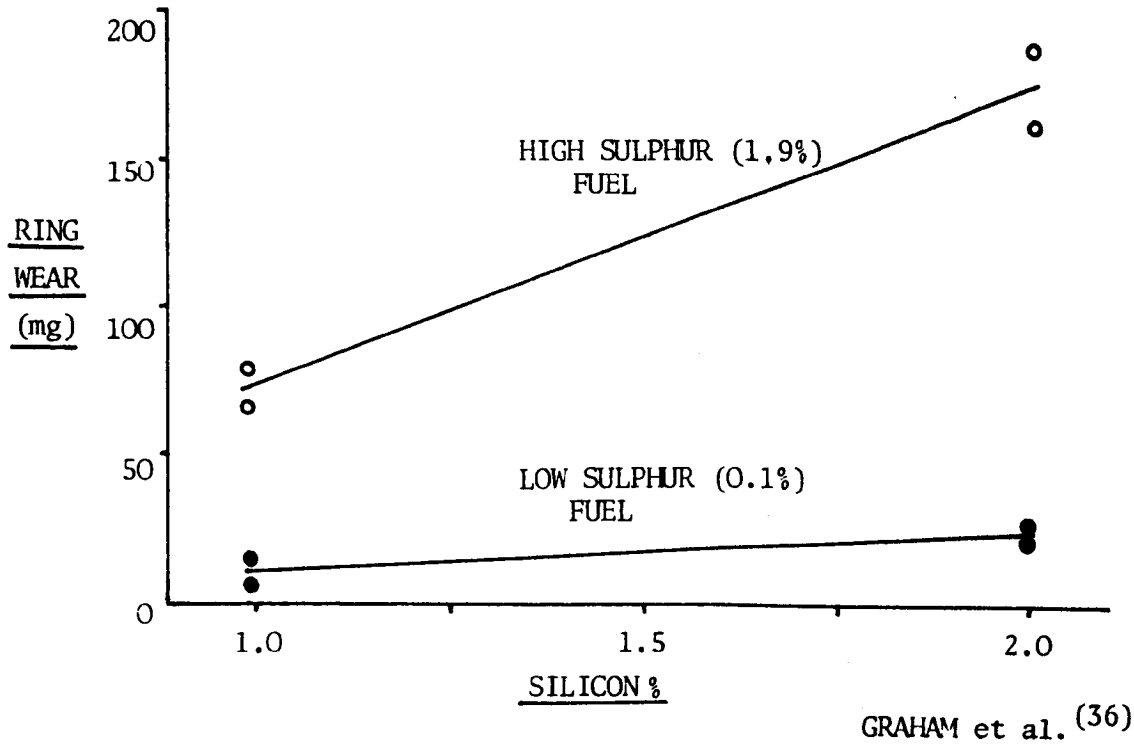

FIG. 11 Influence of fuel sulphur on ring wear.

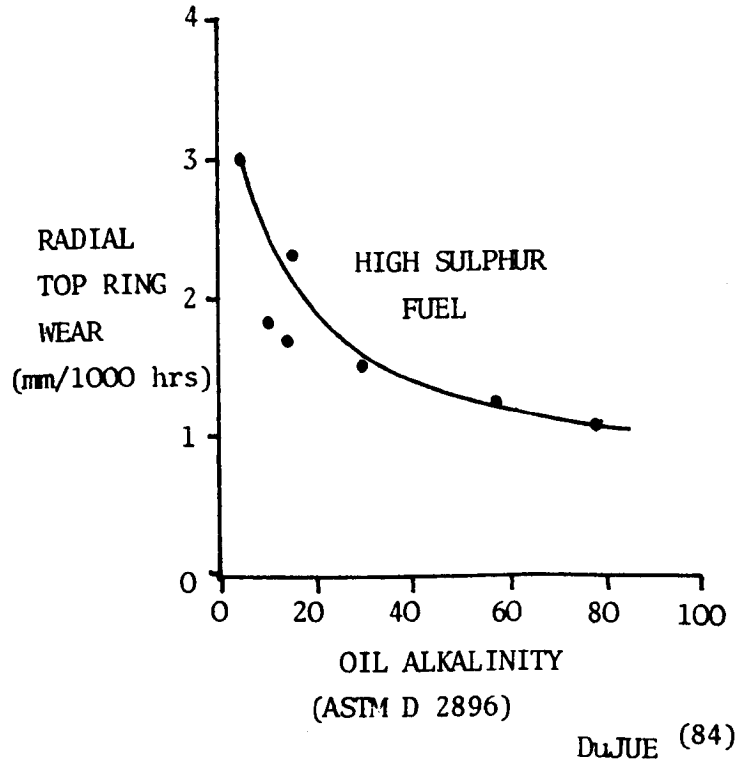

FIG. 12 Wear increase on top ring due to corrosion in the engine.

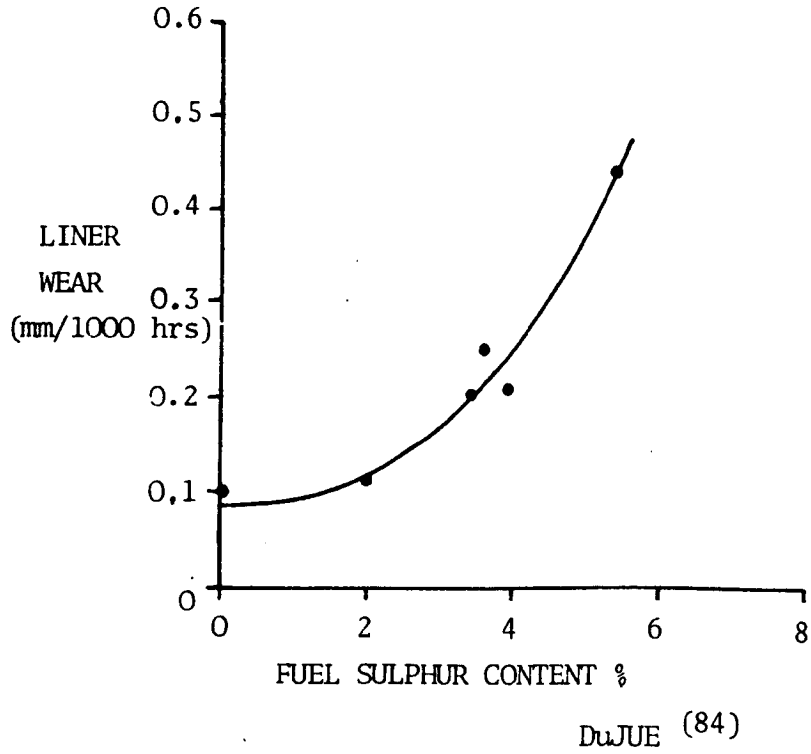

FIG. 13 Liner wear rates using high sulphur fuels.

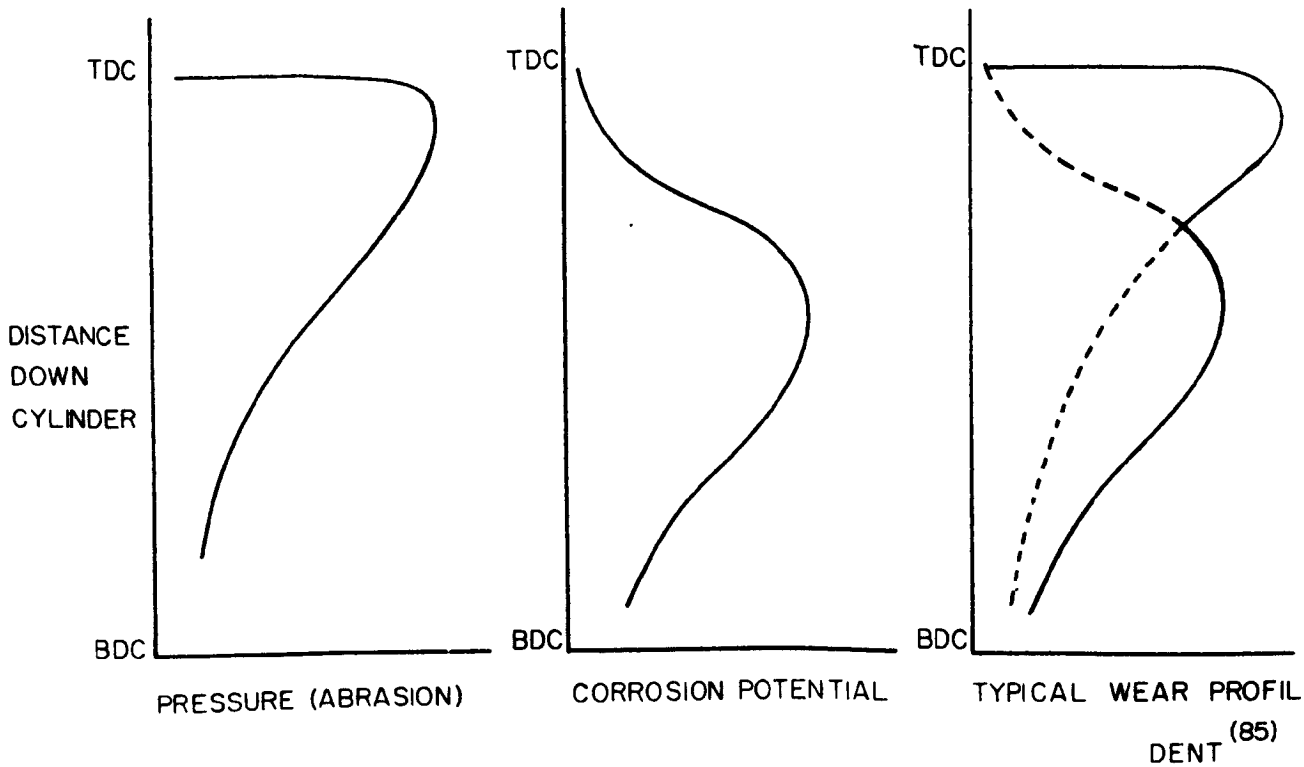

FIG. 14 Liner wear profile down the engine stroke resulting from abrasion and corrosion.

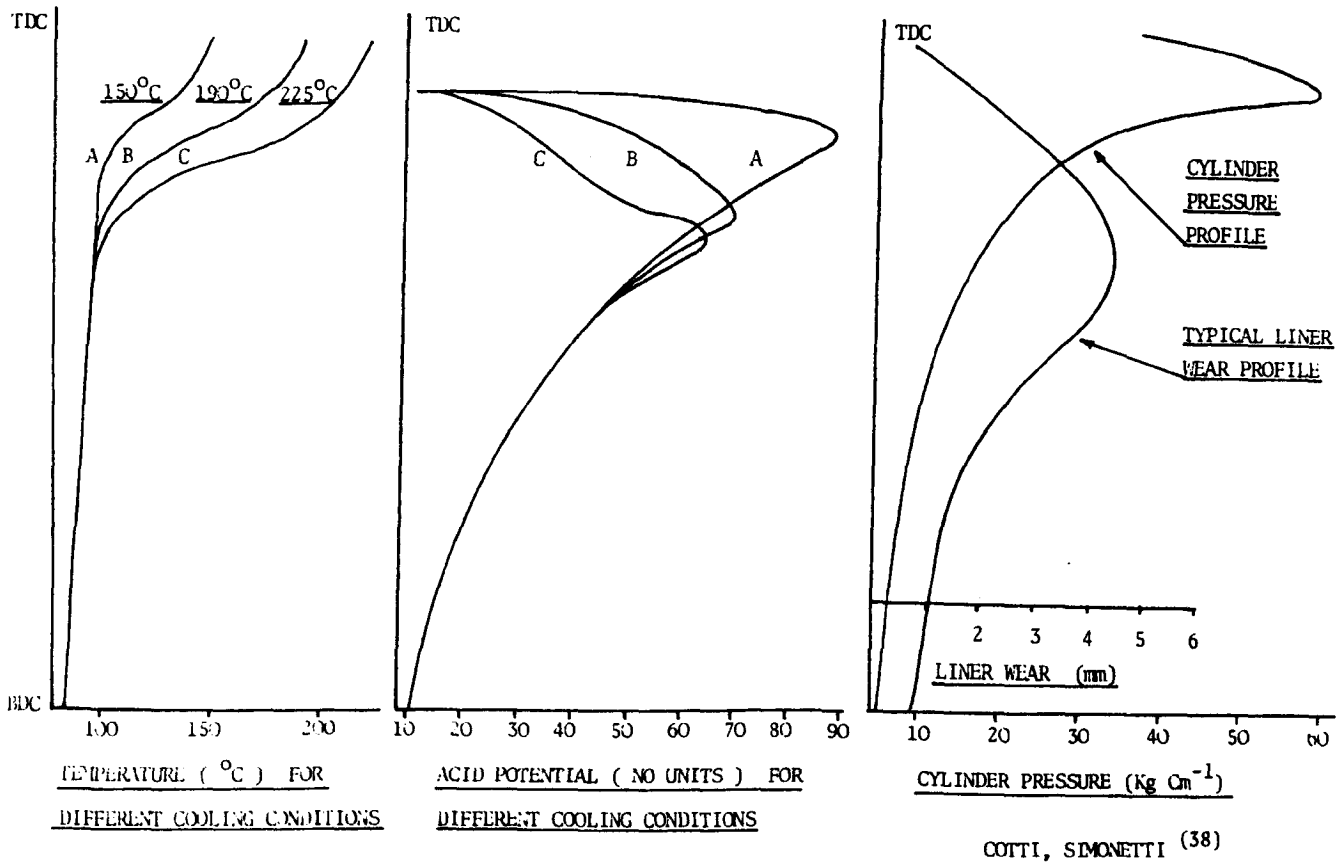

FIG. 15 Temperature, corrosion potential, gas pressure and liner wear profile for an engine running on a 3.0% sulphur residual fuel.

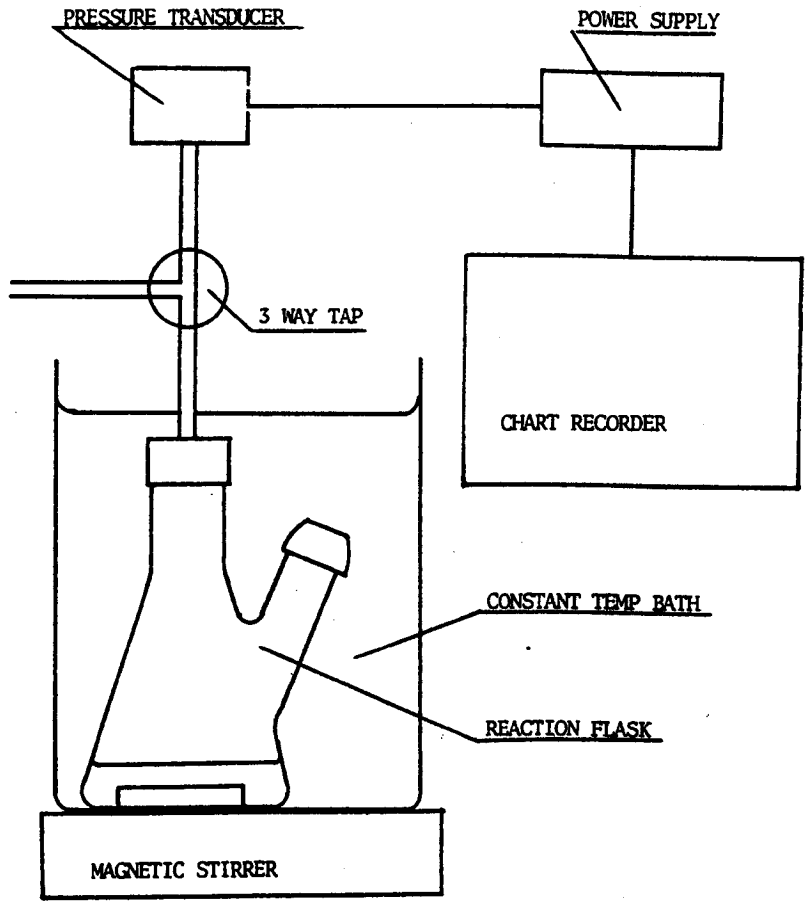

FIG. 16 Schematic diagram of corrosion rig.

SAMPLE	TYPE	C %	Si %	Mn %	P %	Cu %
A	HIGH PHOSPHORUS	2.83	1.25	1.0	0.63	-
B	HIGH COPPER	3.15	1.20	0.9	0.25	0.9
C	RIG PLATE SPECIMEN	3.17	2.05	0.46	0.25	-
D	LOW COPPER	3.56	2,14	0.54	0.025	-
E	HIGH COPPER	3.42	2.27	0.47	0.10	0.83
F	EN 42	0.75/0.82	0.10/0.35	0.6/0.8	-	-
G	MARTENSITIC	0.75/0.82	0.10/0.35	0.6/0.8	-	-
H	PETTER LINER	2.26	2.07	0.51	1.05	-

TABLE 17 Analysis of corrosion test samples.

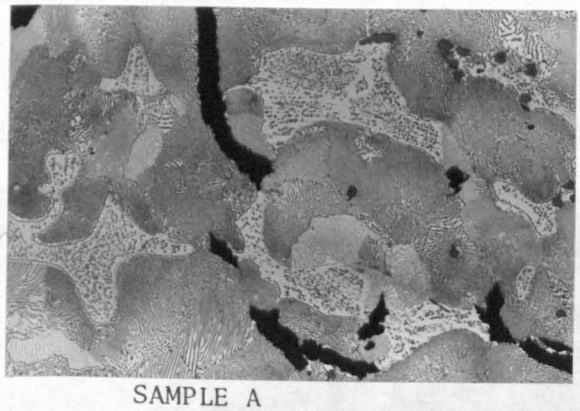

SAMPLE A

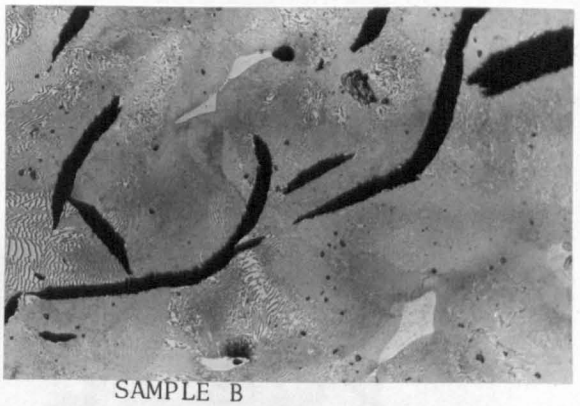

SAMPLE B

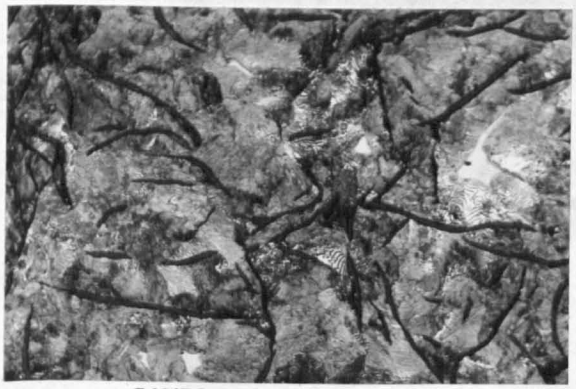

SAMPLE C

SAMPLE D

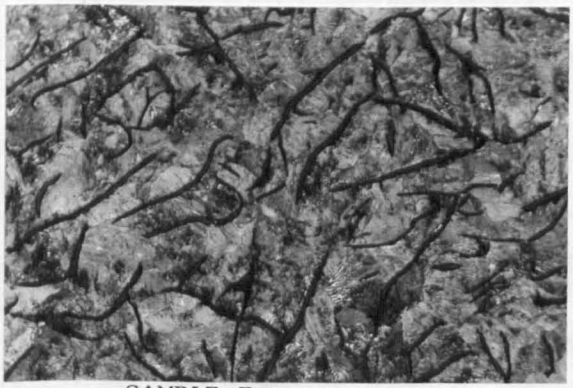

SAMPLE E

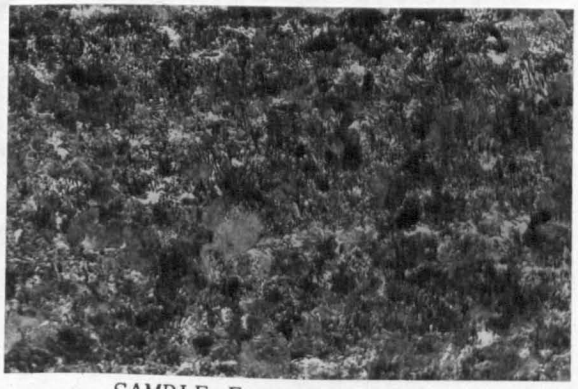

SAMPLE F

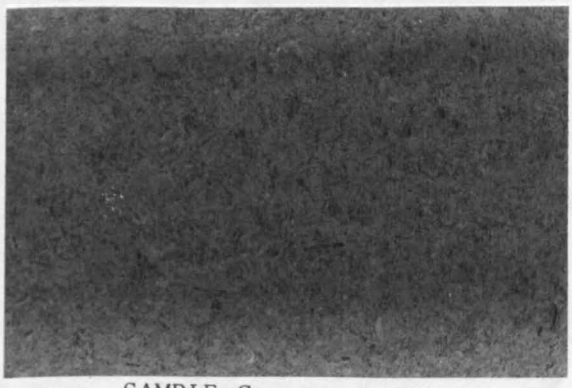

SAMPLE G

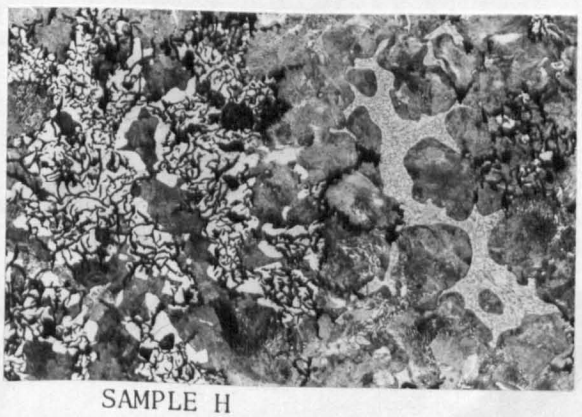

SAMPLE H

FIG. 18 Microstructures of corrosion test samples. X100

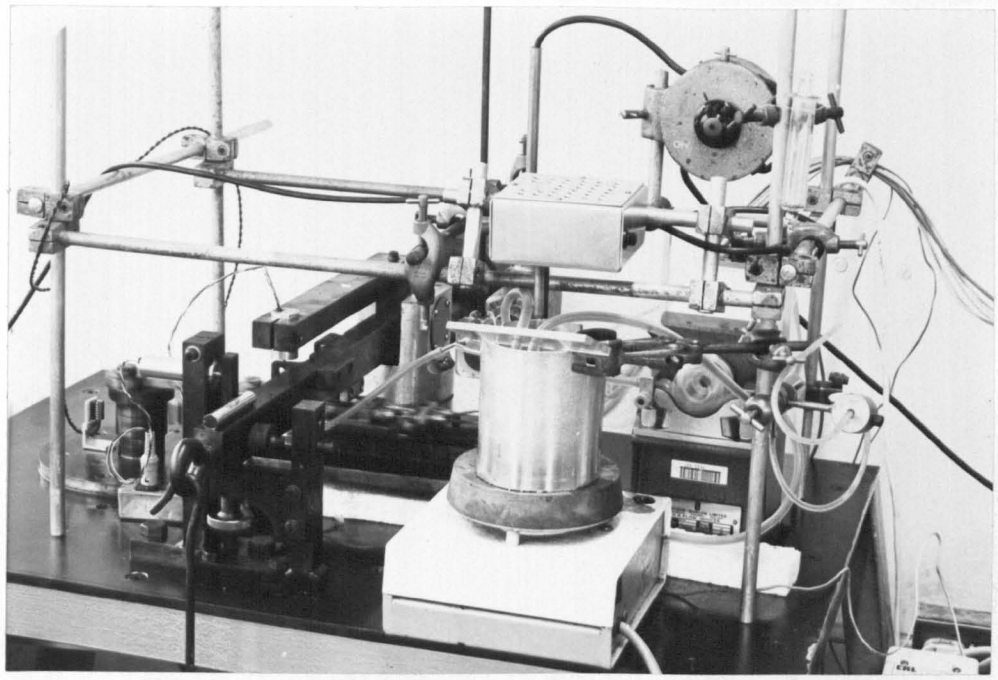

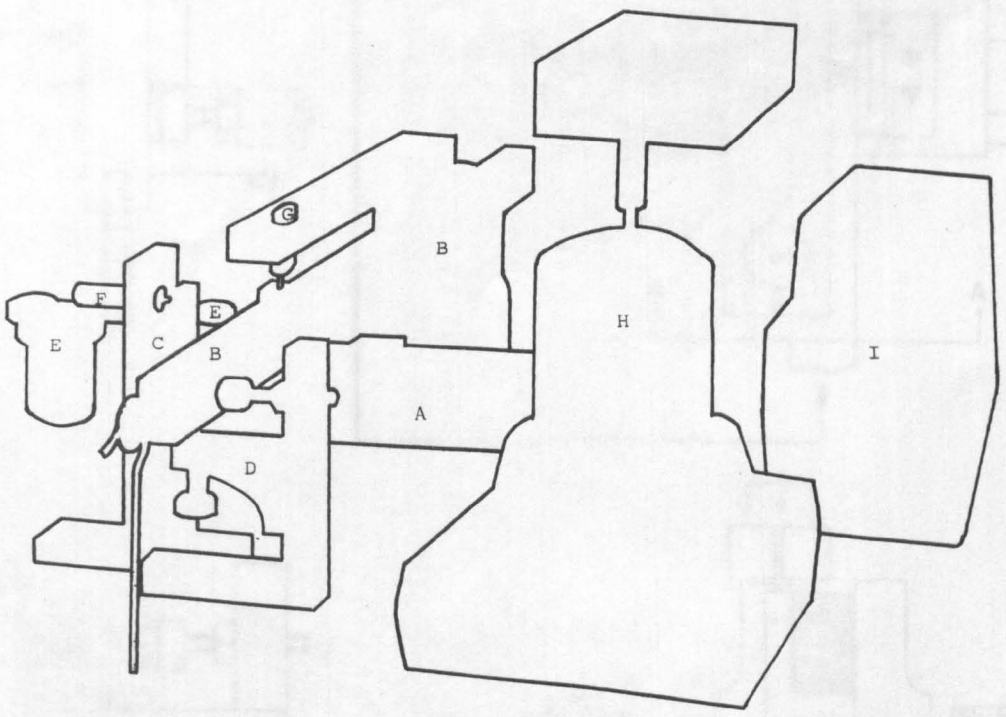

A) Base plate, bath and specimens.
B) Wear arm and pivot.
C) Friction post.
D) Adjustable stop.
E) Connecting rod and excentric drive.
F) Force transducer.
G) Wear transducer.
H) Oil reservoir and heater.
I) Peristaltic pump.

FIG. 19 a Reciprocating wear rig.

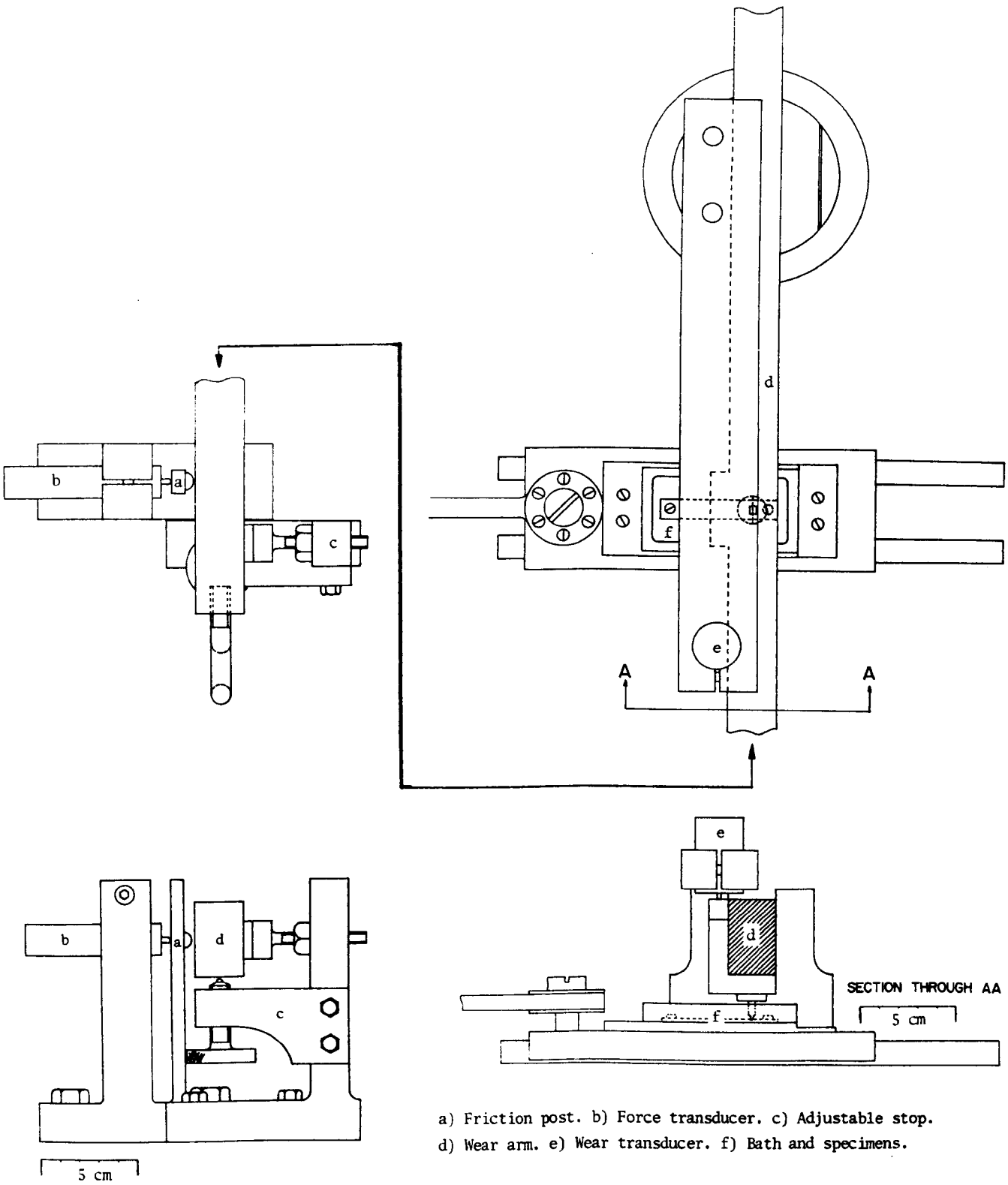

a) Friction post. b) Force transducer. c) Adjustable stop.
d) Wear arm. e) Wear transducer. f) Bath and specimens.

FIG. 19 Diagram of final wear rig design with the pin held in a pivoted arm.

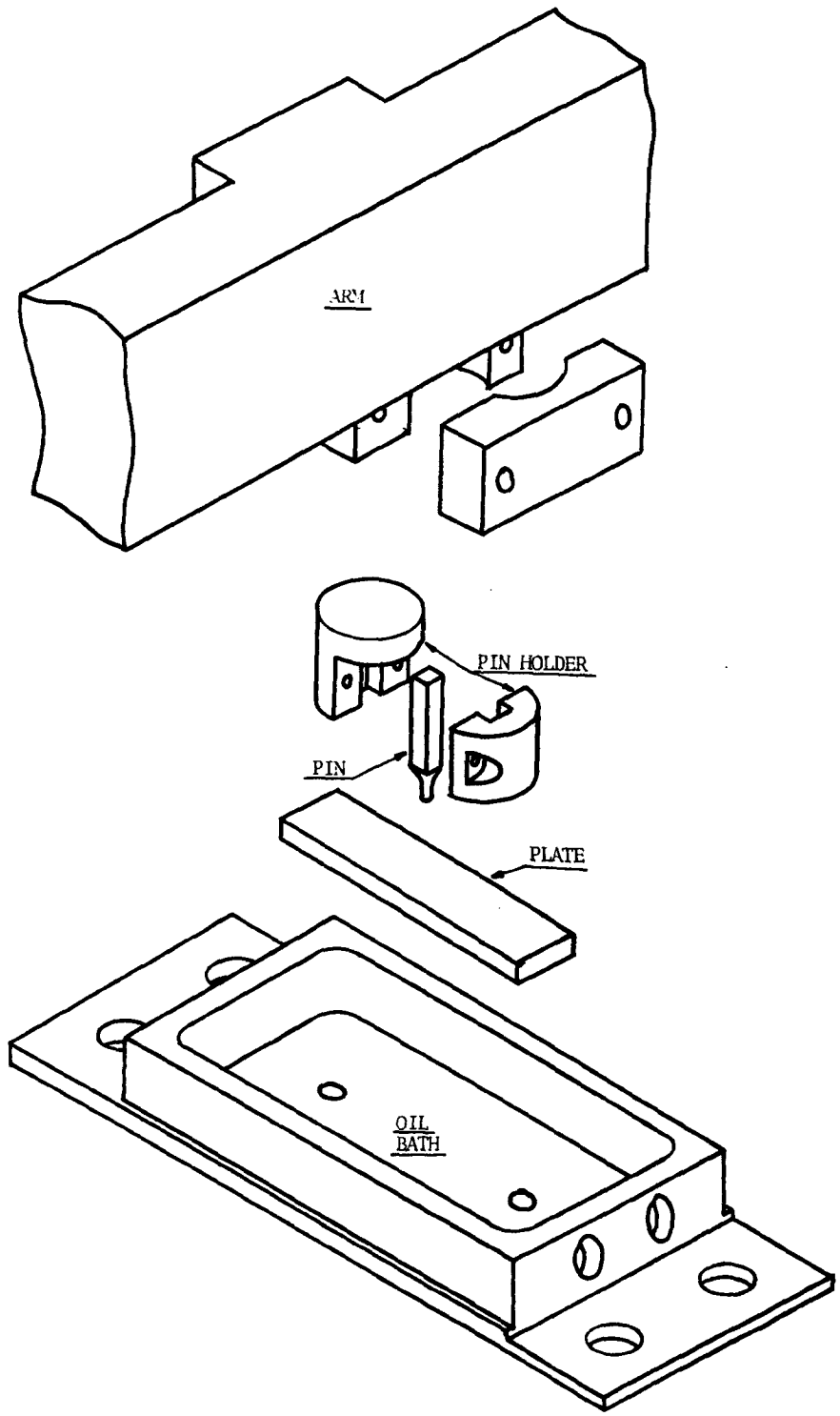

FIG. 20 Pin and plate assembly.

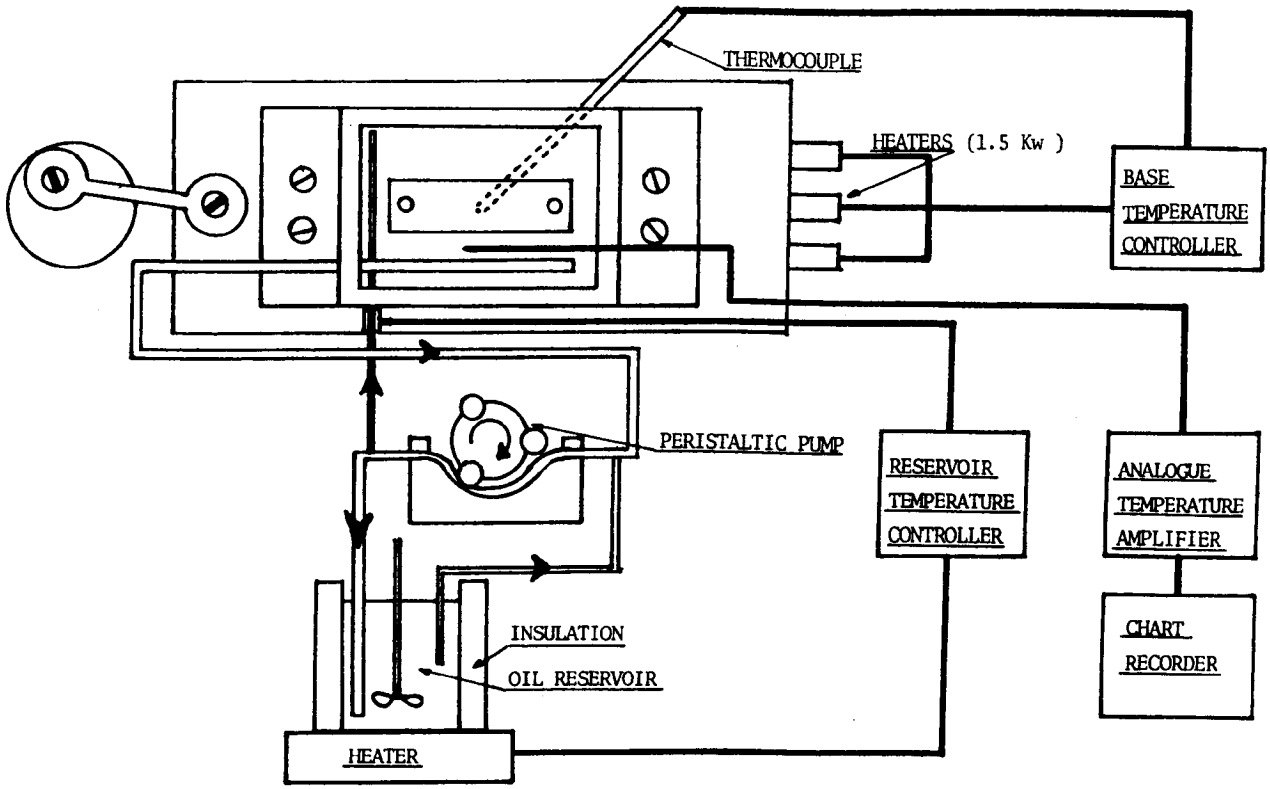

FIG. 21 Diagram of oil system and temperature control loops.

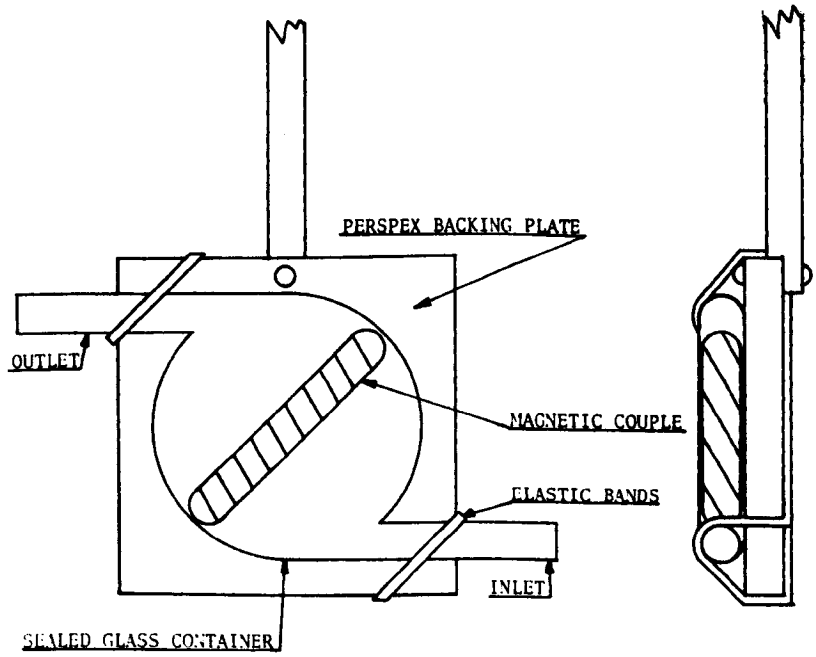

FIG. 22 In-line oil mixing unit.

FUEL and OIL	
FUEL	0.18 % Sulphur Distillate Fuel.
CYLINDER OIL	ELO 1036.
CRANKCASE OIL	ESSOLUBE 30.
RUNNING CONDITIONS	
12 hours at 800 rpm	Brake load 7 lb.
12 hours at 800 rpm	Brake load 12.5 lb.
OIL FEED RATE	
0 - 6 hours	Maximum delivery.
6 - 12 hours	5.6 g/hr.

TABLE 23 Running-in conditions for Petter engine tests.

FUEL and OIL	
FUEL (Test A)	0.18 % Sulphur undoped Distillate Fuel.
(Test B)	3.5 % Sulphur doped Distillate Fuel.
CYLINDER OIL	ELO 1036, FEED 5.6 g/hr.
CRANKCASE OIL	ESSOLUBE 30.
ENGINE CONDITIONS	
Cylinder head water outlet temp. 130 - 140 ^{o}F.	
Mid-top cylinder outlet water temp. 60 $\pm$ 3 ^{o}F.	
Bottom cylinder outlet water temp. 110 ^{o}F Max.	
CRANKCASE OIL TEMPERATURE	116 ^{o}F approx.
CRANKCASE OIL PRESSURE	25 lb/in^2 Min.
BRAKE LOAD	14 lb. Min.
ENGINE SPEED	860 rpm.
FUEL FLOW	5 ml/200secs.
INLET AIR PRESSURE	7 in. Mercury.

TABLE 24 Long term test conditions for the high sulphur doped distillate fuel test.

HOURS RUNNING	INTERVAL (hours)	HOURS RUNNING	INTERVAL (hours)
5	5	95	20
24	19	105	10
30	6	120	15
50	20	130	10
75	25	144	14

TABLE 25 Oil sampling intervals for Petter test.

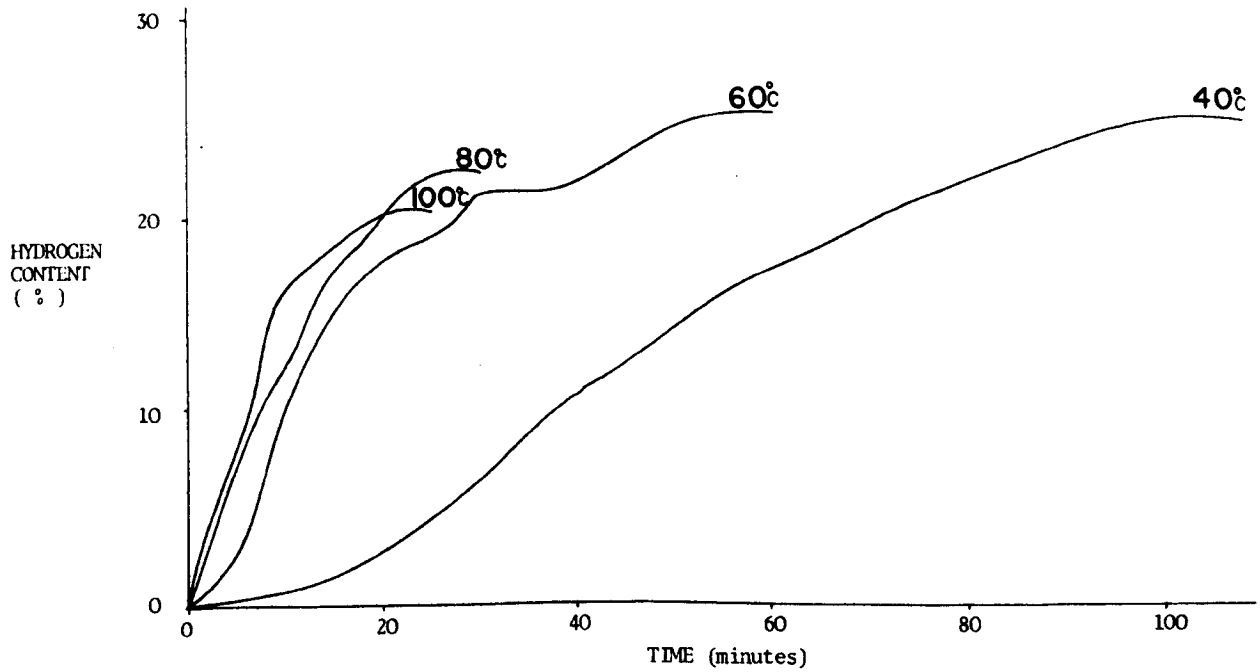

FIG. 26 Corrosion rates for different test temperatures.

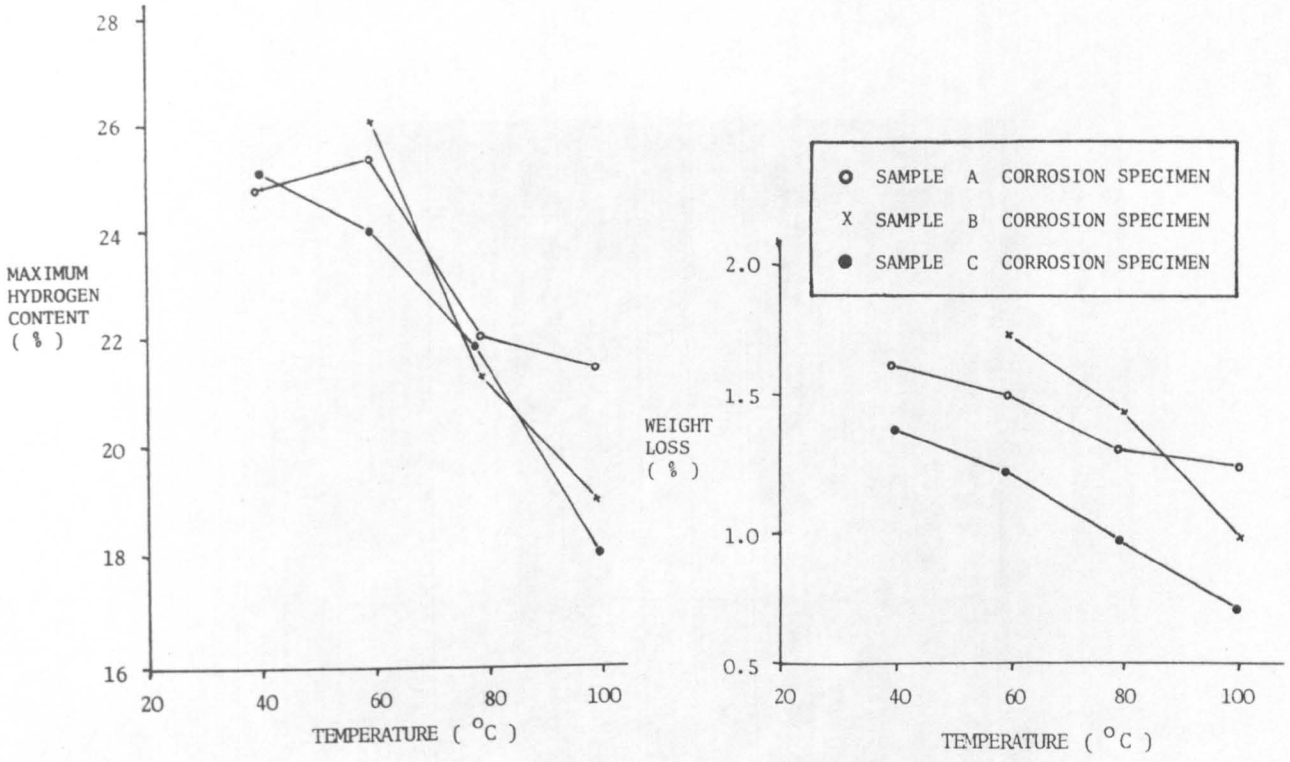

FIG. 27 Total corrosion of first series of corrosion specimens.

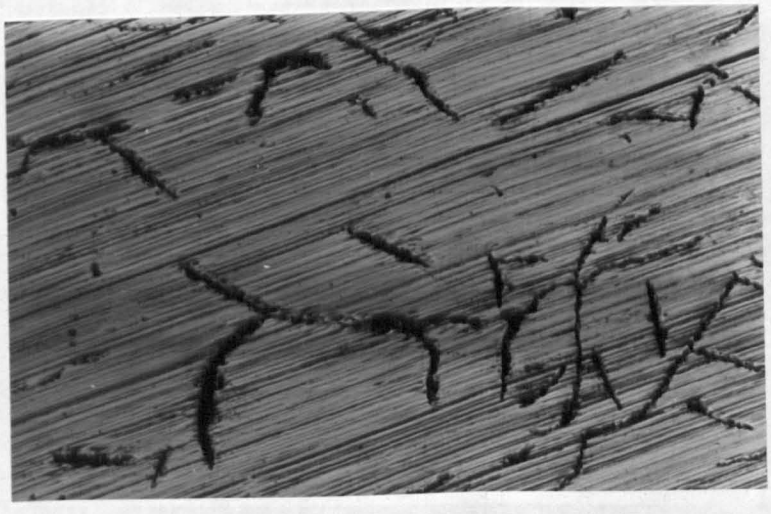

FIG. 28 Original ground surface of typical corrosion specimen. X100

FIG. 29 Stimulation of corrosion by graphite. X1000

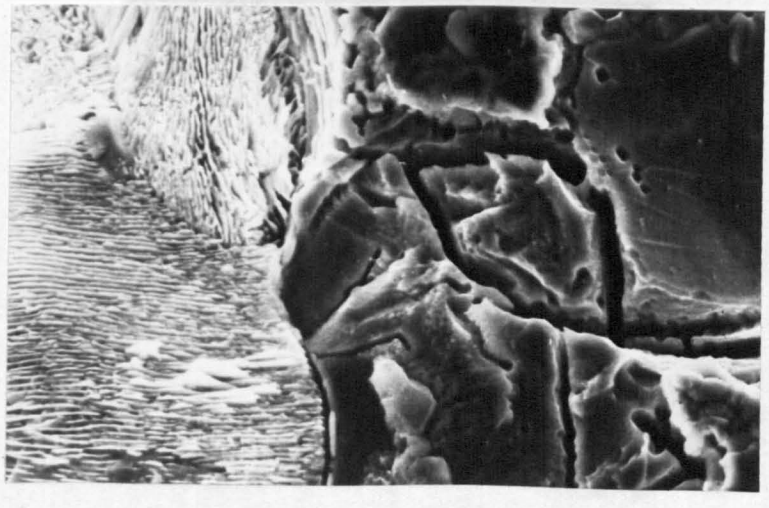

FIG. 30 Selective corrosion of pearlite. X2000

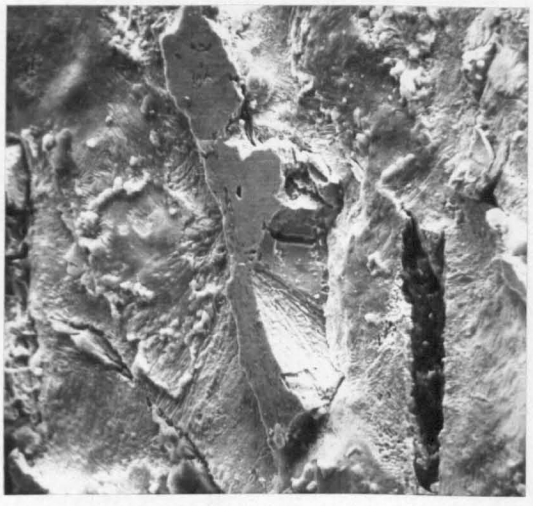

FIG. 31 Relatively unattacked phosphide eutectic. X200

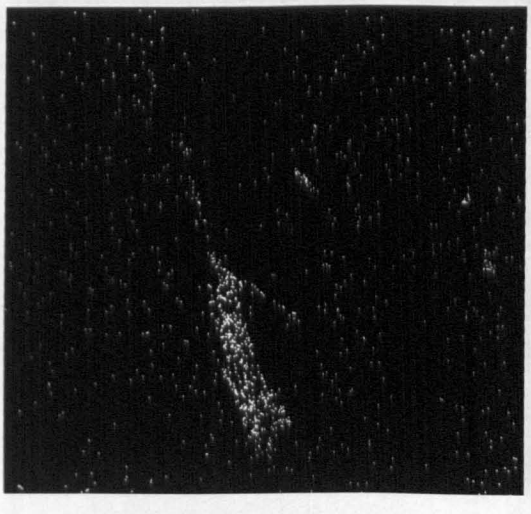

FIG. 32 E.P.M.A. for phosphorus over area shown in Fig. 31. X200

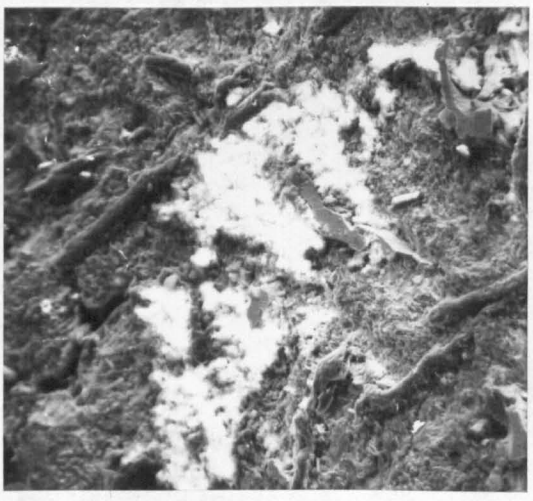

FIG. 33 Deposit on surface of some corrosion samples. X50

FIG. 34 E.P.M.A. for sulphur over area shown in Fig. 33. X50

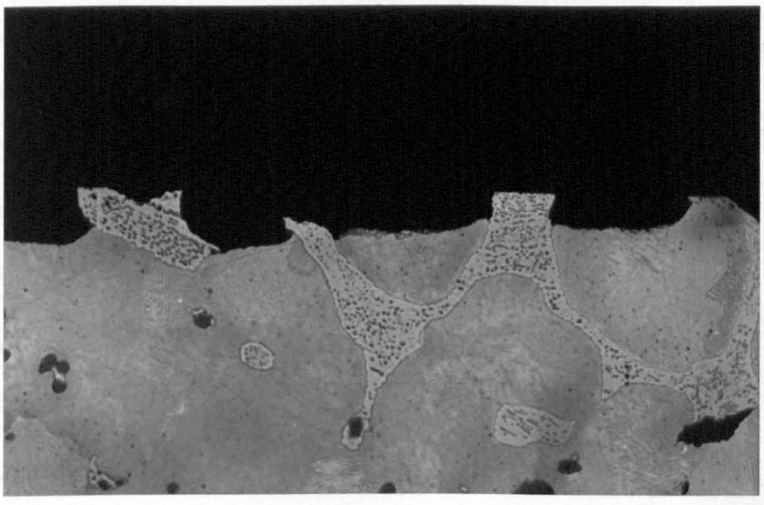

FIG. 35 Section normal to the surface of type A corrosion specimen (see Table 17). X200

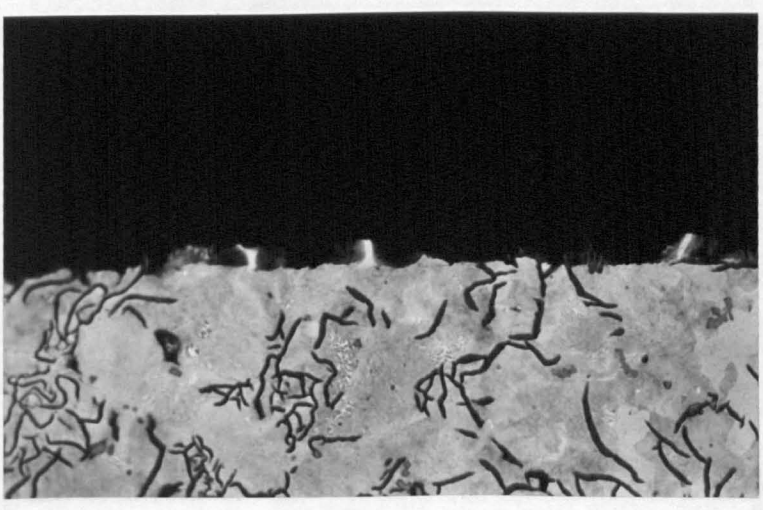

FIG. 36 Section normal to the surface of type C corrosion specimen. X200

SAMPLE	TYPE	HYDROGEN EVOLVED (%)	CALCULATED DISOLVED Fe (g)
D	LOW COPPER	0.65	4.5×10^{-2}
E	HIGH COPPER	0.6o	4.2×10^{-2}
F	EN 42	0.35	2.6×10^{-2}
G	MARTENSITIC	0.32	2.2×10^{-2}
H	PETTER LINER	2.40	18.7×10^{-2}

TABLE 37 Total corrosion of second series of corrosion specimens.

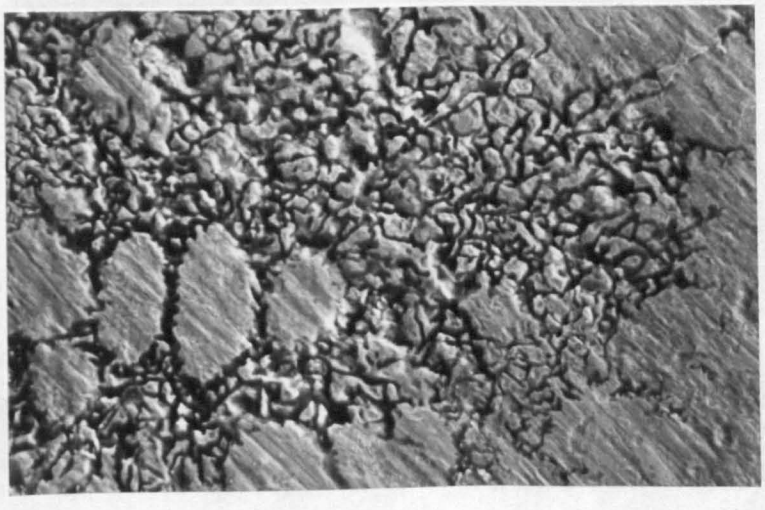

FIG. 38 Stimulation of corrosion by graphite on type H specimen (Petter engine liner material). X350

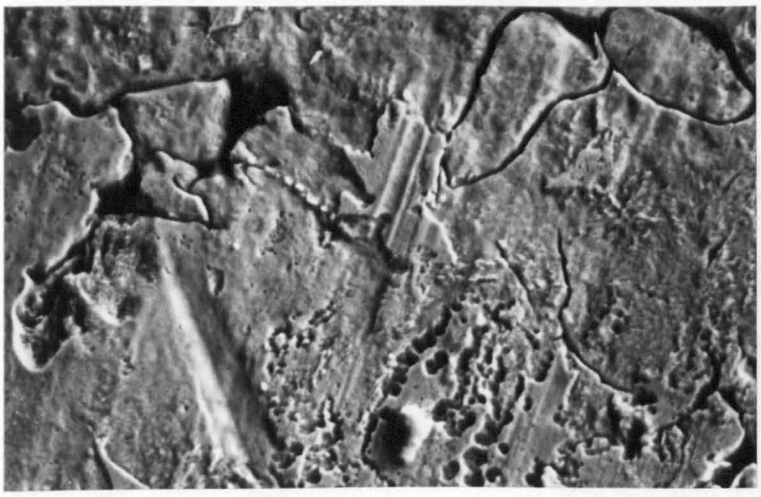

FIG. 39 Lack of corrosion on phosphide eutectic. X500

FIG. 40 E.P.M.A. for phosphorus over area shown in Fig. 39. X500

FIG. 41 Corrosion revealing internal structure of phosphide eutectic. X700

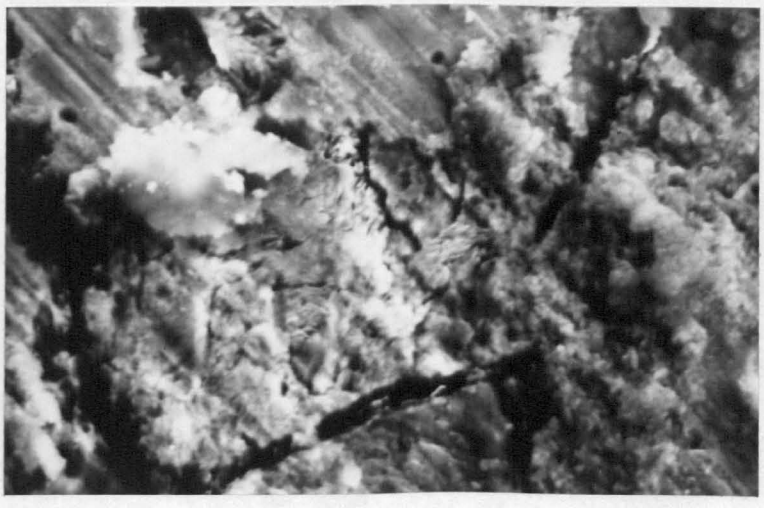

FIG. 42 More severe corrosion in areas of no surface film. X750

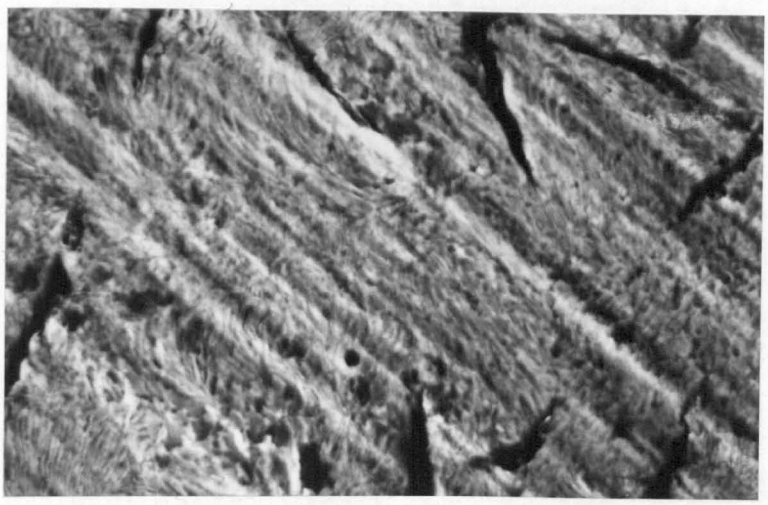

FIG. 43 Corrosion of type E specimens (see Table 17). X800

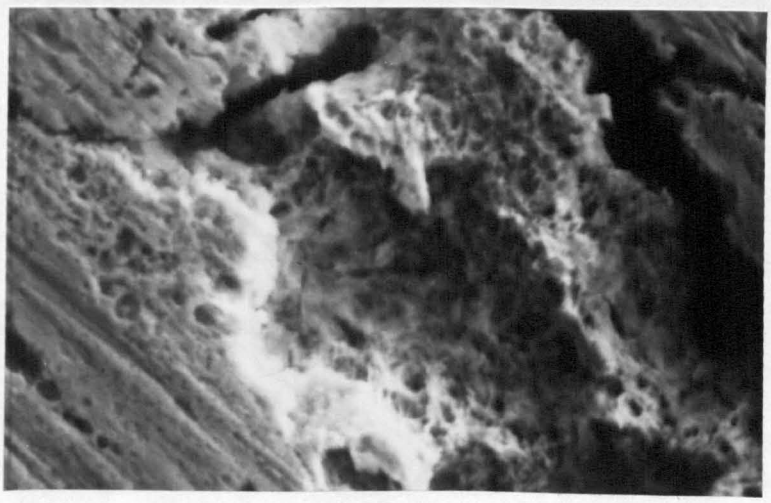

FIG. 44 Corrosion of Martensitic specimen. X1000

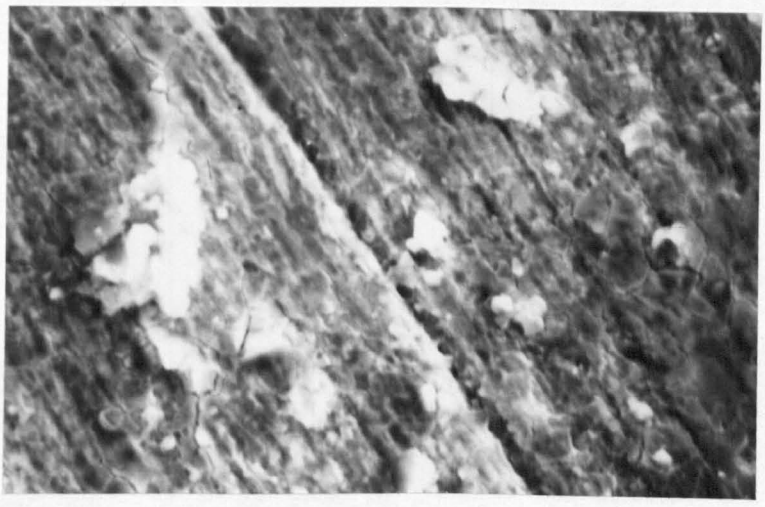

FIG. 45 Corrosion of fully pearlitic steel specimen. X1100

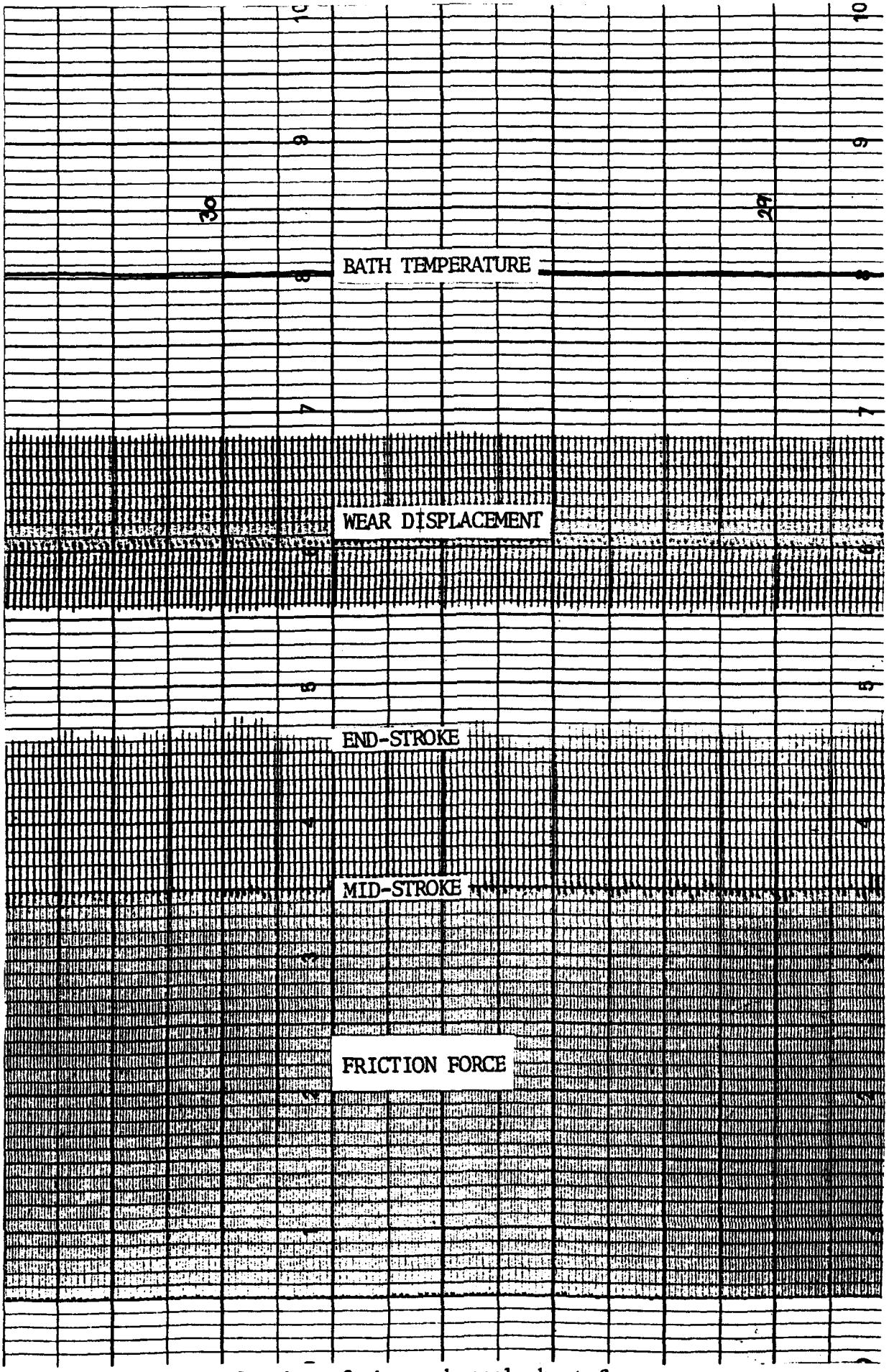

FIG. 46 Section of three channel chart from reciprocating wear rig.

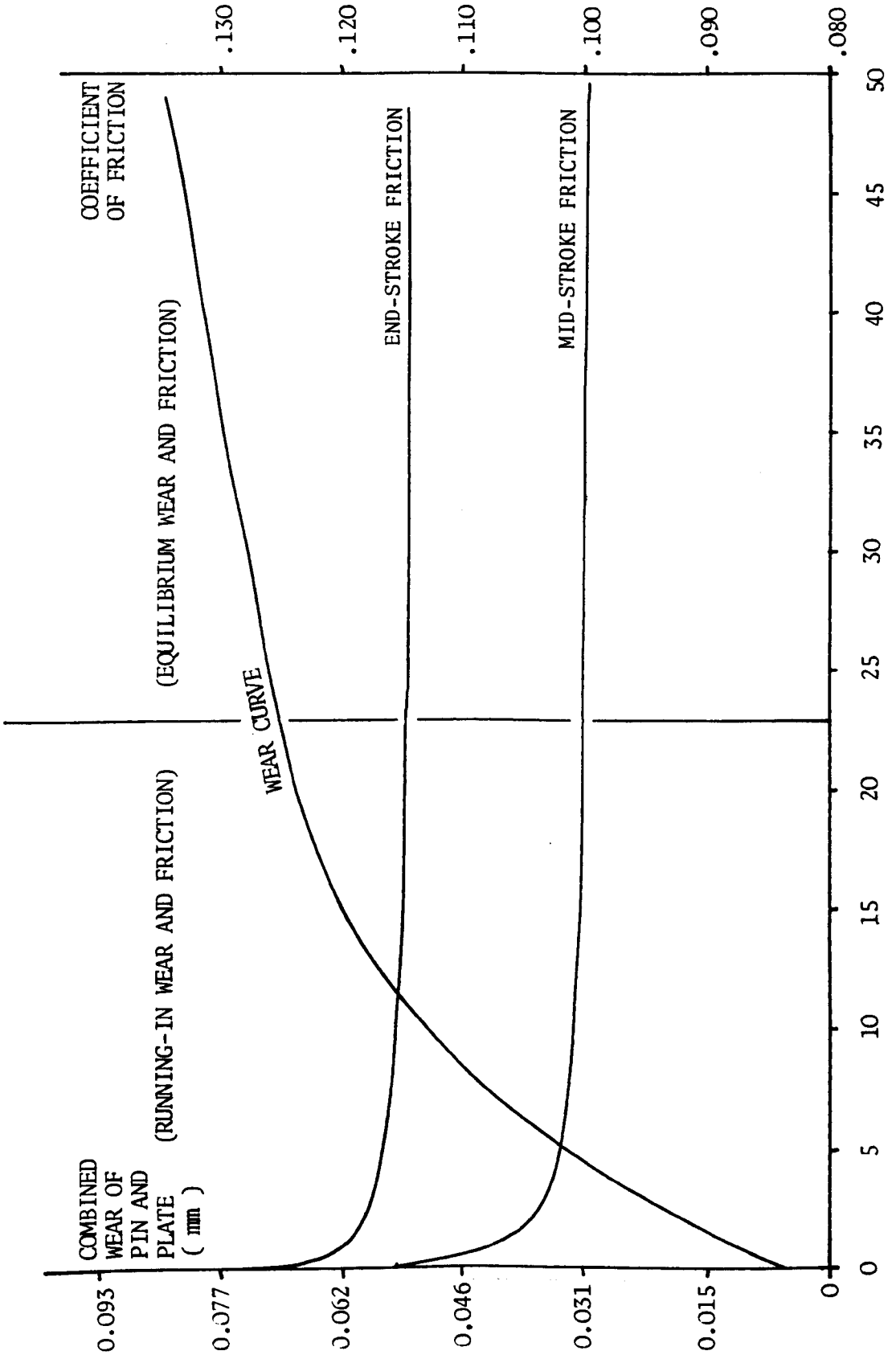

FIG. 47 Wear and frictional force plotted for complete test.

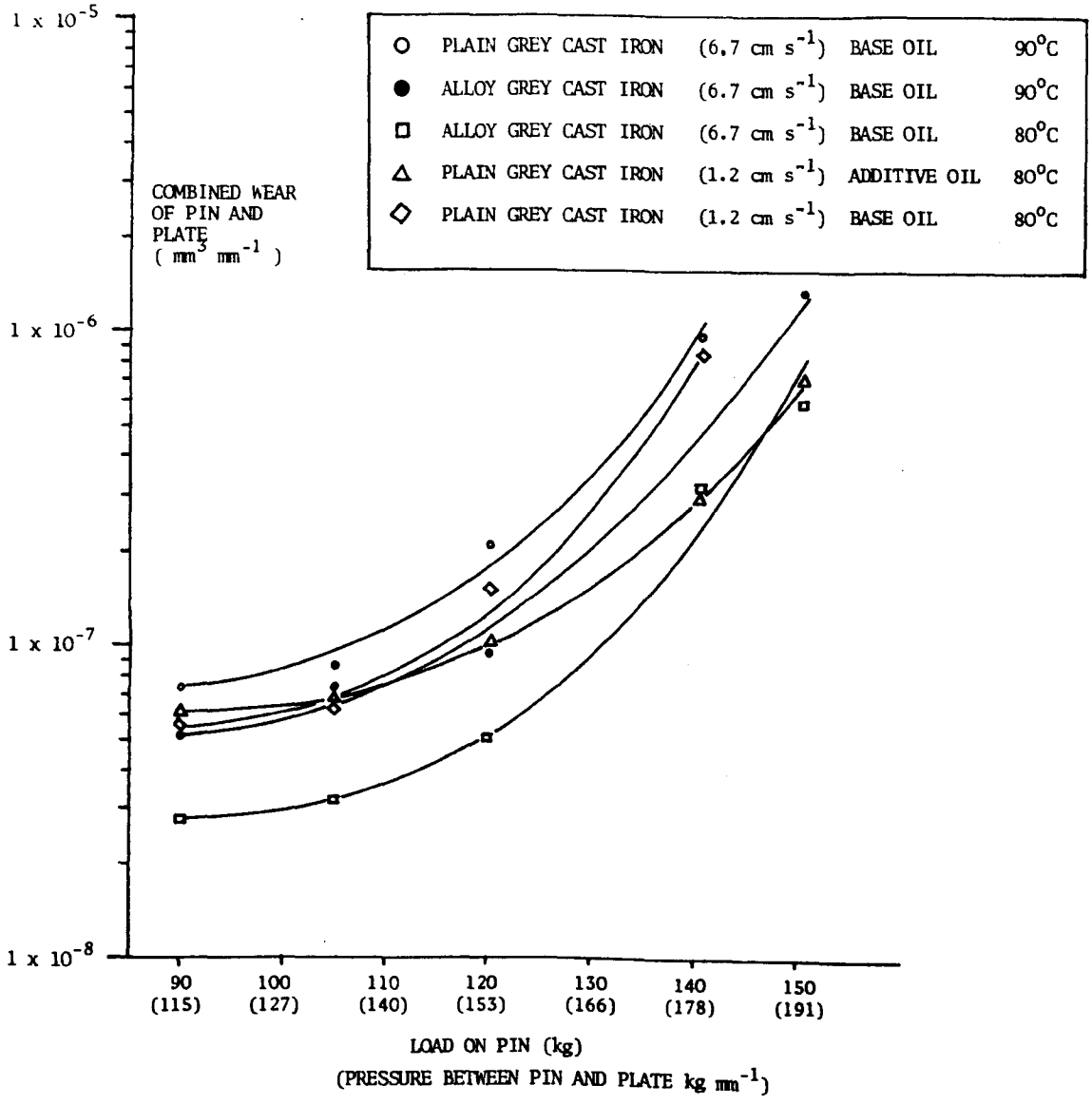

FIG. 48 Calculated wear rates for several lubricant, speed, load and temperature conditions.

CAST IRON PLATE MATERIAL TYPE	MAXIMUM SPEED, (cm^{-1})	TEMPERATURE (^{o}C)	OIL TYPE	OIL VISCOSITY (Cs)	WEAR RATE ($mm^{3} mm^{-1}$)	PERCENTAGE WEAR
ALLOY	6.7	80	BASE	13	5.2×10^{-8}	25
ALLOY	6.7	90	BASE	13	9.4×10^{-8}	45
PLAIN	1.2	80	ADDITIVE	17	1.1×10^{-7}	53
ALLOY	1.2	80	BASE	13	1.4×10^{-7}	67
PLAIN	1.2	80	BASE	13	1.5×10^{-7}	71
PLAIN	6.7	90	BASE	13	2.1×10^{-7}	100

TABLE 49 Comparison of wear rates at 120 Kg load.

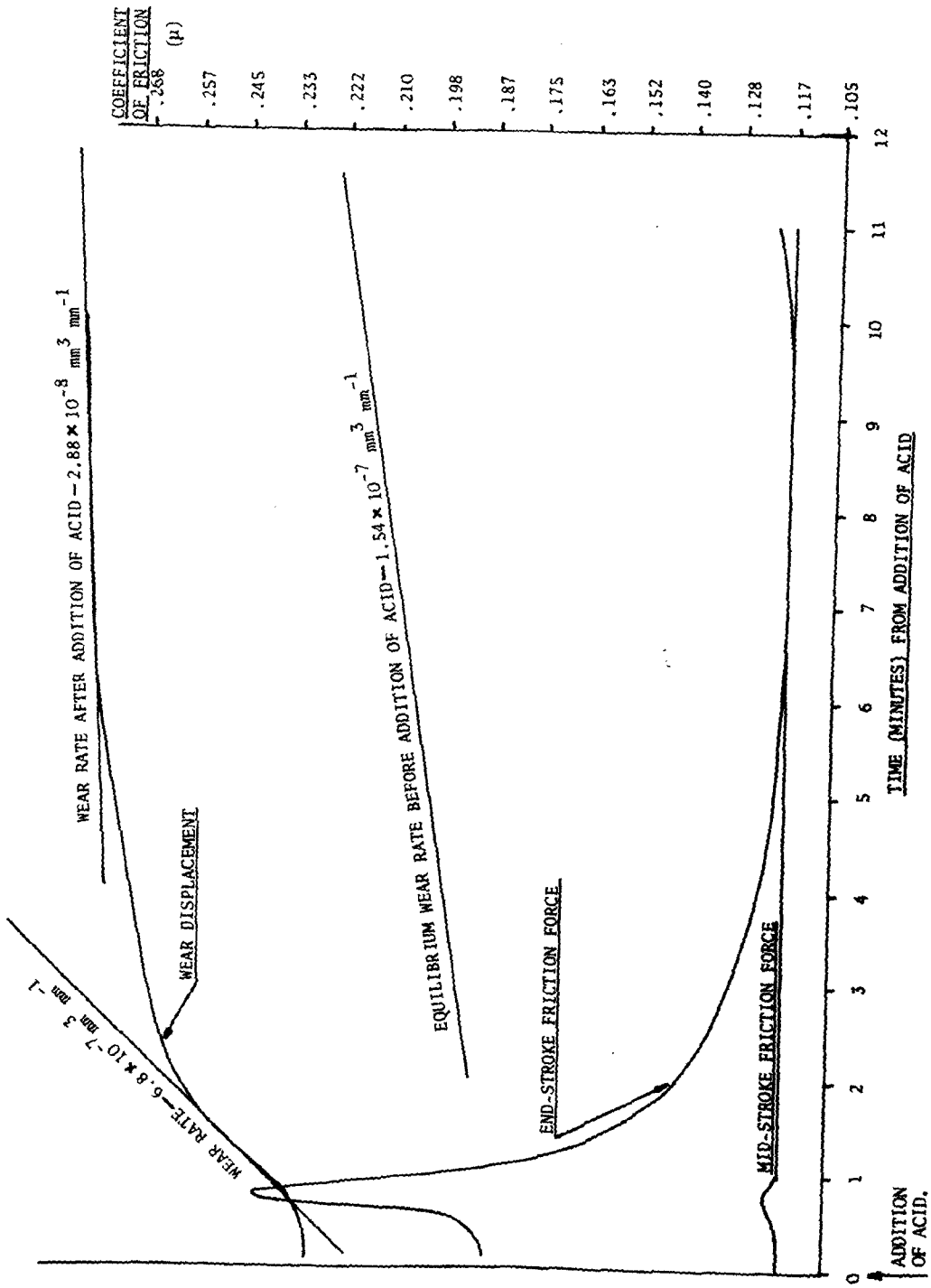

FIG. 50 Effect of acid addition on wear and friction.

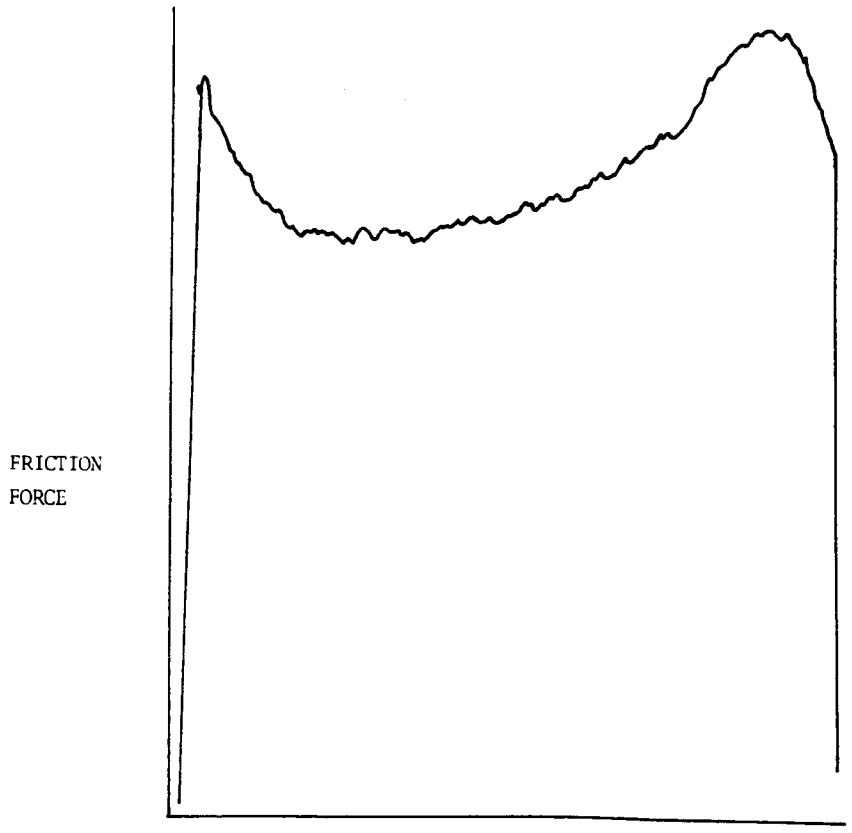

FIG. 51 Oscilloscope trace of friction force over one pass during equilibrium wear.

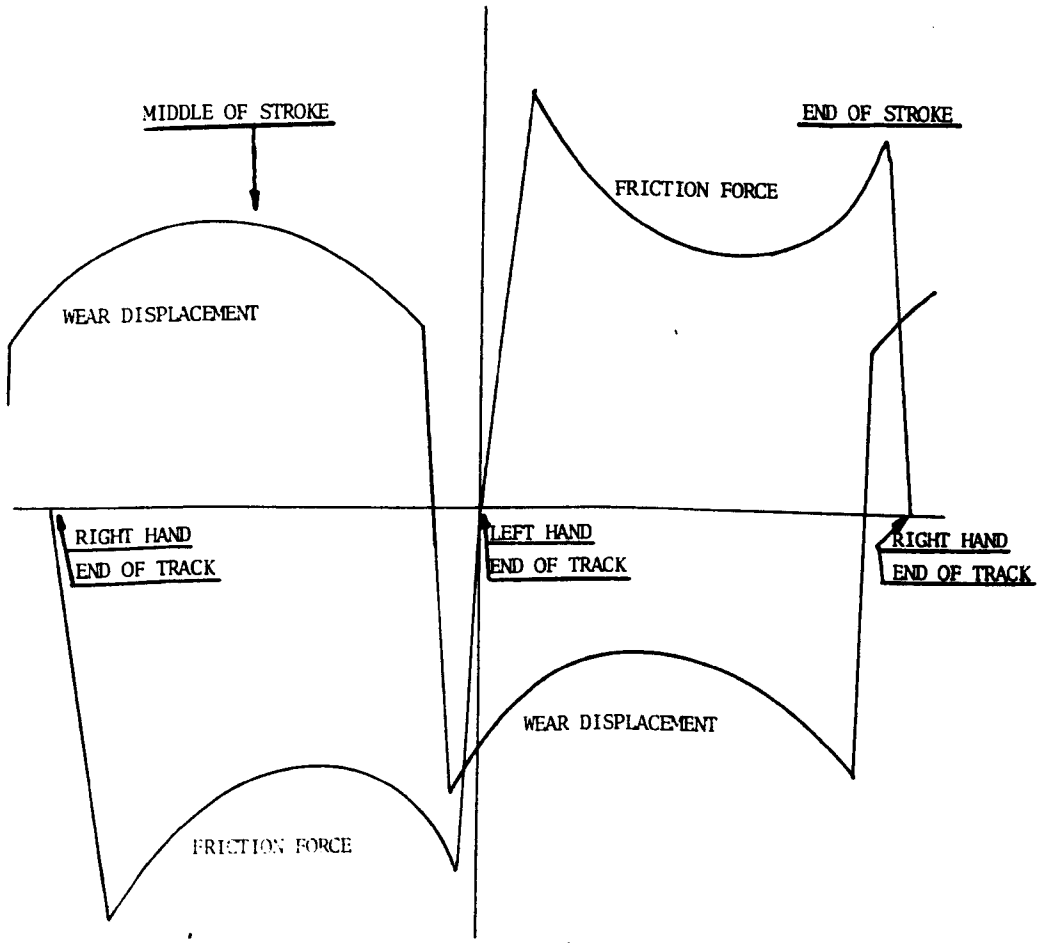

FIG. 52 Frictional force measured by transducers on either side of arm.

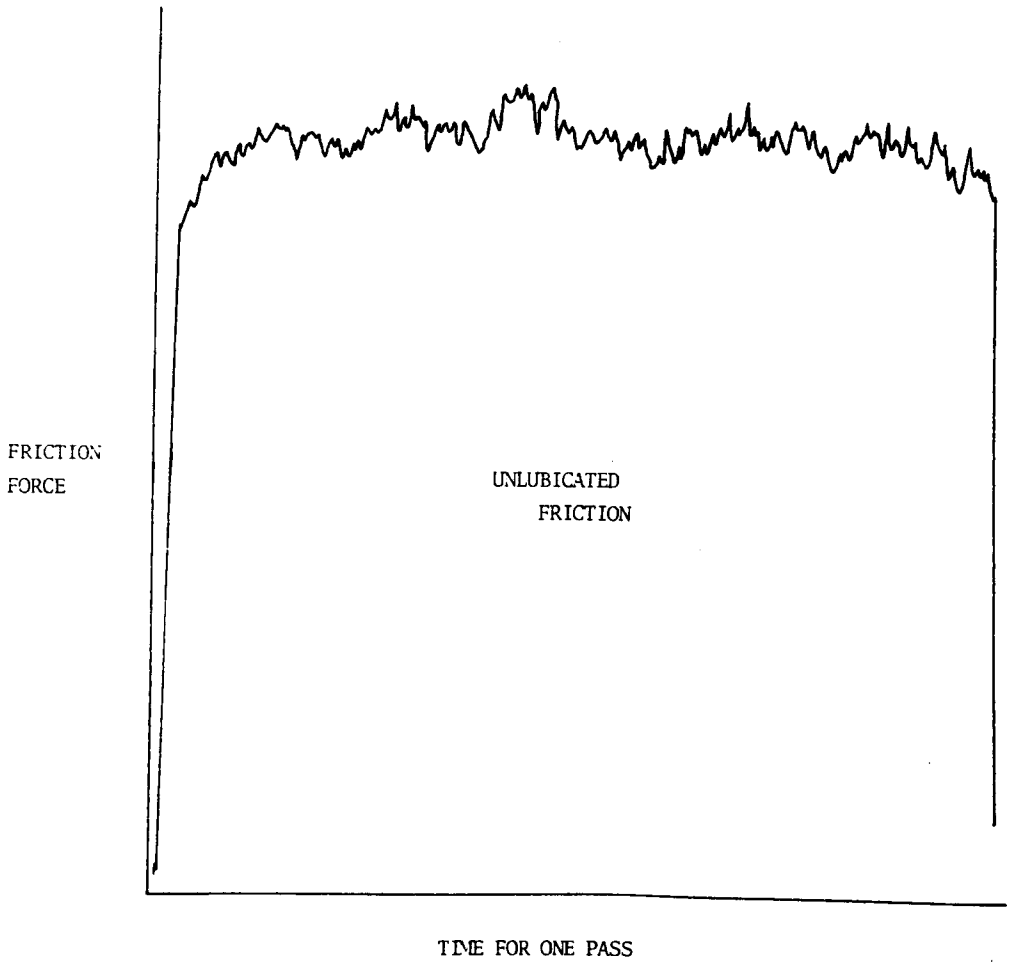

FIG. 53 Oscilloscope trace of dry friction force over one pass during equilibrium wear.

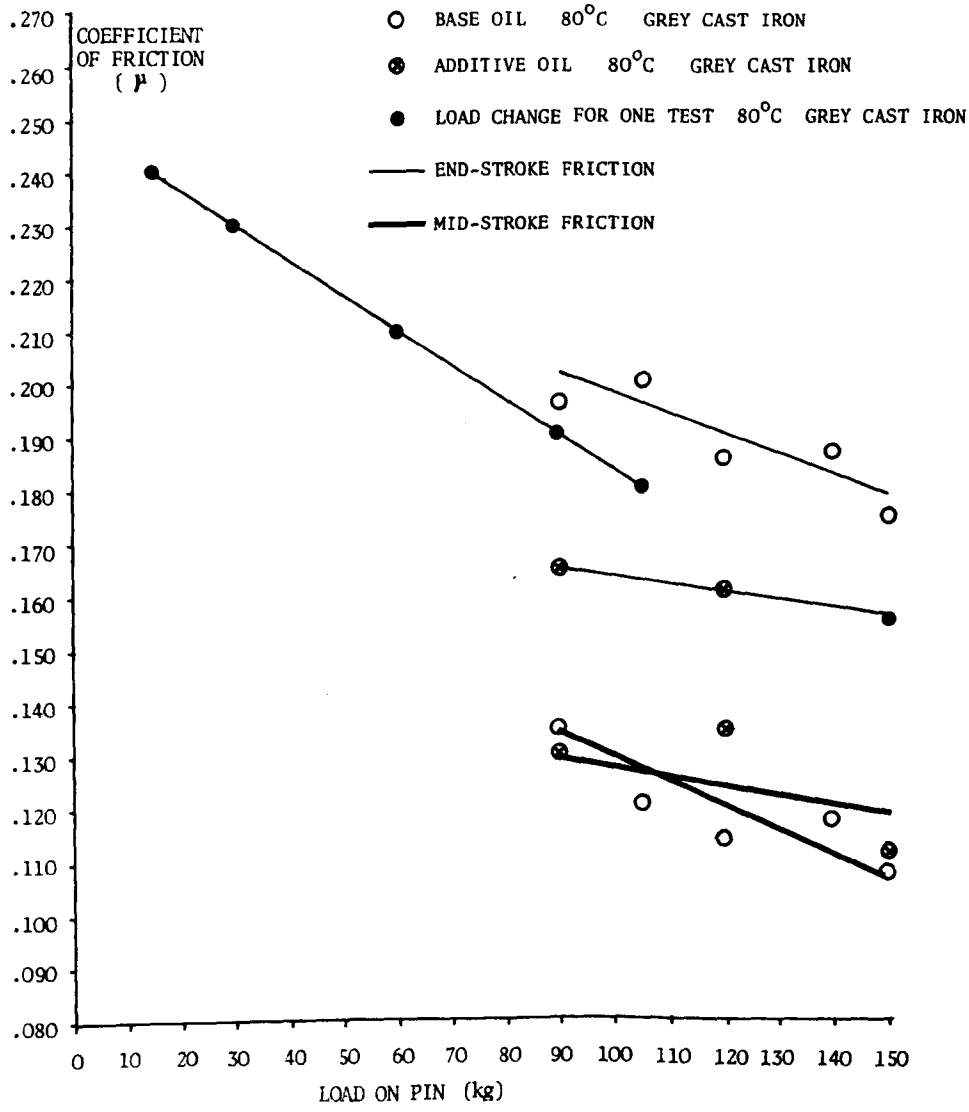

FIG. 54 End and mid-stroke friction coefficients for base and additive oils.

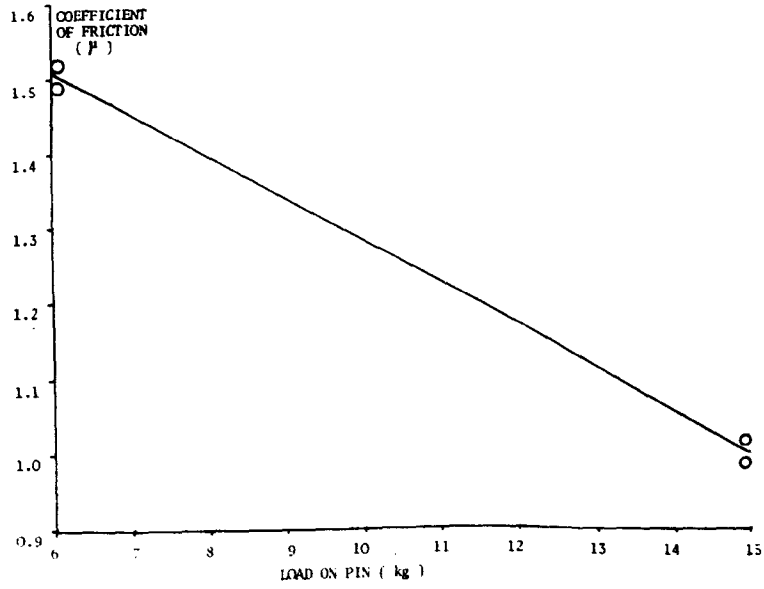

FIG. 55 Friction coefficients for dry wear tests.

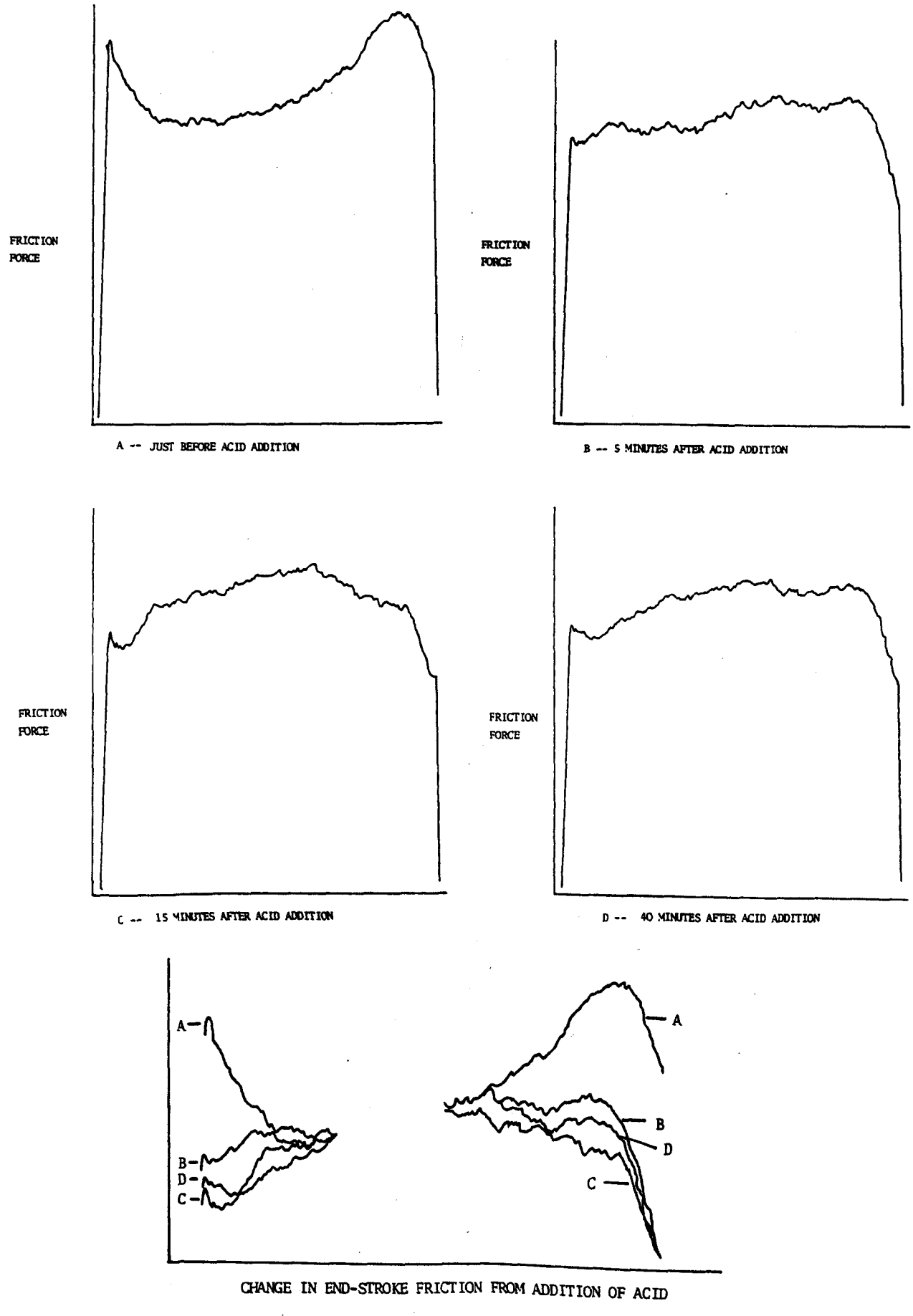

FIG. 56 Oscilloscope friction change along the stroke for acidified portion of test.

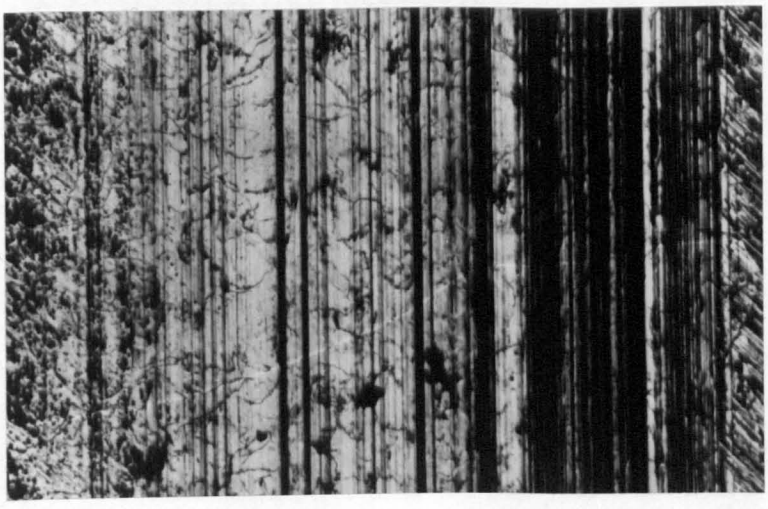

FIG. 57 Grooves along track length. X70

FIG. 58 Smooth surfaces between the grooves. X500

FIG. 59 Taper section through unacidified plate wear track. X200

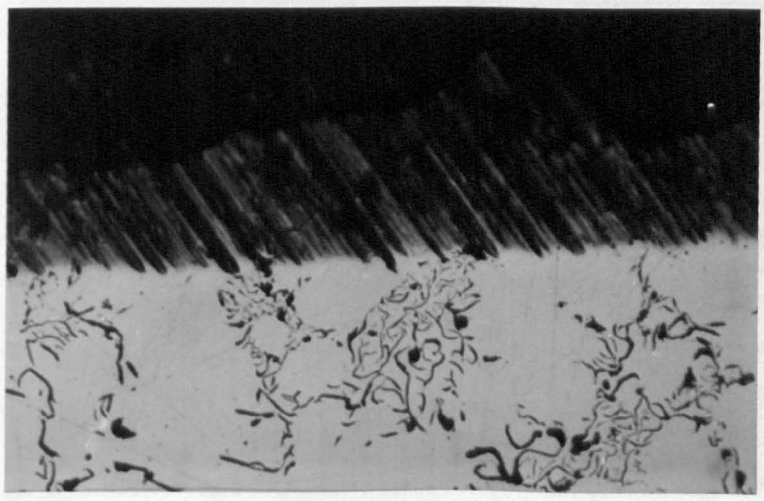

FIG. 60 Taper section through original ground surface. X200

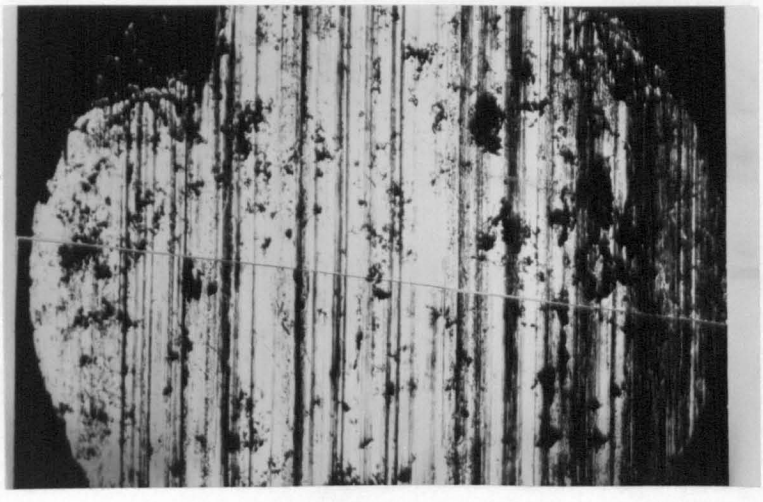

FIG. 61 Grooves over pin surface along direction of reciprocation. X70

FIG. 62 Differential abrasion allowing hard phases to be seen on pin surfaces. X200

FIG. 63 Deposit on wear track in grooves of the original grinding marks. X500

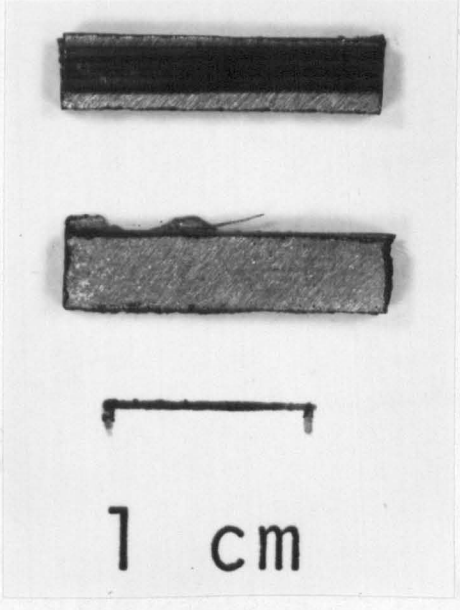

FIG. 64 Comparison of an area of wear track deposit with a section of plate material away from the track. (X.P.S. specimens).

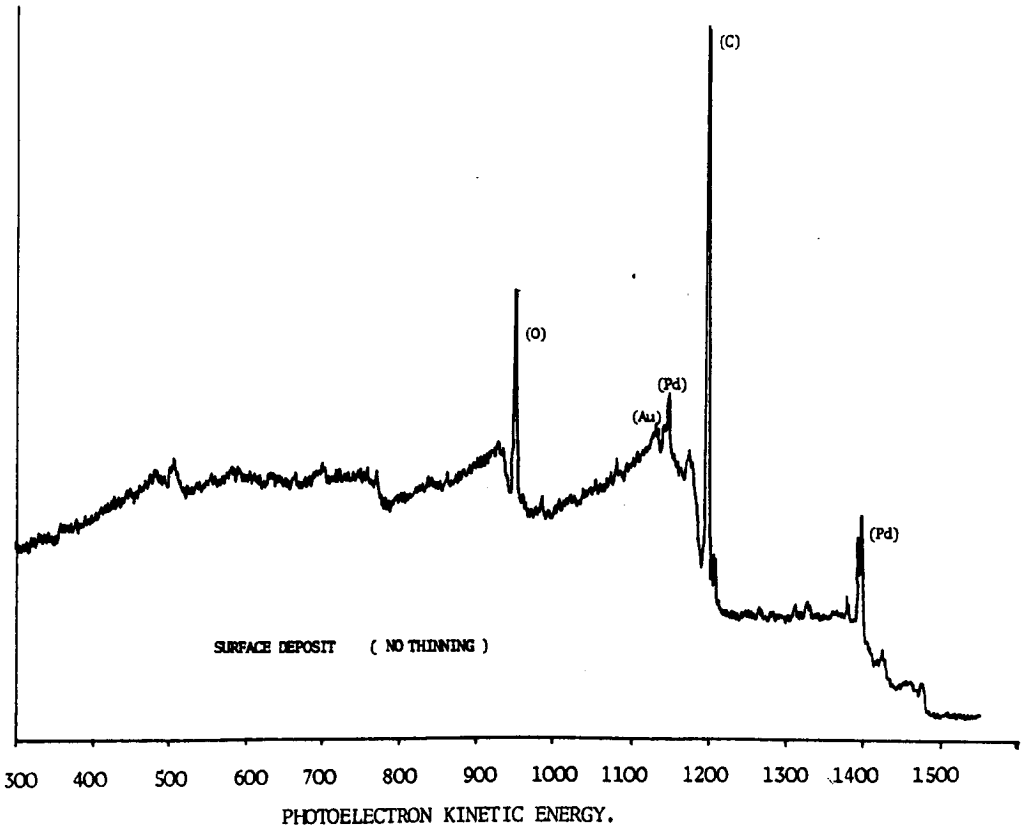

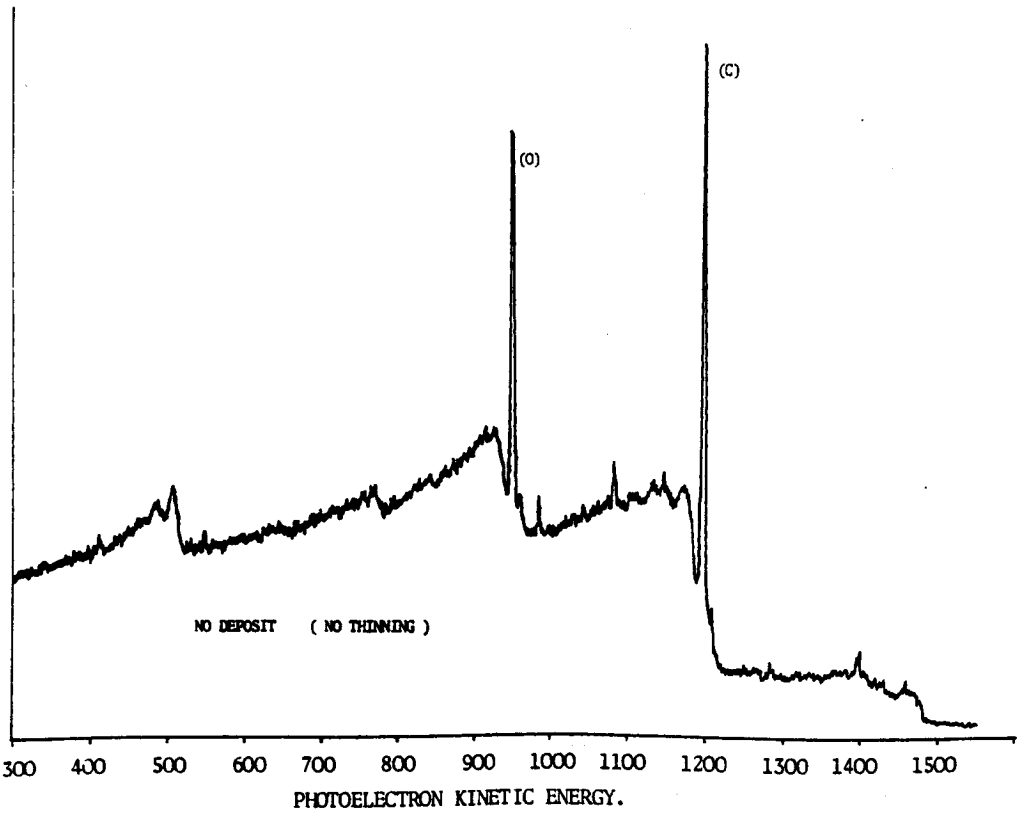

FIG. 65 X.P.S. spectrum before ion beam etching of the surface.
(Al Kα, 1487 eV)

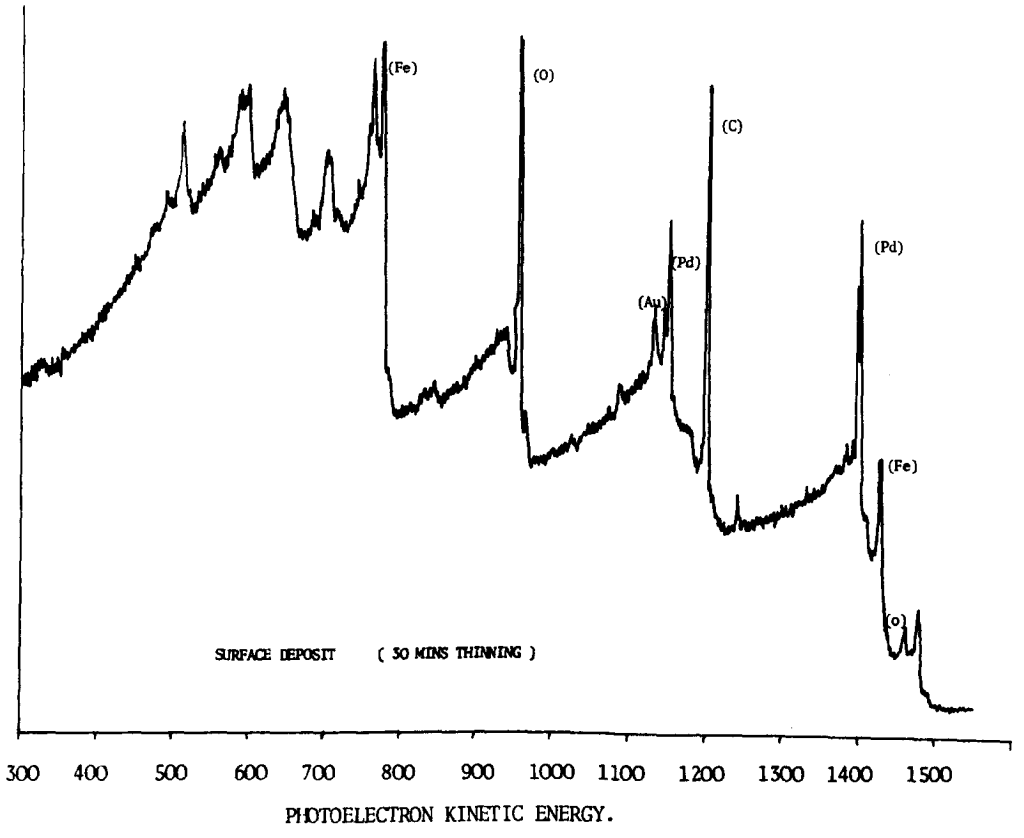

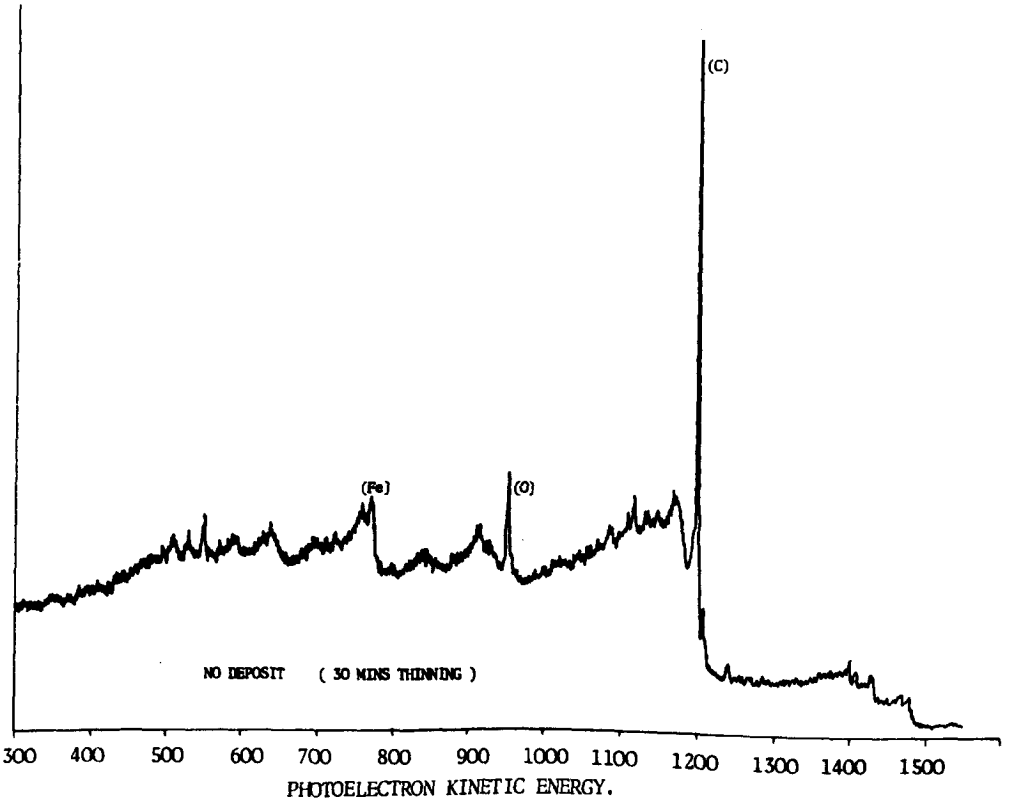

FIG. 66 Spectrum after 30 minutes etching.

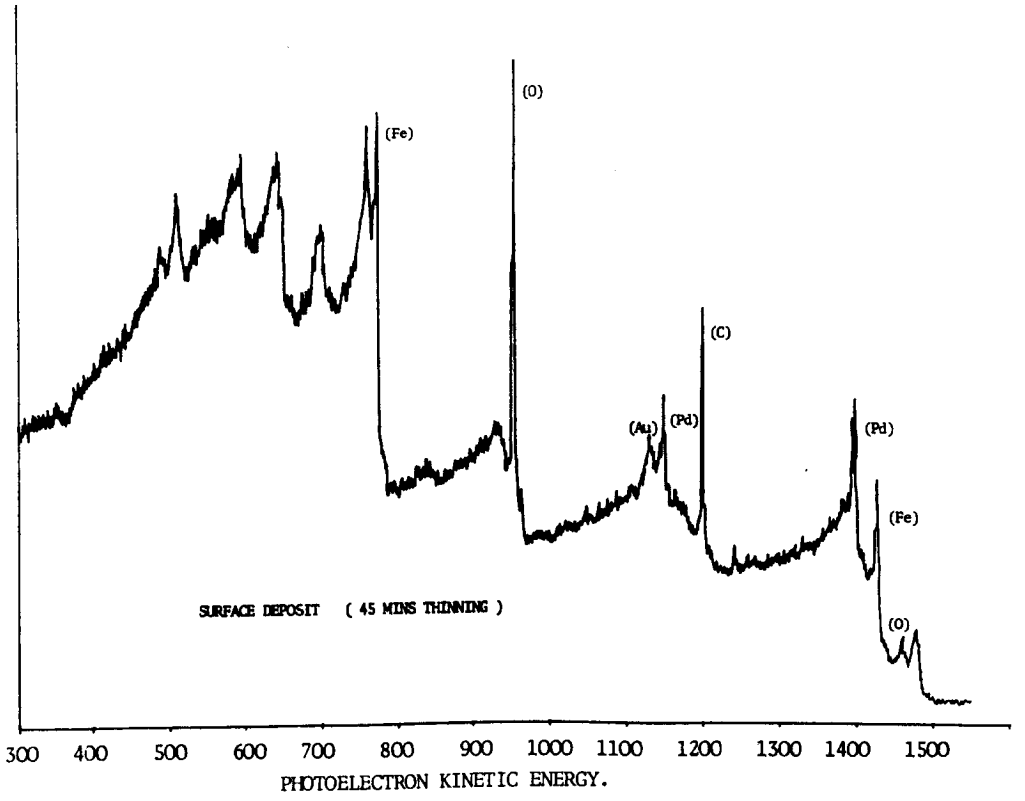

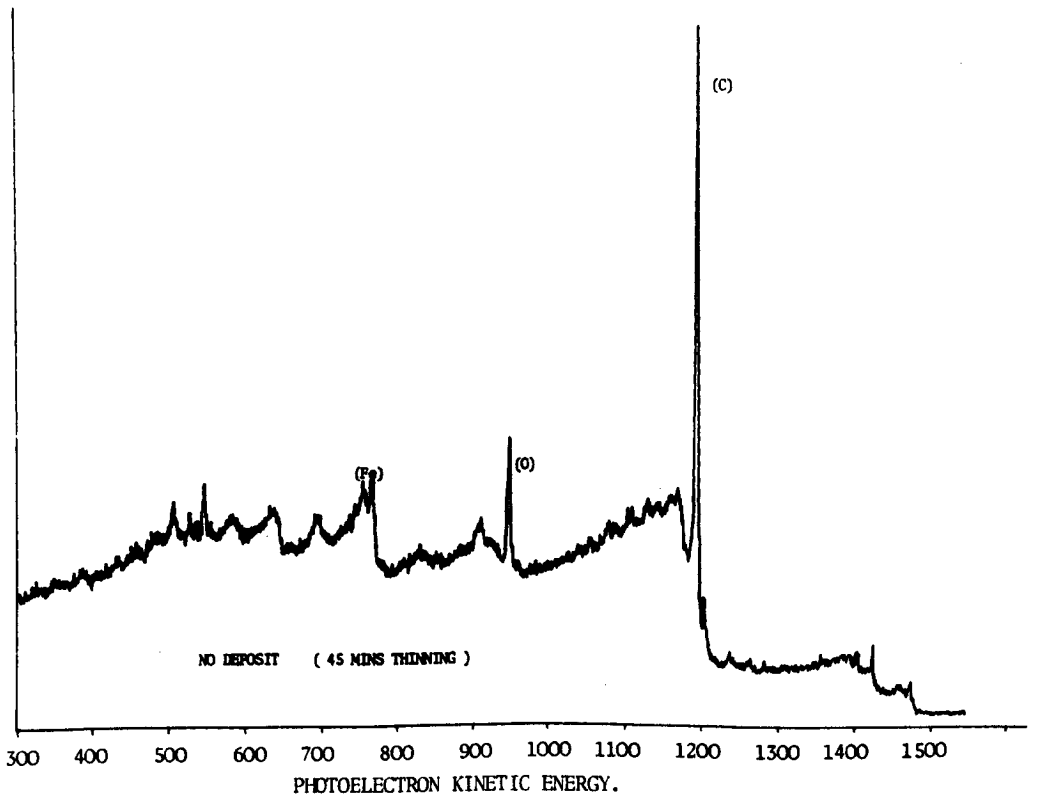

FIG. 67 Spectrum after 45 minutes etching.

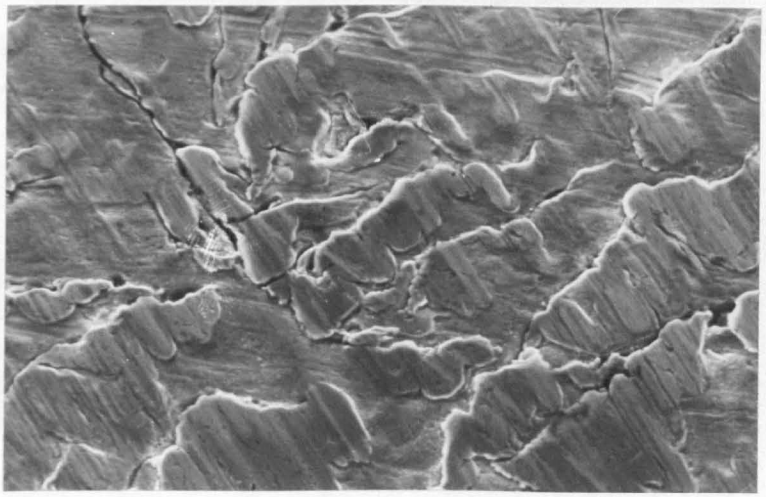

FIG. 68 Plate surfaces subject to corrosion and abrasion before conditions were balanced to simulate engine wear. X500

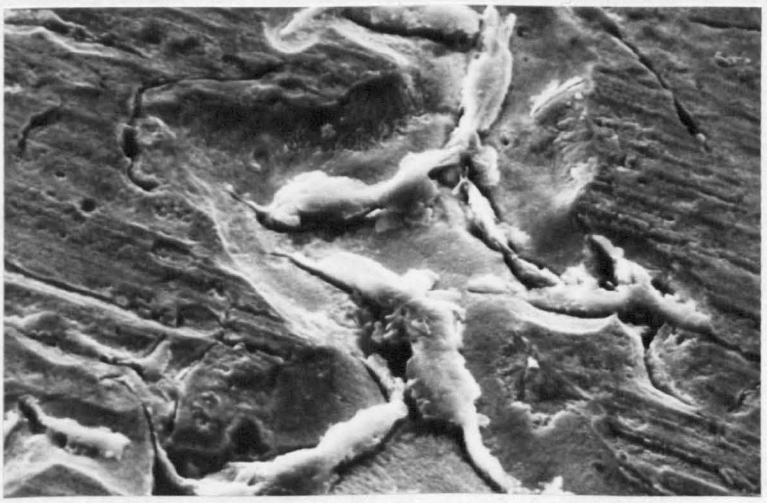

FIG. 69 Graphite stimulation of corrosion in areas subject to no abrasion. X1000

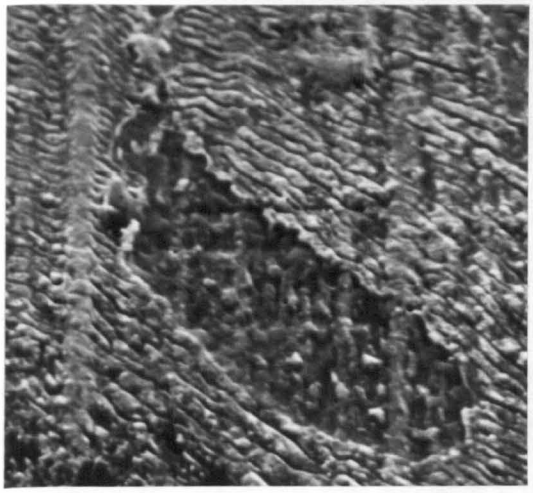

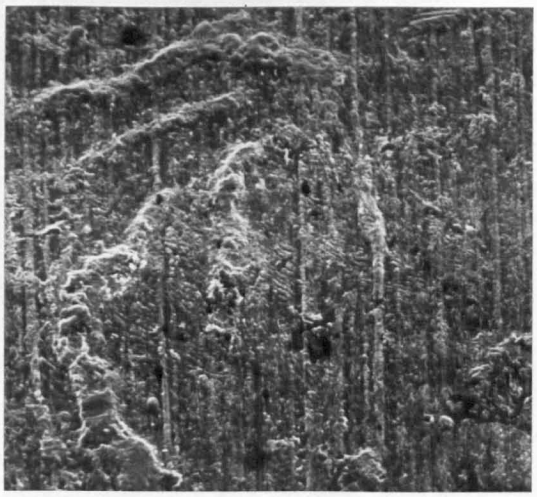

FIG. 70 Replicas of wear near T.D.C. from marine engine using residual fuel. X2000 and X500

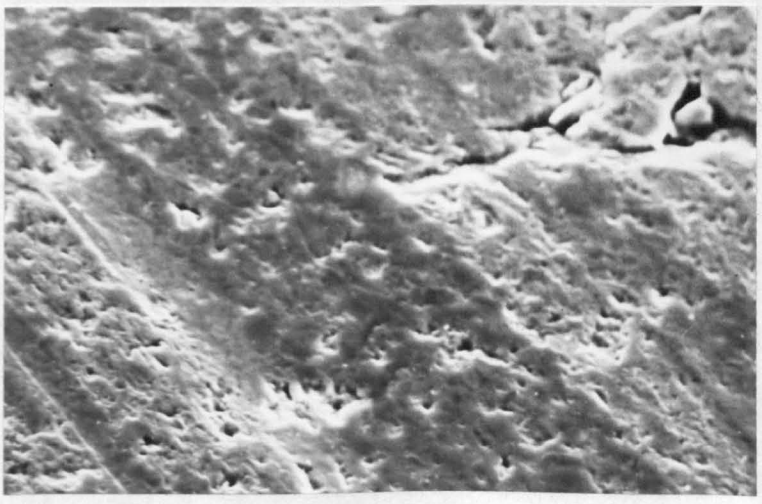

FIG. 71 Deposit on wear track at the end of the stroke after acidification of the lubricant. X2000

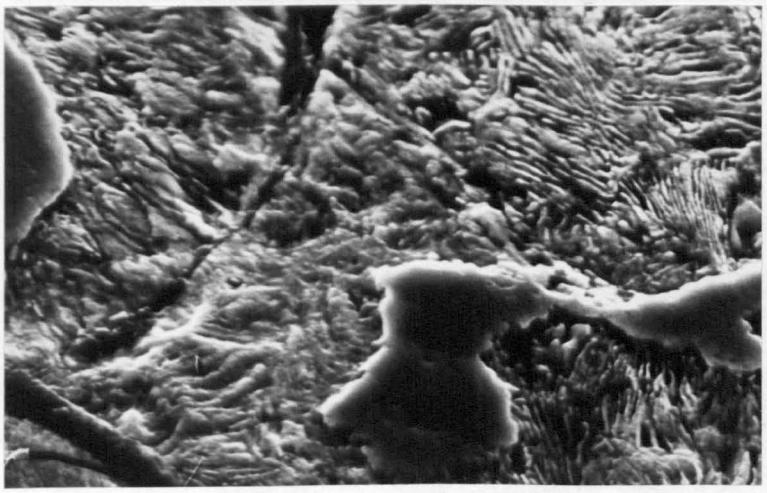

FIG. 72 Corrosion of pearlite on the wear track of an acidified test. X5000

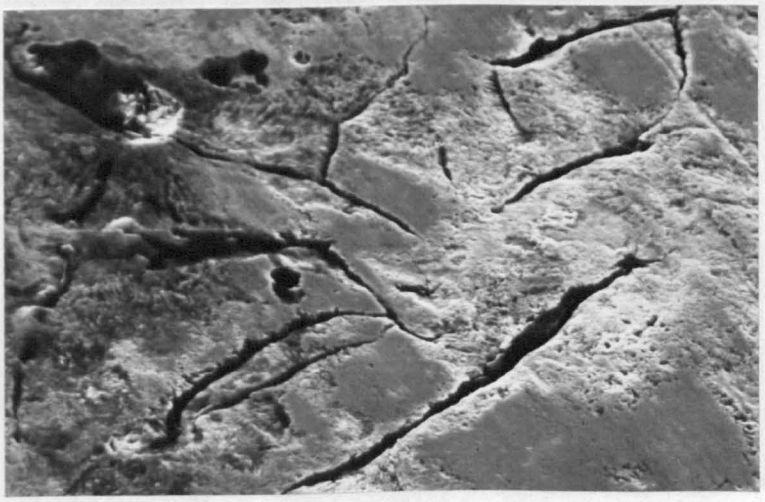

FIG. 73 Plate surface subject to corrosion and abrasion after conditions were balanced to simulate engine wear. X2000

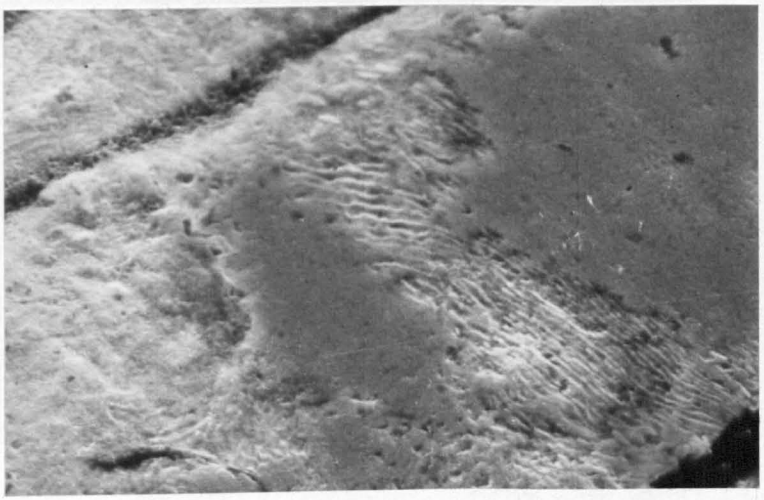

FIG. 74 Corrosion of pearlite in area shown in Fig. 73. X5000

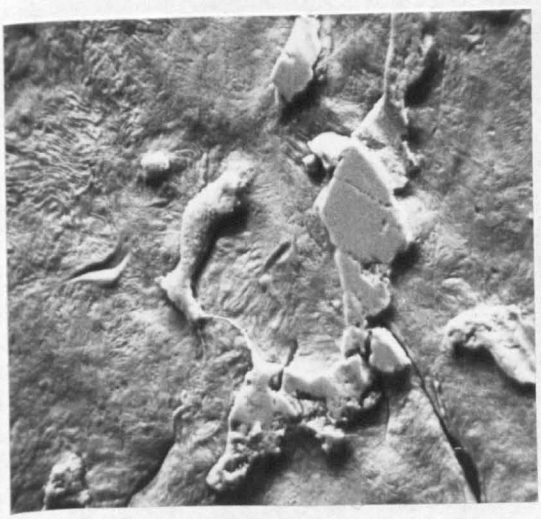

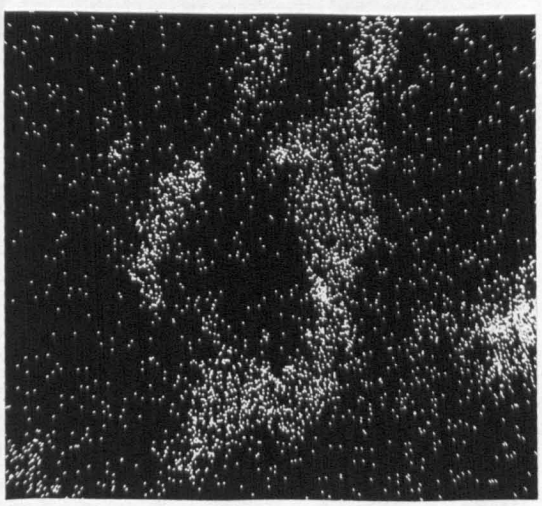

FIG. 75 Phase with lower wear rate on specimen plate surface. EPMA for phosphorus. X1000

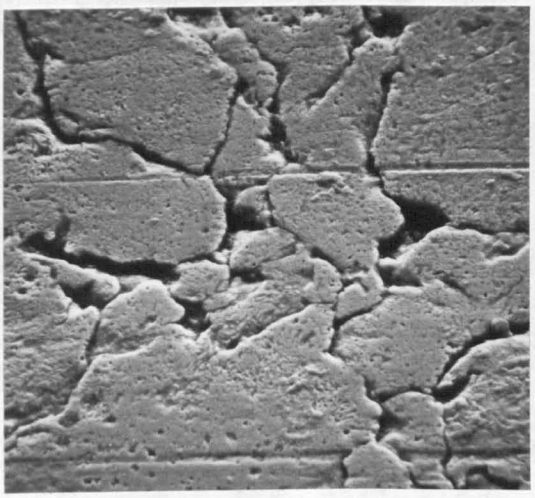

FIG. 76 Areas of film on the surface of an alloy cast iron plate specimen from an acidified test. X1000

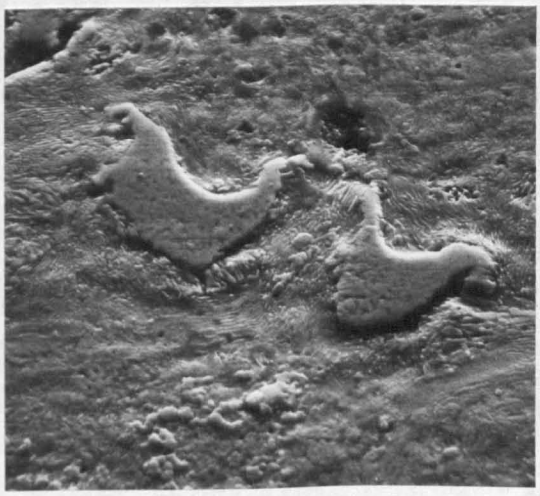

FIG. 77 Internal structure of phosphide eutectic on the plate surface of an acidified wear rig test. X2000

FIG. 78 Phosphide eutectic and pearlite on pin surface of an acidified test. X2000

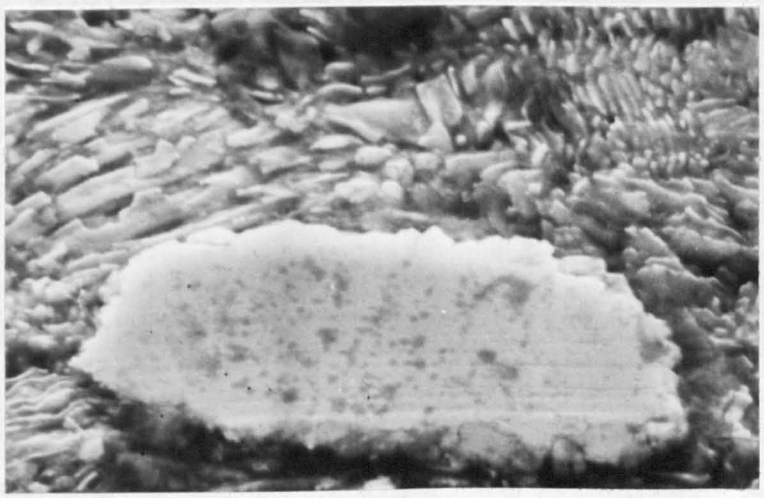

FIG. 79 Unattacked phosphide eutectic and iron carbide on pin surface. X5000

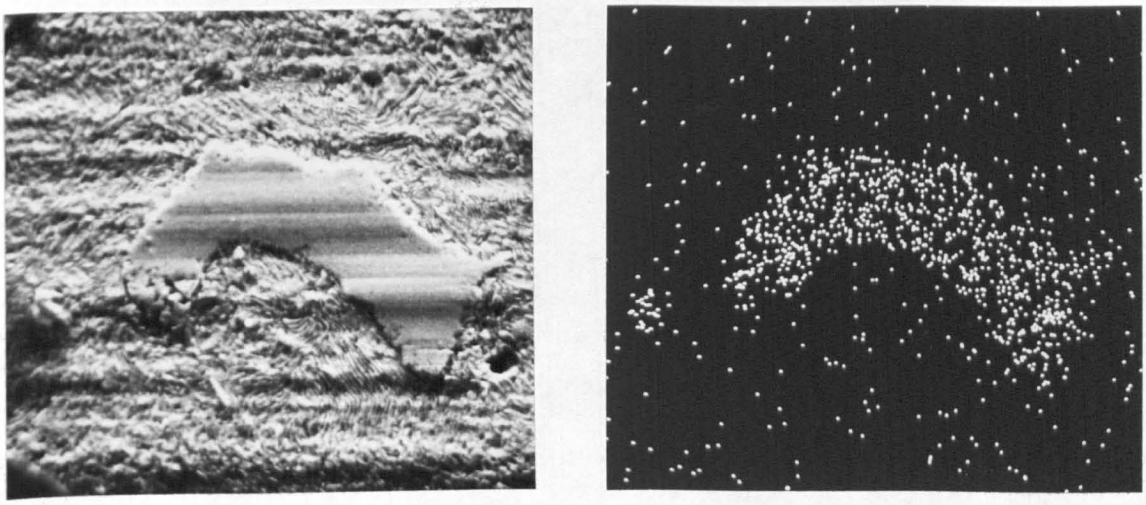

FIG. 80 Phosphide eutectic area standing above the matrix material on pin wear surface. EPMA for phosphorus. X2000

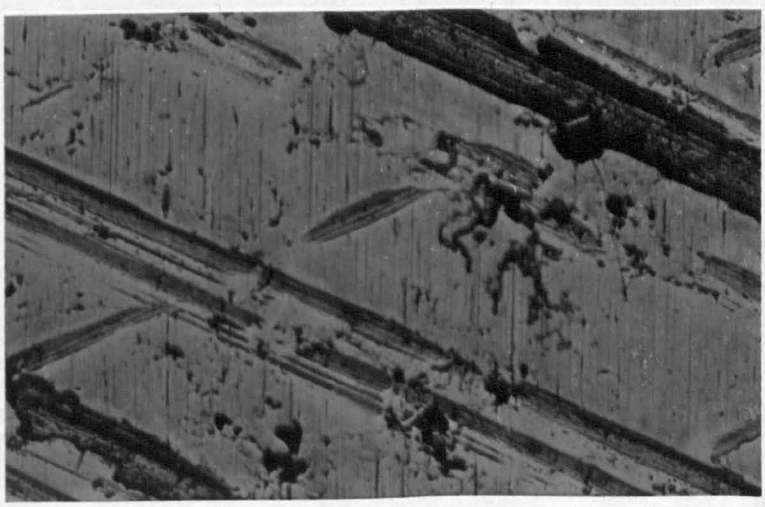

FIG. 81 Remains of original honing at the end of the test over top and middle of the low sulphur liner bore. X200

FIG. 82 Evidence of lightly etched phosphide eutectic after 144 hours running on liner surface near the top of the stroke of the low sulphur test. X100

FIG. 83 Hardly any wear near the bottom of the stroke after 144 hours running on the liner run on low sulphur fuel. X100

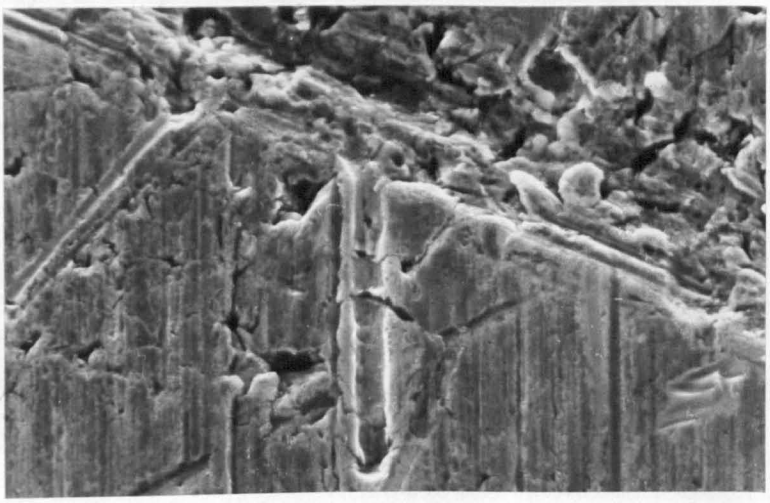

FIG. 84 Abrasion damage over the top and middle of the low sulphur test liner after 144 hours. X1000

FIG. 85 Staining over the top of the stroke at 180° to the oil feed hole after 144 hours using high sulphur fuel. X200

FIG. 86 Evidence of corrosion revealing the phosphide eutectic structure in areas similar to FIG. 85. X100

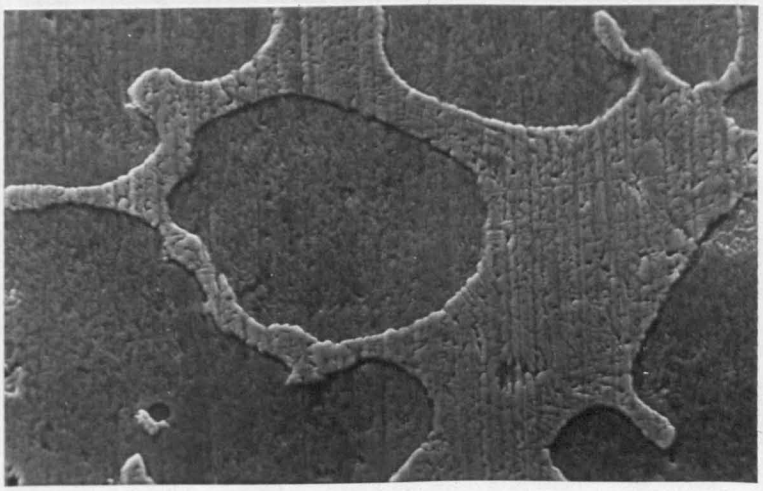

FIG. 87. Internal corrosion of phosphide eutectic which appears to be standing above the level of the matrix in areas similar to FIG. 85. X2000

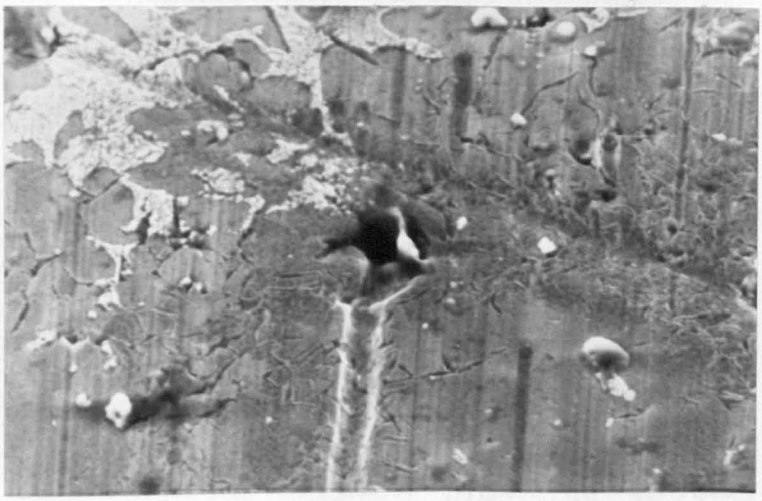

FIG. 88 Cavities on liner surface after 144 hours from which large abrasive grooves eminate top of bore at 180° to oil feed hole using high sulphur fuel. X500

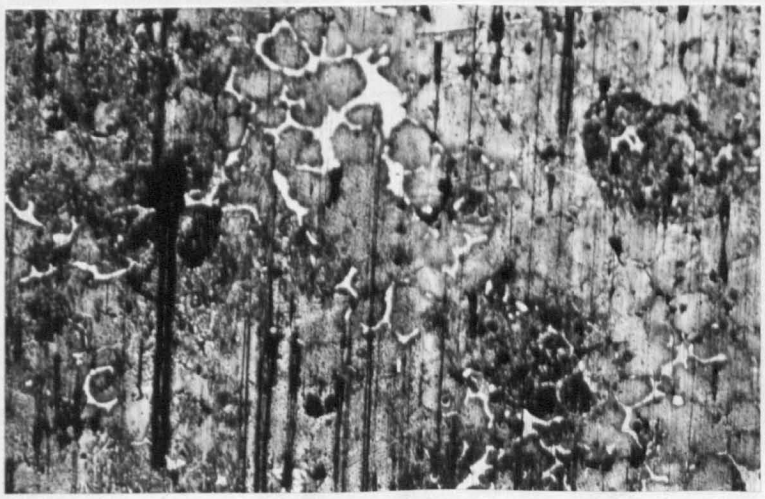

FIG. 89 Corrosive wear over middle of bore using high sulphur fuel. X100

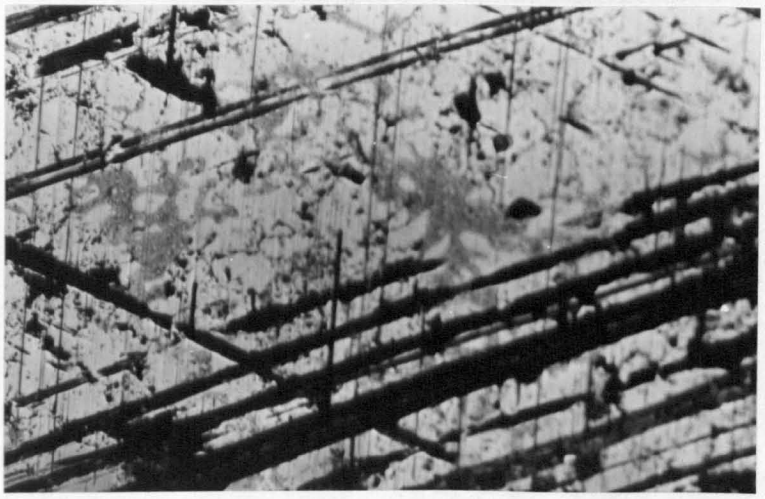

FIG. 90 Corrosive wear over bottom of stroke for high sulphur fuel test. X100

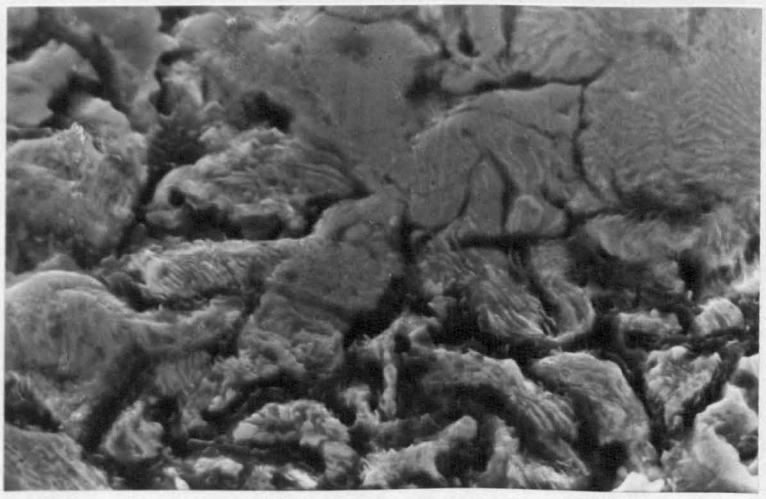

FIG. 91 Graphite stimulation of corrosion at bottom of liner at 180° to oil feed hole. High sulphur fuel test. X5000

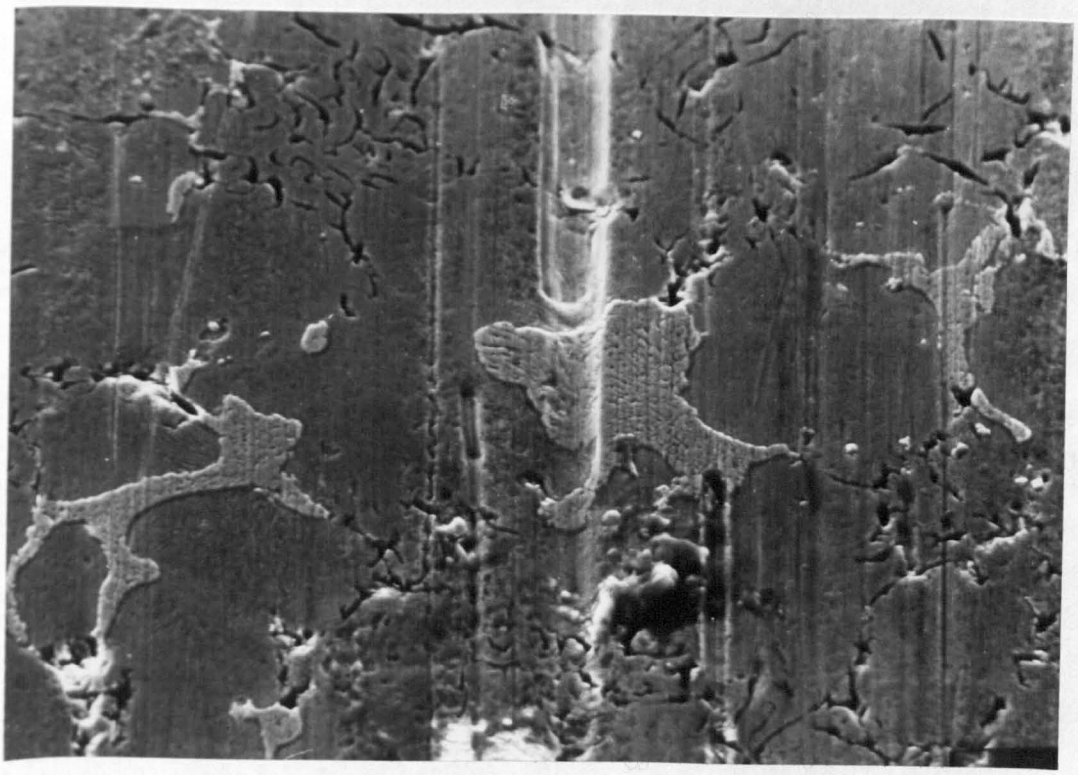

FIG. 92 Range of abrasive damage in addition to corrosion of matrix and phosphide eutectic phase. Some abrasion leading from the edge of the hard phase. X700

FIG. 93 Corrosion and abrasion on high sulphur test liner surface after 144 hours over top of stroke at 0^{o} to the oil feed hole. X2000

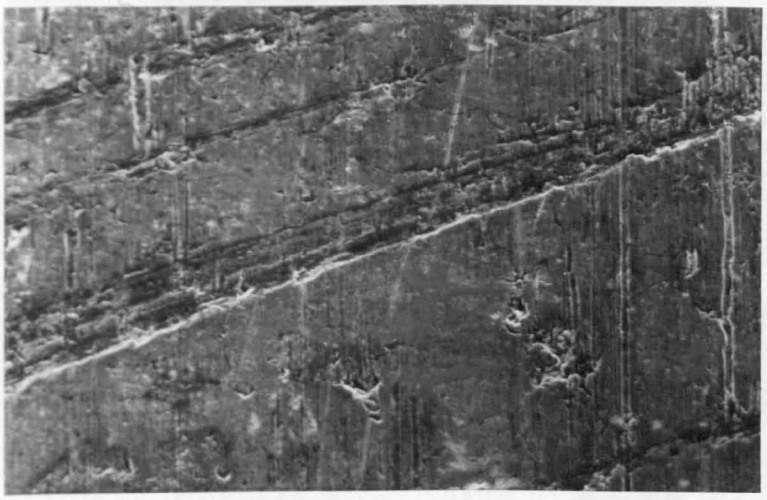

FIG. 94 Remains of original honing over top of stroke. Conditions as in Fig. 93. X100

FIG. 95 Remains of original honing over middle of stroke. Conditions as in Fig. 93. X200

FIG. 96 Wear only in localised areas at bottom of stroke. Conditions as in Fig. 93. X100

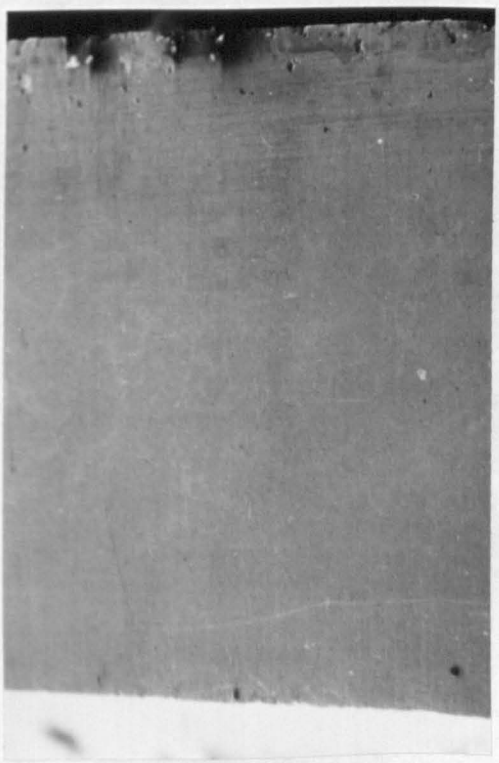

FIG. 97 Second ring rubbing face from high sulphur test after 144 hours. X50

FIG. 98 Second ring rubbing face from low sulphur test after 144 hours. Area on left hand side is original surface finish which has not worn due to manufactured tapered ring section. X50

FIG. 99 Corrosive wear on ring wearing surface. X500

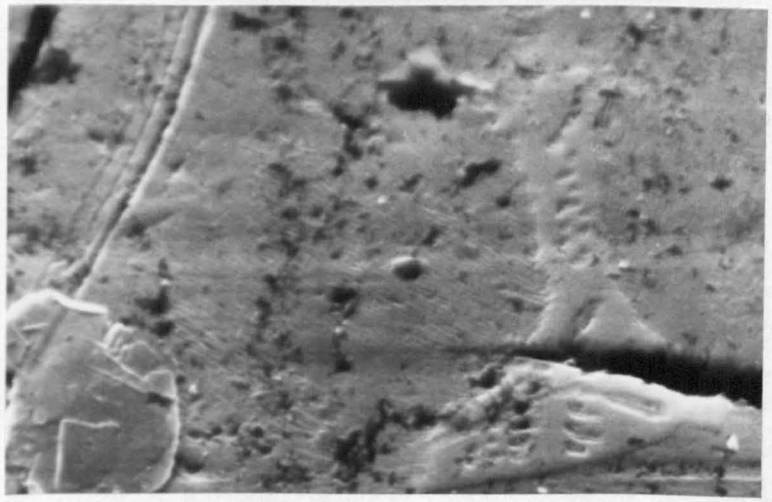

FIG. 100 Corrosion of matrix and phosphide eutectic from low sulphur fuel test. X5000

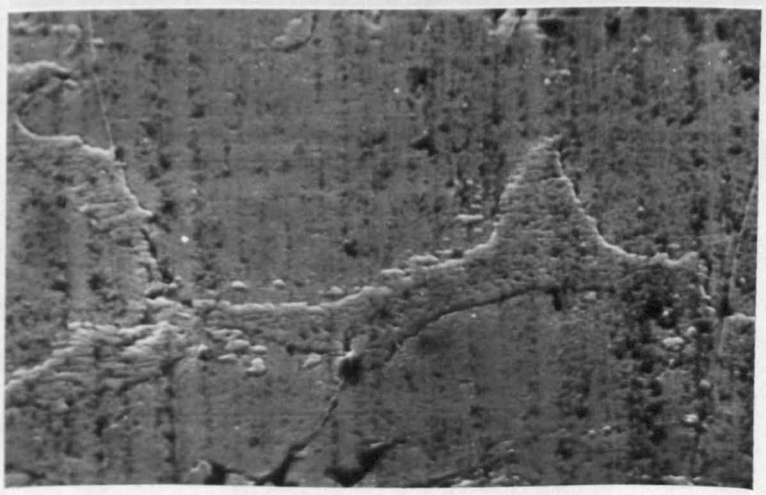

FIG. 101 More extensive corrosion of ring from high sulphur fuel test than for conditions in Fig. 100. X2000

FIG. 102 Taper section at 11.5° through protruding phosphide eutectic on liner at 180° to the oil hole in high sulphur test. X8500

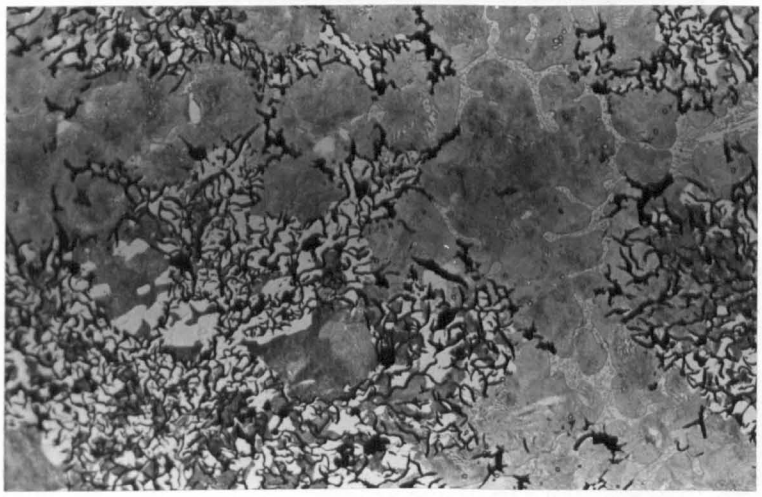

FIG. 103 Microstructure of Petter cylinder liner material. X200

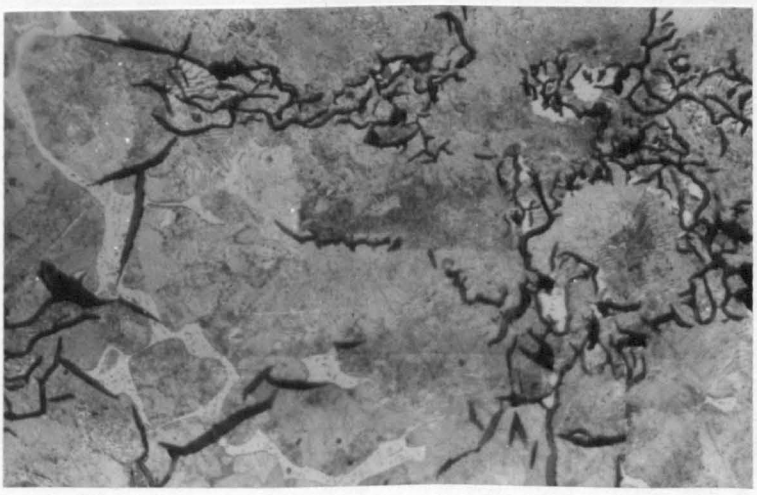

FIG. 104 Microstructure of Petter piston ring material. X200

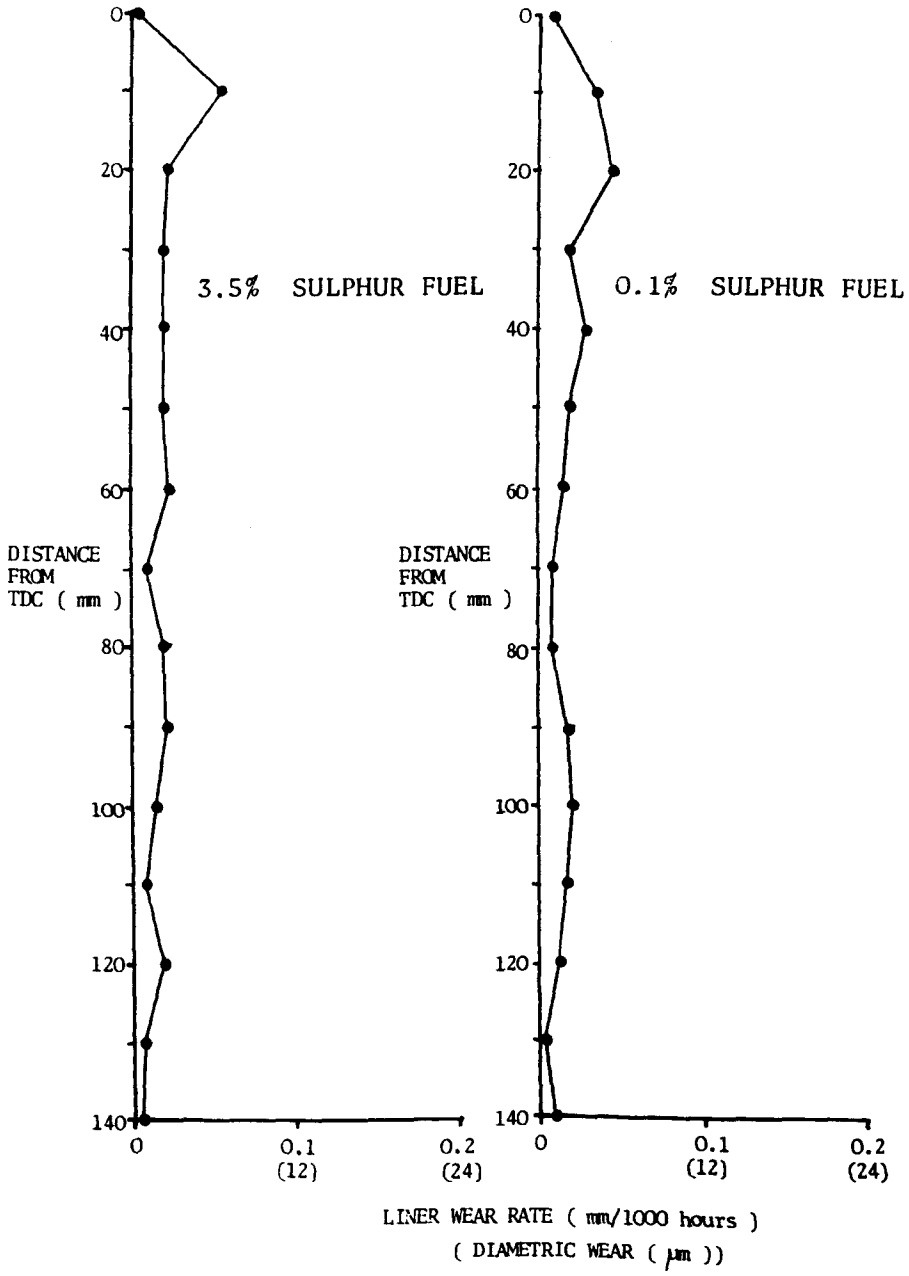

FIG. 105 Profile measurements down liner bore at end of test for low and high sulphur fuels.

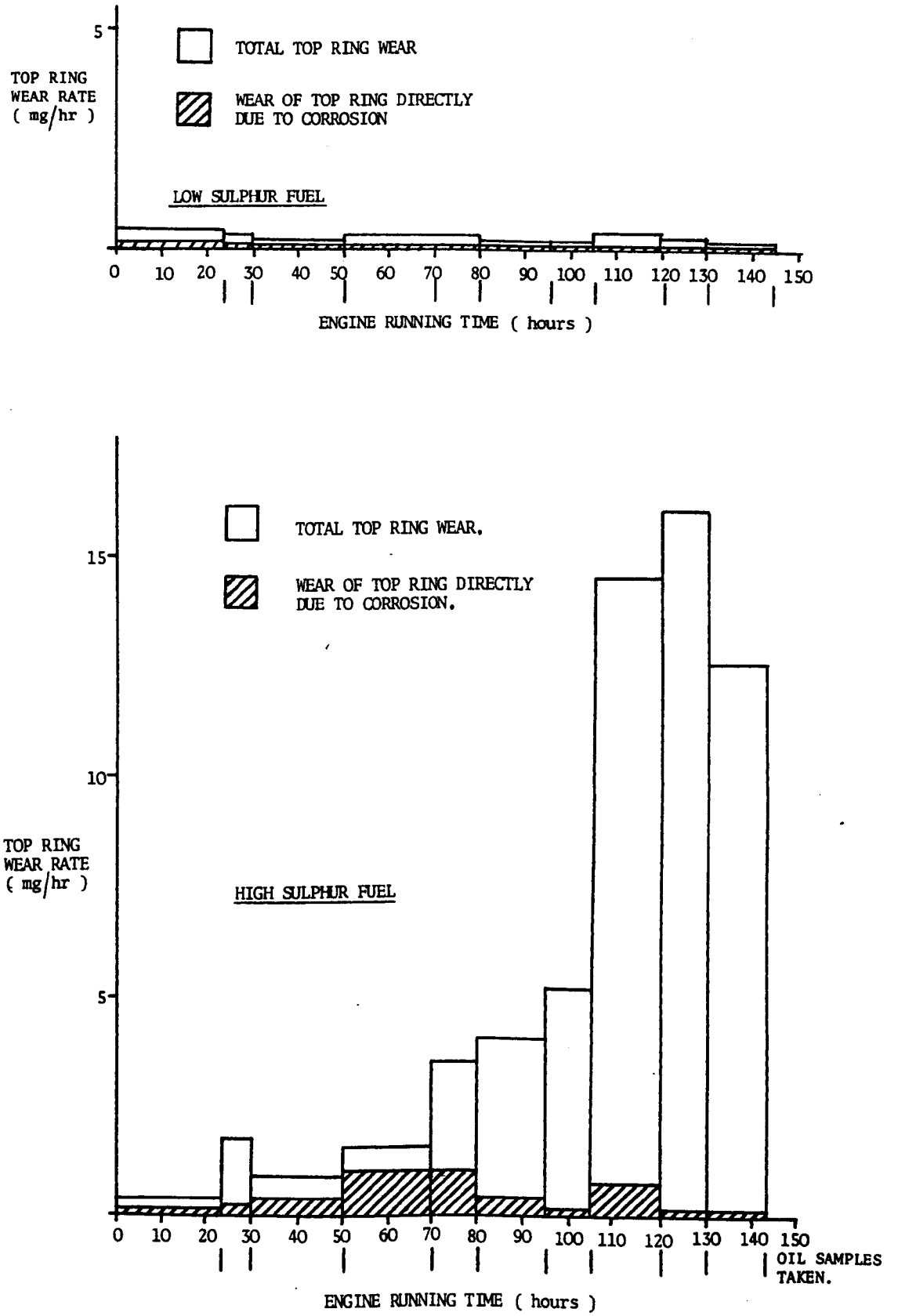

FIG. 106 Total piston ring wear measured by radioactive particle pickup in the oil drains and wear attributed directly to corrosion for both tests.

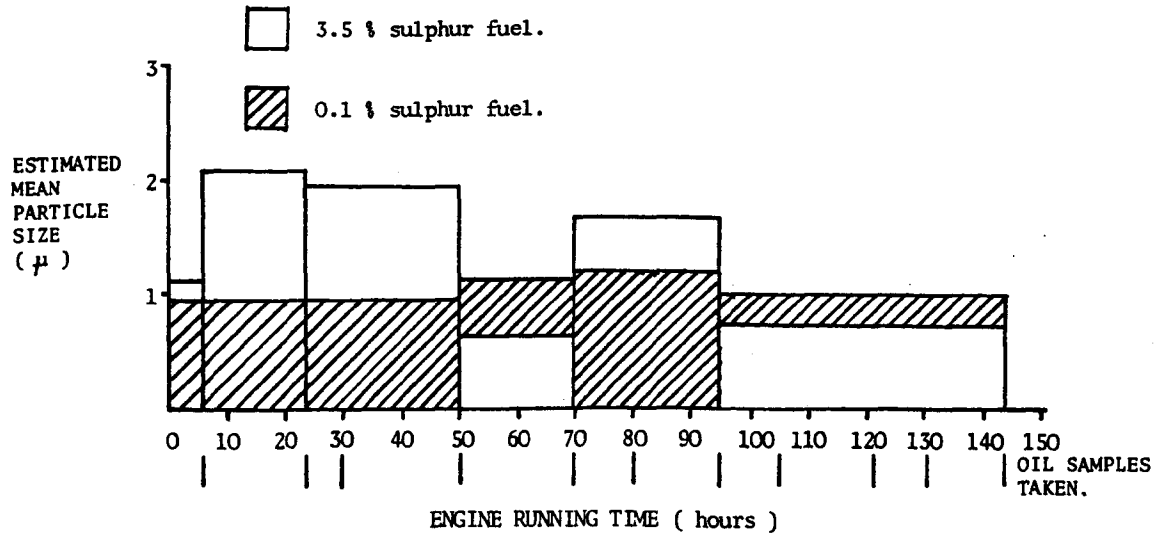

FIG. 107 Average particle size from ferrographic analysis of oil sample debris for both tests.

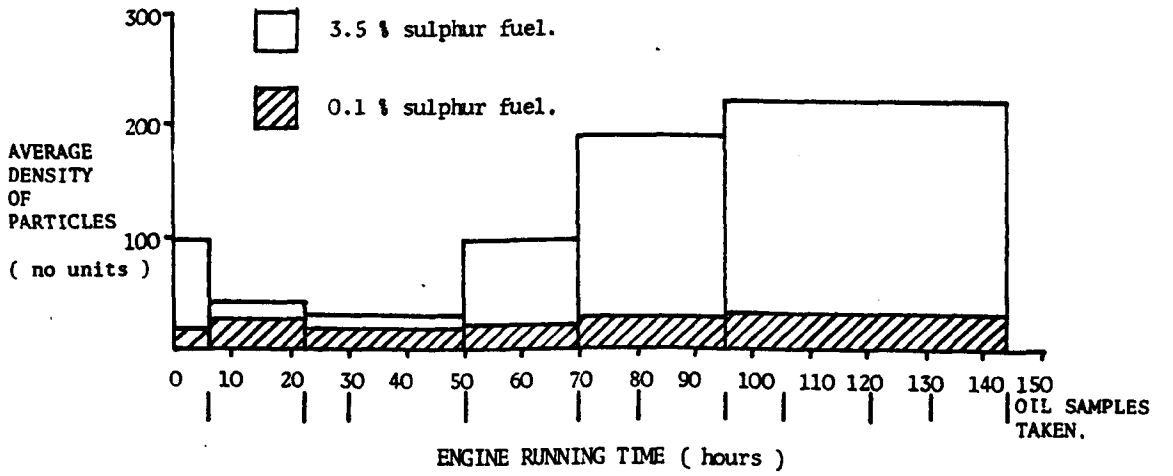

FIG. 108 Average particle density of debris on ferrographic slides on same samples as in Fig. 107.

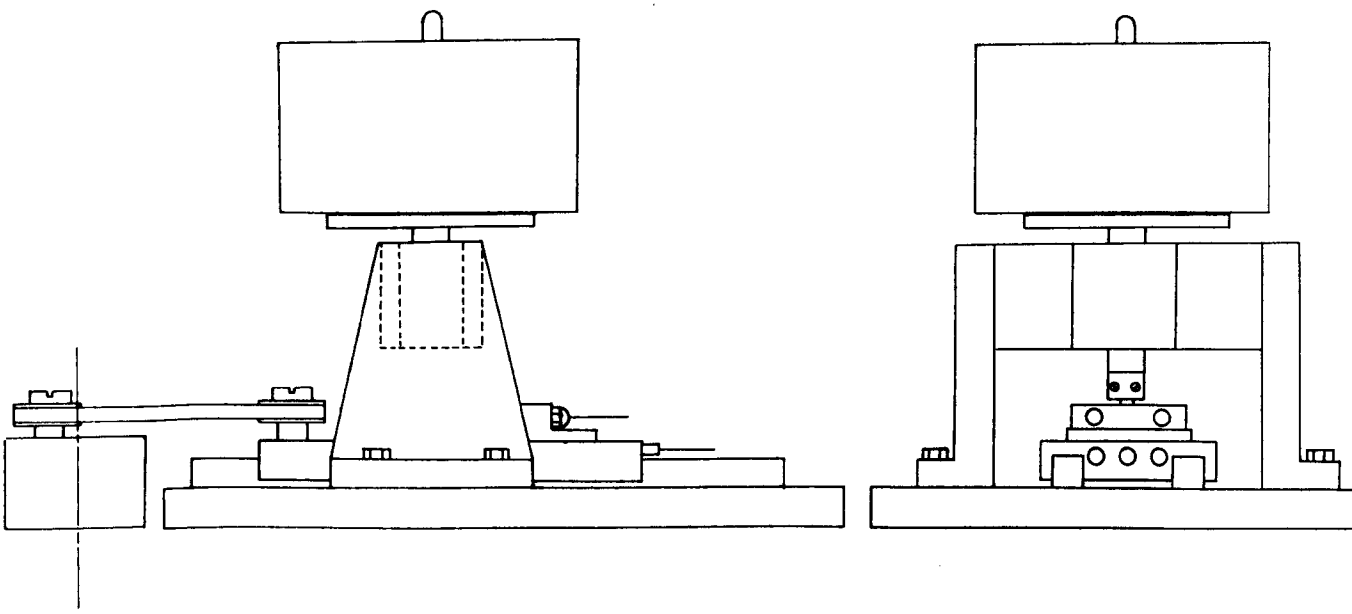

FIG. 109 Design of unsuccessful gantry system for loading of specimens.

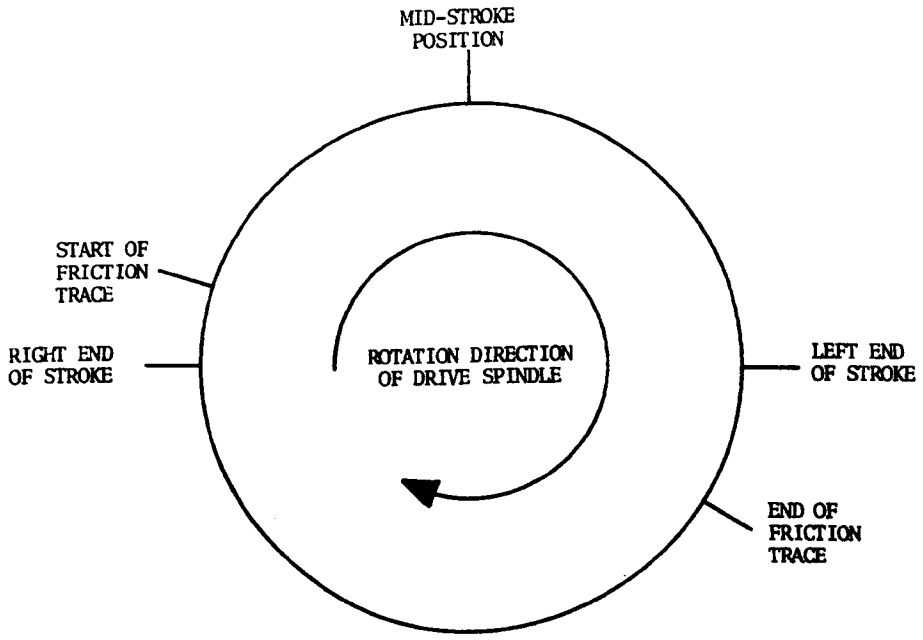

FIG. 110 Frictional force transducer output response through one revolution of drive spindle.

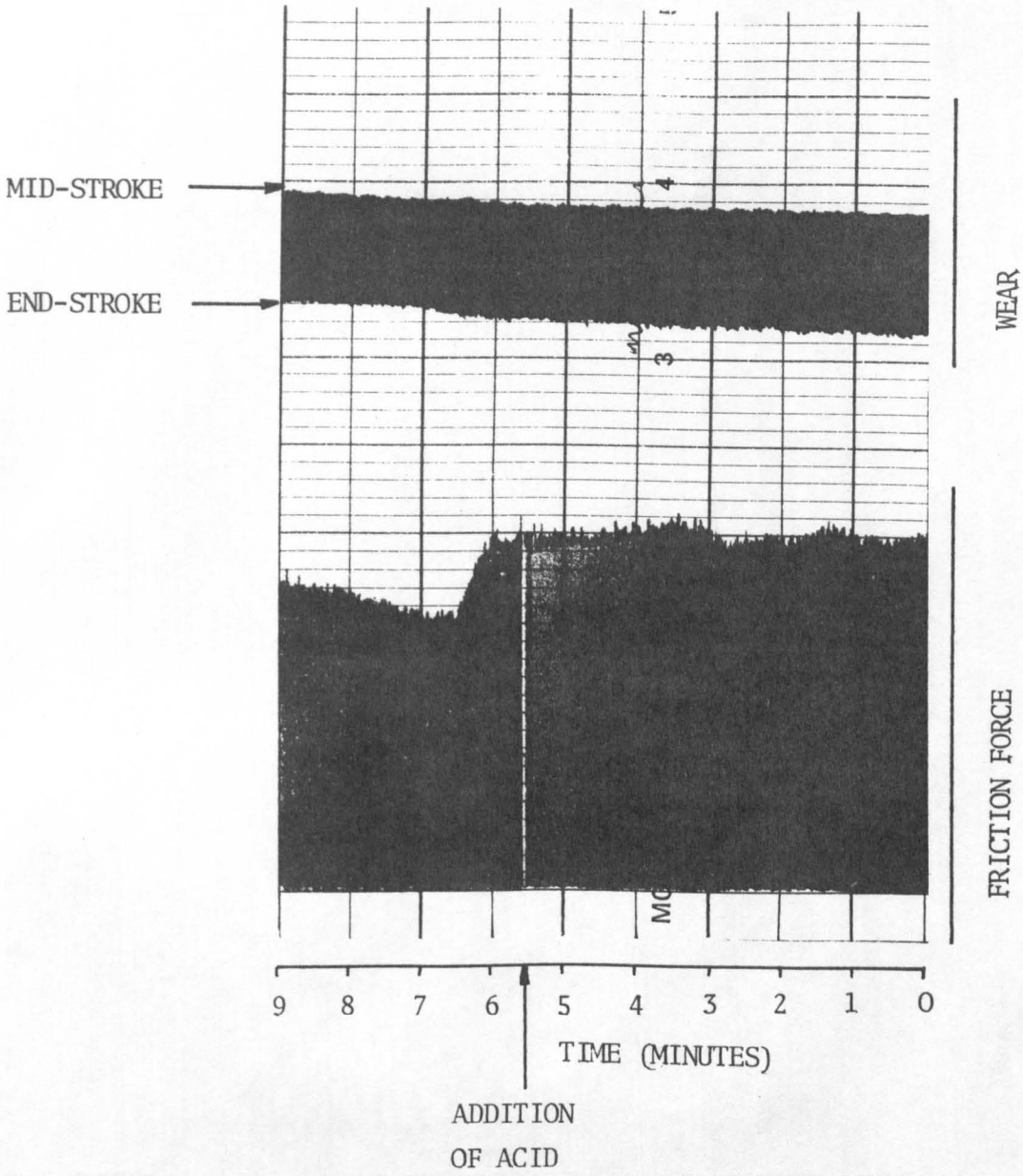

FIG. 111 Effect of acid addition on wear and friction transducer outputs. (see also FIG. 52)

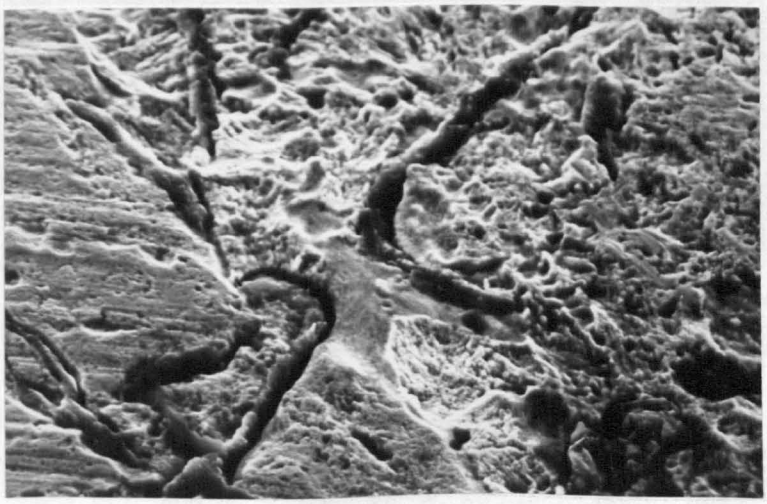

FIG. 112 Corrosion at edge (left) and beside the wear track (right) from an acidified rig test. X1000

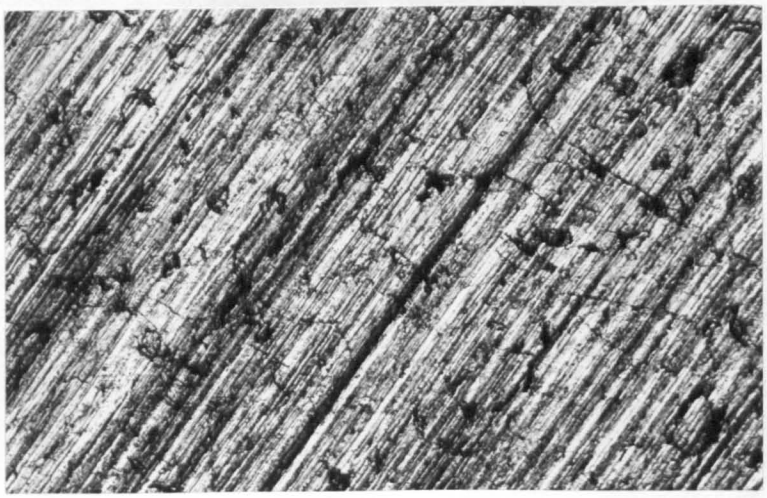

Plate surface
X100

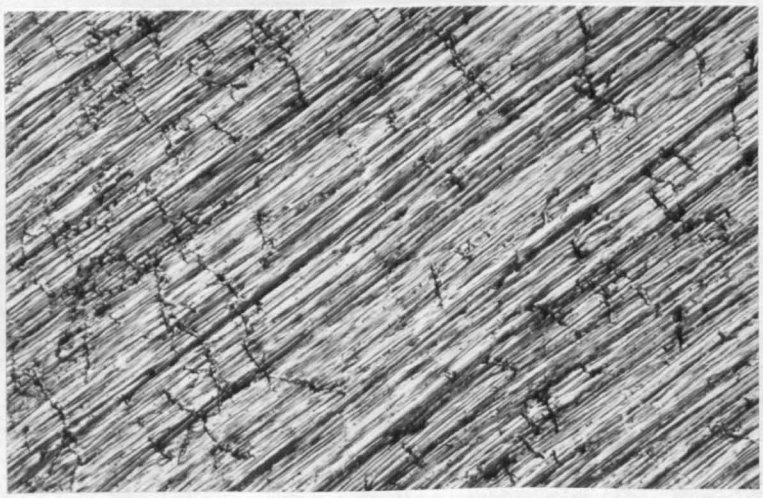

Pin surface
X100

FIG. 113 Original surfaces of rig plate and pin specimens.